SOURCE LOCALIZATION IN THE PRESENCE OF SENSOR MANIFOLD UNCERTAINTIES AND SYNCHRONIZATION ERROR

A Thesis Presented to the Faculty of Graduate School

University of Missouri – Columbia

In Partial Fulfillment

Of the Requirements for the Degree

Master of Science

---

by

Yue Wang

Dr. Dominic K.C. Ho, Thesis Supervisor

May 2011

The undersigned, appointed by the dean of the Graduate School, have examined the thesis entitled

SOURCE LOCALIZATION IN THE PRESENCE OF SENSOR MANIFOLD UNCERTAINTIES AND SYNCHRONIZATION ERROR

presented by Yue Wang

a candidate for the degree of Master of Science

and hereby certify that, in their opinion, it is worthy of acceptance.

Dr. Dominic K.C. Ho

Dr. Tony Han

Dr. Yi Shang

ACKNOWLEDGEMENTS

First, I would like to sincerely thank my advisor, Dr. Dominic Ho, for his intellectual and patient guidance. Without his help and guidance, I would not be able to complete my research.

I would also like to express my gratitude to Dr.Tony Han, Dr.Yi Shang for their time and consideration in reading my dissertation, and or their suggestions in completing my research.

I would like to thank Ming Sun, Le Yang, Zhenhua Ma, Liyang Rui, Shanjie Chen, my colleagues in the Communications Lab.

I would like to express my sincere thankfulness to my father, Weimin Wang, my mother, Yirong Shi, and all my other family members. Without your love, support and encouragement, I would not be able to accomplish my goal.

I also want to say thank you to all my friends. Thanks for the help from all of you.

Abstract

Passive source localization is a commonly used technology which can be applied to many areas, such as radar, sonar, microphone array, sensor network and wireless communication system. If an unknown source radiates some signals, the signal will be received by some receivers. The source location can be estimated based on the received signals using passive source localization technology. A lot of positioning methods have been derived on this subject, such as time of arrivals (TOAs), time differences of arrival (TDOAs), angle of arrivals (AOAs).

This thesis is mainly based on Chan and Ho's two stage closed form TDOAs source localization method. However, Chan and Ho's method assume the sensor positions are known and all of the sensors are perfectly synchronized.

Three topics that affect the accuracy of the source localization are discussed in this thesis in the presence of sensor position manifold uncertainties, in the presence of clock-bias error and in the presence of both sensor position manifold uncertainties and clock-bias error.

At first, we develop an estimator for source localization when measurement noise and sensor position manifold uncertainties are present. We modify a weighting matrix that accounts for the sensor position manifold error to improve the source location estimation. Then, we use simulation to analyse the performance of the proposed estimator. The simulation result shows that the proposed method reaches the CRLB performance for both the near-field and distant sources in the small error region. Furthermore, the proposed method has been provn that its performance reaches CRLB theoretically.

Secondly, we develop an algorithm for source localization in the presence of measurement noise and unknown but fixed clock offsets. The main idea of this estimator is to group the sensors with the same synchronization clocks together to form m_N sub-arrays. We transformed the original TDOA values to the new TDOA values of which the reference sensors are different for different sub-arrays so that the clock offsets are eliminated within a sub-array. The simulation results show that the proposed method reaches the CRLB performance for both the near-field and distant sources in the small error region. The performance of the proposed method in reaching CRLB has been provn theoretically under the small noise condition.

Finally, we develop an estimator for source localization in the presence of measurement noise,

sensor position manifold uncertainties and clock-bias error. The weighting matrix takes into account of the measurement noise and the sensor position manifold uncertainties. In addition, we group the sensors with the same synchronization clocks together to form m_N sub-array and use the new transformed TDOA values which allow us to eliminate the clock offsets within a sub-array. The simulation result shows that the proposed method reaches the CRLB performance for both the near-field and distant sources in the small error region. The performance of reaching the CRLB has been proved theoretically under the small noise condition.

Contents

Chapter 1

Introduction

1.1 Background

Passive source localization is a commonly used technology which can be apply in many areas, such as radar [1,2], sonar [3-6], microphone array [7-9], sensor network [10-14] and wireless communication [15-18] system. If an unknown source radiate some signal, and the signal will be received by some receivers. The source location can be estimate base on the received signals using the passive source localization technology. After many years study on this subject, a lot of methods have been derived using time of arrivals(TOAs), time differences of arrival(TDOAs) [19-25], angle of arrivals(AOAs) [26-28].

TOA refers to the travel time of a radio signal from a single transmitter to a remote single receiver. TOA after multiplied by signal propagation speed is the distance from the transmitter to the receiver. TOA defines a circle at the receiver position in which the emitting source will lie. In absence of noise, the source location is at the intersection of the circles from three receivers. Because TOA method need the absolute time of arrival,time stamping the signal and synchronization between transmitter and receiver is needed. Figure 1.1 shows the TOA localization approach, where s_1, s_2, s_1 are receivers. the intersection of the three circles is the source location.

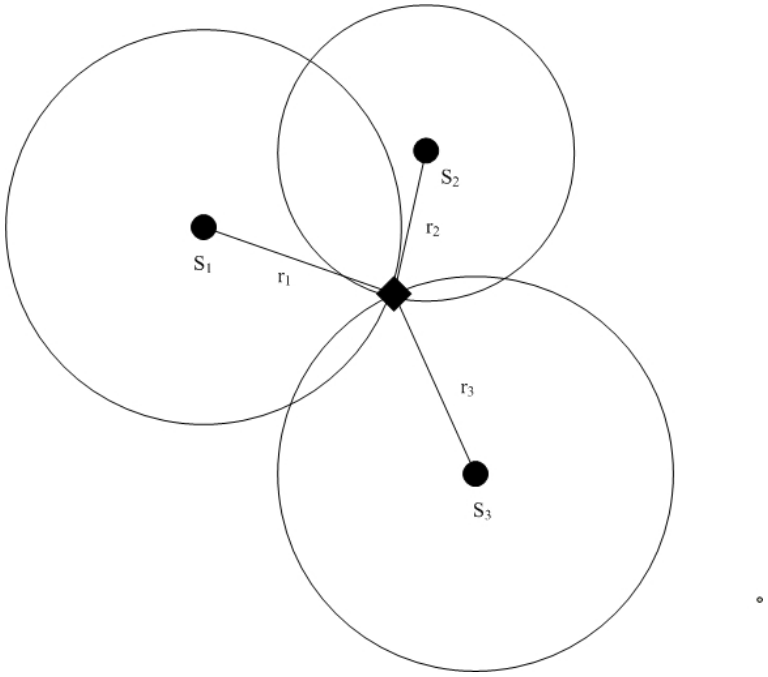

Figure 1.1: Source localization using TOAs

TDOA is the difference of arrival time of a source signal arrived at two different receivers. TDOAs can be calculated by subtraction of two TOA measurements, or it can be obtained by cross-correlating the two received signal. A constant TDOA locus is a hyperbola. Source location can be estimated by solving a nonlinear hyperbolic equations. Both TOA and TDOA techniques need synchronization. However, no time-stamping the signal is needed for TDOA. Figure 1.2 will illustrates the TDOA localization methods, where s_1, s_2, s_1 are receivers. The intersection of hyperbolic curves give the location.

AOA refers to angel of arrival. AOA uses direction information instead of distance information to estimate the source location. AOA defines a bearing line that passes through the source. Figure 1.3 demonstrates the AOA localization method, where s_1, s_2, s_1 are receivers, The intersection of bearing lines is the source location.

This thesis is based on TDOAs for source localization. The proposed estimators, however, can be easily extended to TOA and AOA position localization algorithm in a straight forward manner.

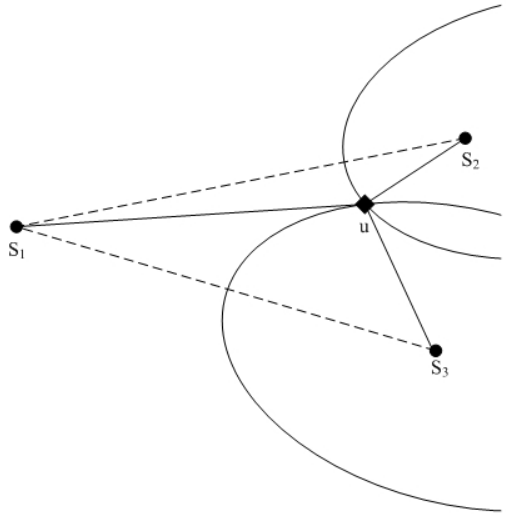

Figure 1.2: Source localization using TDOAs

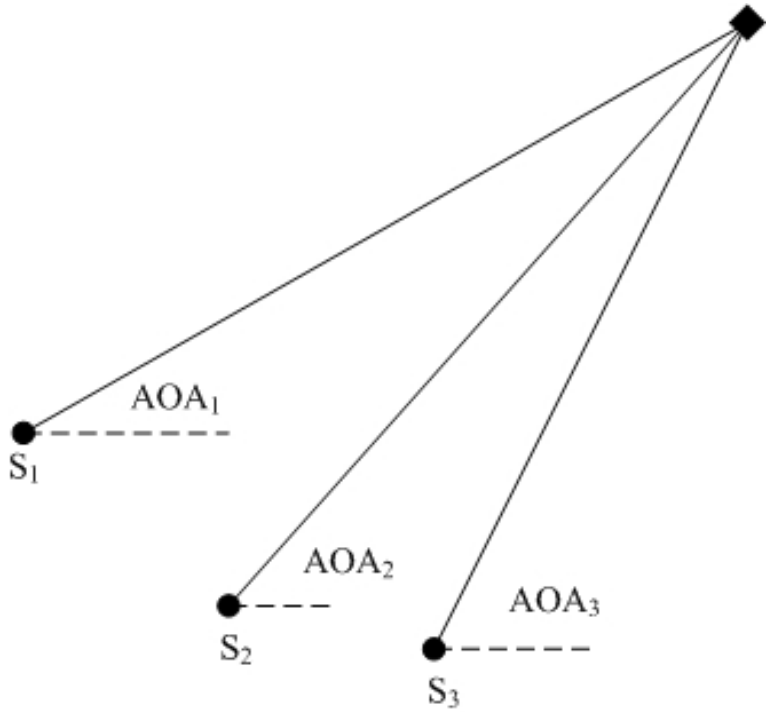

Figure 1.3: Source localization using AOAs

1.2 Localization Accuracy

Localization accuracy depend on different factors, for example, measurement noise, geometric distribution of the sensor and source, nonlinear of sight, sensor position error and clock-bias error. In this thesis, we will discuss sensor position manifold uncertainties and clock-bias error and combination of the two error.

1.2.1 Manifold Uncertainty

Previous study on TDOA localization usually assumes sensor positions are known and accurate. However, sensor positions may have some error. Some previous work has been done on this subject[29,30]. However, they paid more attention on handling independent sensor uncertainties. In practice, sensor uncertainty may have some relations between each other. If these relations are considered, better localization accuracy can be achieved than considering all sensor uncertainty as independent Gaussian noise.

For example, in Figure 1.4, the entire sensor array contains two sub-arrays. The sensors in each sub-array are mounted at fixed position. In this case, each sub-array can be drifted and all its sensors have the same amount of position error. If all the sensors have independent error, it will be sixteen dimensions of uncertainty. However, since all sensors in one sub-array move together, it only has four dimensions of uncertainty. So, there is some hope that the estimation accuracy can be improved.

1.2.2 Clock Bias Uncertainty

The TDOA localization method needs synchronization among the sensors. However, a sensor array may have more than one clocks. This thesis provide a method which does not need to synchronize different clocks within an array.

Some work has been done in sensor self localization without synchronization [31,32]. It uses differential TDOA (dTDOAs) to cancel out unknown clock offsets. However, it requires all sensors to transmit some signals. In this thesis, sensors don't need to transmit signals. Source location can be estimated using a passive sensor array. For example, consider Figure 1.5 where,

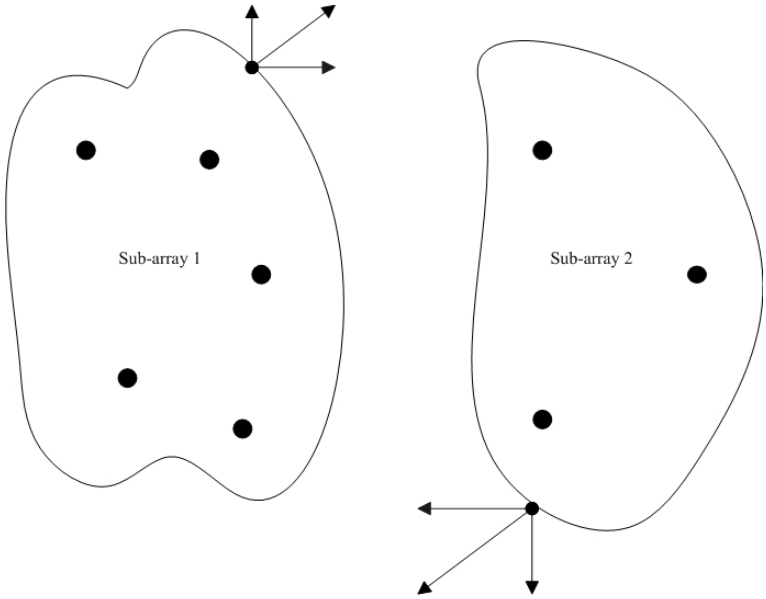

Figure 1.4: Illustration of manifold sensor uncertainty

s_1, s_2, s_1, are receivers and r_1, r_2, r_3 are TOAs. we have two clocks and the receivers have the same clock are grouped together. Each sub-array has one own clock, clock 1 and clock 2. we choose sensor 1 as reference sensor, the TDOAs are $r_{21} = r_2 - r_1$ and $r_{31} = r_3 - r_1$. In absence of TDOAs noise, because s_1 and s_3 have different clocks and hence r_{31} contains clock bias. As result, using r_{21} and r_{31} to localize the source will give very large localization error.

1.2.3 Manifold error and Clock Bias uncertainty

The two kinds of error may happen at the same time, and this thesis will consider this situation as well Figure 1.6 illustrate this situation, which both manifold sensor uncertainty and clock bias error exist.

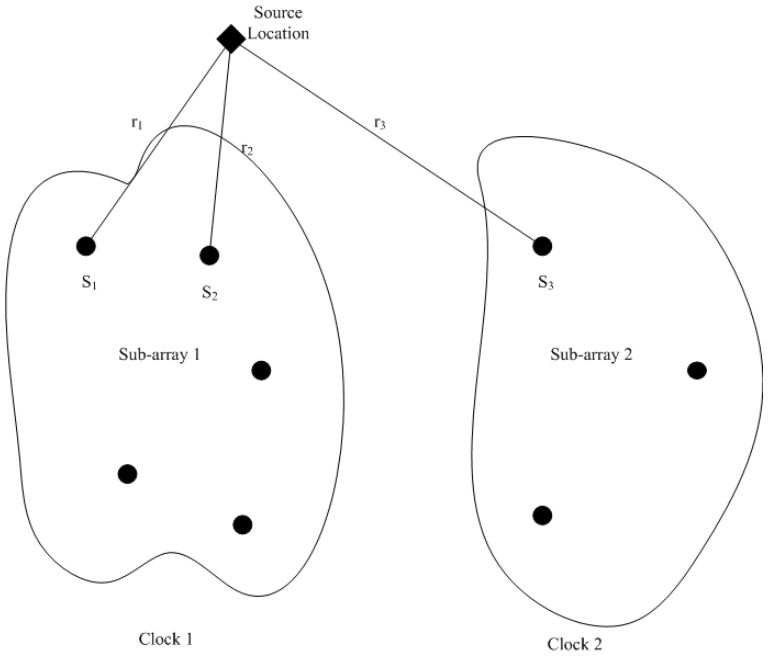

Figure 1.5: Illustration of clock bias uncertainty

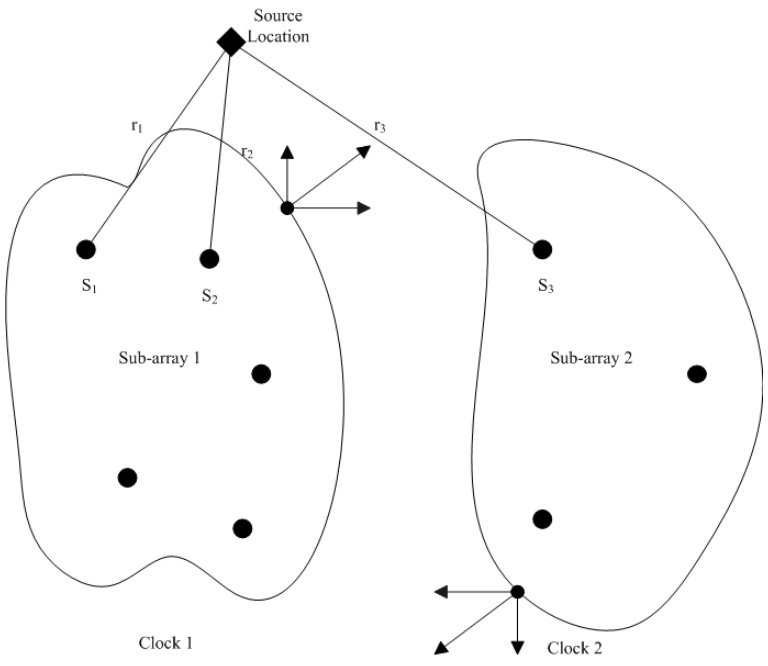

Figure 1.6: Illustration of in the presence of sensor position manifold uncertainties and clock-bias uncertainties

1.3 Motivation

1.3.1 Manifold Uncertainty

In a sensor array, quite often sensors are fix on a structure and the structure may be moved or rotated because of wind, vibration. In this situation, the position uncertainties of al the sensors in the structure are the same. If the dependency can be explored properly, a more accurate source location estimate can be achieved than considering all sensor uncertainties are independent.

For example, consider a sensor array with a number of sensor mounted, which is placed along the highway to detect wild animals that might cross the road. The sensing system is need to inform the driver to avoid the accident. But, because of the wind, the rain and the vibration caused by vehicles, the position of the sensor array may be moved or rotated. But the relative position of the sensors remain unchanged. We shall call this sensor position uncertainties as sensor manifold uncertainties.

1.3.2 Clock Bias Uncertainty

If a sensor array has several sub-arrays, and each sub-array has its own clock, different sub-arrays will have clock bias with one another.When their clock are not synchronized. for example, this could be due to the large geometric distances among the sub-arrays. This thesis will provide a method to solve this problem.

For example, consider the situation that one sensor array has several sub-arrays. The sub-arrays are separated and the sensors in one sub-array is close to each other. Sensors can be synchronized using Bluetooth technology. Because of the small range coverage of Bluetooth, only sensors in the same sub-array can be synchronized. Each sub-array has its own clock and the clock of different sub-arrays are not synchronized. In this case, method proposed in this thesis can be applied.

1.3.3 Combination of Manifold and Clock Bias Uncertainty

If one sensor array has several sub-arrays that are far from each other, each sub-array has its own clock. When the sub-arrays are fixed on several objects, the sensors will have manifold uncertainty. In this case, it is reasonable to propose a algorithm which can handle both manifold uncertainty and clock bias uncertainty together.

1.4 Contribution

This thesis addresses the problem of TDOA localization in the presence of sensor manifold uncertainties and /or synchronization clock bias errors. The main contributions include:

(1) The study of localization accuracy in the presence of these errors. through the CRLB analysis based on Gaussian noise model.

(2) The development of estimators to obtain the optimum source location estimate.

(3) The analysis of the proposed estimators.

For the first contribution, the study through the CRLB analysis based on Gaussian noise model.

For the second contribution, three algorithms are proposed in the thesis. The first one is to solve source localization in the presence manifold uncertainty of the sensors. Since the position uncertainties in different sensors are related dimension of uncertainties can be reduced. Estimation accuracy can be improved by exploring manifold sensor error uncertainties than assuming all sensor uncertainties are independent. If there is no relationship among the sensor positions, the method proposed in this thesis also can handle this situation. The new method can be viewed as an generalization for the previous study of independent position errors as well.

The second algorithm is the estimation of the source position in the presence of clock bias error among different sub-arrays in a sensor array. It can be applied to the situation where a sensor array has more than one clock and only the sensors within a sub-array can have perfect synchronization.

The third estimator is to address the situation when both manifold sensor uncertainties and clock bias uncertainties are presence at the same time.

For the third contribution, we have conducted the analysis of the performance of the proposed estimators in both simulations study and theoretical proofs. The three proposed estimators achieve optimal performance both in simulation and in theory over the small error region.

Chapter 2

Localization Basics

In this Chapter, we will introduce some basic topics in localization, including basic idea about the Cramr-Rao lower Bound(CRLB), the TDOA localization algorithm, the Taylor-series technique and the closed-form two-stage algorithm.

2.1 Cramer-Rao lower Bound(CRLB)

Cramer-Rao lower Bound(CRLB) provide a lower bound on the variance of any unbiased estimator[33,34]. It gives optimal variance and alerts us if it is impossible to find an unbiased estimator whose variance is less than the bound.

CRLB is obtained from probability density function(PDF) of the collection of data measurements $\boldsymbol{x}$ that is parameterized with respect to the unknown parameter $\boldsymbol{\theta}$. It is assumed that if PDF satisfies

$$E\left[\frac{\partial lnp(\mathbf{x};\boldsymbol{\theta})}{\partial \boldsymbol{\theta}}\right] = 0 \tag{2.1}$$

Then the variance of any unbiased estimator $\hat{\theta}$ must satisfies

$$cov(\hat{\boldsymbol{\theta}}) \geq -E\left[\frac{\partial^2 lnp(\mathbf{x};\boldsymbol{\theta})}{\partial \boldsymbol{\theta}\boldsymbol{\theta}^T}\right]^{-1} \tag{2.2}$$

In this thesis, we will compare compare CRLB with simulation result to see if mean-square error reach CRLB which is the optimal permance. Then, we will prove variance of the estimated source location is equals to CRLB theoretically

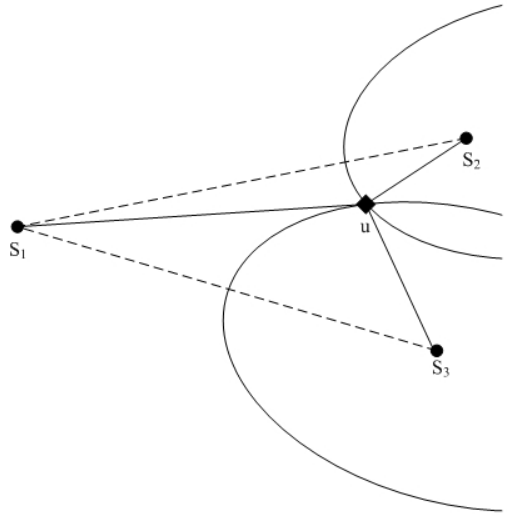

Figure 2.1: Source localization using TDOAs

2.2 TDOA localization

As mentioned in Chapter 1, TDOA is the difference of arrival time of a source signal arrived at two different receivers. A constant TDOA locus is a hyperbola. Source location can be estimated by solving a set of nonlinear hyperbolic equations.

Figure 2.1 shows a example of TDOA localization. $\mathbf{s}_1, \mathbf{s}_2, \mathbf{s}_3$ are receivers. The intersection of hyperbolic curves is the source location. We shall denote the true distance between the source and i_{th} receiver as r_i^o

$$r_i^o = \|\mathbf{u}^o - \mathbf{s}_i\| \tag{2.3}$$

where $\| * \|$ represents the 2-norm. TDOA measurement, after multiplied by the signal propagation speed, between sensor i and sensor 1 is

$$r_{i1} = r_i - r_1 + n_{i1}, i = 2, 3, \ldots, M \tag{2.4}$$

n_{i1} is the TDOA noise, that is assumed to be zero-mean Gaussian noise In TDOA localization, we use the measurements $r_{i1}, i = 2, 3, \ldots, M$ to estimate source location $\mathbf{u}^o$.

2.3 Taylor-series Method

The basic idea of Taylor-series method [19] is an iterative algorithm to locate the source. It starts with a initial guess and improving the estimation at each step by adding the local linear least-sum square error correction to the previous estimation. Let $\mathbf{u}^o = [x^o, y^o, z^o]^T$ to be the source location. Sensor positions are represented by $\mathbf{S} = [\mathbf{s}_1^T, \ldots, \mathbf{s}_M^T]$ where $\mathbf{s}_i = [x_i, y_i, z_i]^T$ for i=1, ..., M is the sensor position of the i^{th} sensor. The range from source to the i^{th} sensor is

$$r_i^o = \|\mathbf{u}^o - \mathbf{s}_i\| = \sqrt{(x^o - x_i)^2 + (y^o - y_i)^2 + (z^o - z_i)^2} \tag{2.5}$$

Then the true TDOA is related to $\mathbf{u}^o$ by

$$r_{i1}^o = r_i^o - r_1^o, i = 2, 3, \ldots, M. \tag{2.6}$$

Let n_{i1} be TDOA noise for the i^{th} sensor. We represent r_{i1} as

$$r_{i1} = r_{i1}^o + n_{i1}. \tag{2.7}$$

In matrix form

$$\mathbf{f}(\mathbf{u}^o) = \mathbf{T} = \mathbf{M} - \mathbf{E} \tag{2.8}$$

where

$$\mathbf{T} = \begin{bmatrix} r_{21}^o & \ldots & r_{M1}^o \end{bmatrix}^T \tag{2.9}$$

$$\mathbf{M} = \begin{bmatrix} r_{21} & \ldots & r_{M1} \end{bmatrix}^T \tag{2.10}$$

$$\mathbf{E} = \begin{bmatrix} n_{21} & \ldots & n_{M1} \end{bmatrix}^T \tag{2.11}$$

The error term $\mathbf{E}$ has a covariance matrix $\mathbf{Q}$.

$$\mathbf{Q} = E\left[\mathbf{E}\mathbf{E}^T\right] \tag{2.12}$$

If $\mathbf{u}_g$ is the guess value then we can express the true source location $\mathbf{u}^o$ as

$$\mathbf{u} = \mathbf{u}_g + \Delta\mathbf{u} \tag{2.13}$$

We expand $\mathbf{f(u)}$ in Taylor-series

$$\mathbf{f}(\mathbf{u}) \mid_{\mathbf{u}=\mathbf{u}_g} + \mathbf{A}\Delta\mathbf{u} = \mathbf{M} - \mathbf{E} \tag{2.14}$$

where

$$\mathbf{A} = \frac{\partial \mathbf{f}(\mathbf{u})}{\partial \mathbf{u}} = \frac{\partial \mathbf{T}}{\partial \mathbf{u}} \tag{2.15}$$

$$\frac{\partial \mathbf{T}}{\partial \mathbf{u}} = \left[\frac{(\mathbf{u}^o - \mathbf{s}_2)^T}{r_2^o} - \frac{(\mathbf{u}^o - \mathbf{s}_1)^T}{r_1^o}, \ldots, \frac{(\mathbf{u}^o - \mathbf{s}_M)^T}{r_M^o} - \frac{(\mathbf{u}^o - \mathbf{s}_1)^T}{r_1^o} \right] \tag{2.16}$$

(2.14) can be rewritten as

$$\mathbf{A}\Delta\mathbf{u} = \mathbf{W} - \mathbf{E} \tag{2.17}$$

where

$$\mathbf{W} = \mathbf{M} - \mathbf{f}(\mathbf{u}) \mid_{\mathbf{u}=\mathbf{u}_g} \tag{2.18}$$

Choosing $\Delta\mathbf{u}$ that gives least weighted squared error

$$\Delta\mathbf{u} = [\mathbf{A}^T\mathbf{Q}^{-1}\mathbf{A}]^{-1}\mathbf{A}^T\mathbf{Q}^{-1}\mathbf{W} \tag{2.19}$$

We update u_g by replace it with

$$\mathbf{u}_g = \mathbf{u}_g + \Delta\mathbf{u}_g \tag{2.20}$$

Then, we repeat (2.19) and (2.20). The final estimate is obtained when $\mathbf{u}_g$ converges to a stable value and $\Delta\mathbf{u}_g$ goes to zero.

Although the Taylor-series method can provide the least weighted squared error estimator for the TDOA localization problem, it needs a initial guess which is close enough to the source location. Otherwise it can only provide local minimum solution rather than the globe minimum source location.

2.4 Closed-form Two Stage Method

Another approach to solve this localization problem is the closed-form two stage solution proposed by Chan and Ho [20]. The advantage of this method is that no initial guess is needed and it is not iterative. This closed form method reaches CRLB in small noise condition. We will introduce the idea of Chan and Ho's two stage method in this section.

Stage 1:

Let $\mathbf{u}^o = [x^o, y^o, z^o]^T$ to be the source location. The sensor positions are represented by $\mathbf{S} = [\mathbf{s}_1^T, \ldots, \mathbf{s}_M^T]^T$ where $\mathbf{s}_i = [x_i, y_i, z_i]^T$ for i=*1*, …, M is the sensor position of the i^{th}

sensor.

The range from source to the i^{th} sensor is

$$r_i^o = \|\mathbf{u}^o - \mathbf{s}_i\| = \sqrt{(x^o - x_i)^2 + (y^o - y_i)^2 + (z^o - z_i)^2} \tag{2.21}$$

Then the TDOA is

$$r_{i1} = r_i - r_1, i = 2, 3, \ldots, M \tag{2.22}$$

Let n_{i1} be TDOA noise for the i^{th} sensor. $n_{i1} = c\Delta t_{i1}$, where Δt_{i1} is TDOA noise and c is the signal propagation speed. we represent r_{i1} as

$$r_{i1} = r_{i1}^o + n_{i1} \tag{2.23}$$

In absence of noise, TDOA for the i^{th} sensor is

$$r_{i1}^o = r_i^o - r_1^o, i = 2, 3, \ldots, M. \tag{2.24}$$

rewrite (2.24) as

$$r_{i1}^o + r_1^o = r_i^o, i = 2, 3, \ldots, M. \tag{2.25}$$

Squaring both sides, gives

$$r_{i1}^{o2} + 2r_{i1}^o r_1^o + r_1^{o2} = r_i^{o2}. \tag{2.26}$$

Substituting (2.21) into (2.26) and simplifying

$$r_{i1}^{o2} + 2r_{i1}^o r_1^o = \mathbf{s}_i^T\mathbf{s}_i - \mathbf{s}_1^T\mathbf{s}_1 - 2(\mathbf{s}_i - \mathbf{s}_1)^T\mathbf{u}^o \tag{2.27}$$

Expressing $r_{i1}^o = r_{i1} - n_{i1}$ and ignoring n_{i1}^2we have

$$r_{i1}^2 - 2r_{i1}n_{i1} + 2r_{i1}r_1^o - 2r_1^o n_{i1} = \mathbf{s}_i^T\mathbf{s}_i - \mathbf{s}_1^T\mathbf{s}_1 - 2(\mathbf{s}_i - \mathbf{s}_1)^T\mathbf{u}^o \tag{2.28}$$

(2.28) can be rewritten as

$$2r_i^o n_{i1} = r_{i1}^2 - \mathbf{s}_i^T\mathbf{s}_i + \mathbf{s}_1^T\mathbf{s}_1 + 2(\mathbf{s}_i - \mathbf{s}_1)^T\mathbf{u}^o + 2r_{i1}r_1^o \tag{2.29}$$

In matrix form, it can be expressed as

$$\boldsymbol{\epsilon}_1 = \mathbf{B}_1\mathbf{n} = \mathbf{h}_1 - \mathbf{G}_1\boldsymbol{\varphi}_1^o \tag{2.30}$$

where

$$\mathbf{B}_1 = 2\begin{bmatrix} r_2^o & & & \\ & r_3^o & & \\ & & \ddots & \\ & & & r_M^o \end{bmatrix} \tag{2.31}$$

$$\mathbf{h}_1 = \begin{bmatrix} r_{21}^2 - \mathbf{s}_2^T\mathbf{s}_2 + \mathbf{s}_1^T\mathbf{s}_1 \\ \vdots \\ r_{M1}^2 - \mathbf{s}_M^T\mathbf{s}_M + \mathbf{s}_1^T\mathbf{s}_1 \end{bmatrix} \tag{2.32}$$

$$\mathbf{G}_1 = -2\begin{bmatrix} (\mathbf{s}_2 - \mathbf{s}_1)^T & r_{21} \\ \vdots & \\ (\mathbf{s}_M - \mathbf{s}_1)^T & r_{M1} \end{bmatrix} \tag{2.33}$$

$$\mathbf{n} = [n_{21}, \ldots, n_{M1}]^T \tag{2.34}$$

$$\boldsymbol{\varphi}_1^o = \begin{bmatrix} \mathbf{u}^o & r_1^o \end{bmatrix}^T \tag{2.35}$$

In this case, weighted least-square (WLS) technique [33] can be applied and the result is

$$\boldsymbol{\varphi}_1 = (\mathbf{G}_1^T\mathbf{W}_1\mathbf{G}_1)^{-1}\mathbf{G}_1^T\mathbf{W}_1\mathbf{h}_1 \tag{2.36}$$

and the covariance matrix of $\boldsymbol{\varphi}_1$ is

$$cov(\boldsymbol{\varphi}_1) = (\mathbf{G}_1^T\mathbf{W}_1\mathbf{G}_1)^{-1} \tag{2.37}$$

The weighting matrix W is calculated using

$$\mathbf{W}_1 = E[\boldsymbol{\epsilon}_1\boldsymbol{\epsilon}_1^T]^{-1} = (\mathbf{B}_1^T\mathbf{Q}\mathbf{B}_1)^{-1} \tag{2.38}$$

Stage 2:

In Stage 2, we make use r_1 in $\boldsymbol{\varphi}_1$ to refine the estimation of the source location. Let $\boldsymbol{\varphi}_2^o = [(x^o - x_1)^2, (y^o - y_1)^2, (z^o - z_1)^2]^T$

$$(\mathbf{u}^o - \mathbf{s}_1) \odot (\mathbf{u}^o - \mathbf{s}_1) = \boldsymbol{\varphi}_2 \tag{2.39}$$

Since $\boldsymbol{\varphi}_1(1:3)$ is an estimator of $\mathbf{u}^o$, ie $\boldsymbol{\varphi}_1(1:3) = \mathbf{u}^o + \Delta\boldsymbol{\varphi}_1(1:3)$, where $\Delta\varphi_1(1:3)$ is the estimation noise. Thus replacing $\mathbf{u}^o$ in (2.39) by $\boldsymbol{\varphi}_1(1:3) - \Delta\boldsymbol{\varphi}_1(1:3)$

$$(\boldsymbol{\varphi}_1(1:3)^o - \mathbf{s}_1) \odot (\boldsymbol{\varphi}_1(1:3)^o - \mathbf{s}_1) - 2(\boldsymbol{\varphi}_1(1:3)^o - \mathbf{s}_1) \odot \Delta\boldsymbol{\varphi}_1(1:3)^o = (\mathbf{u}^o - \mathbf{s}_1) \odot (\mathbf{u}^o - \mathbf{s}_1) \tag{2.40}$$

or

$$2(\boldsymbol{\varphi}_1(1:3)-\Delta\boldsymbol{\varphi}_1(1:3))\odot\Delta\boldsymbol{\varphi}_1(1:3)=(\boldsymbol{\varphi}_1(1:3)-s_1)\odot(\boldsymbol{\varphi}_1(1:3)-s_1)-(\mathbf{u}^o-\mathbf{s}_1)\odot(\mathbf{u}^o-\mathbf{s}_1) \tag{2.41}$$

where the second order noise $\Delta\boldsymbol{\varphi}_1(1:3)\odot\Delta\boldsymbol{\varphi}_1(1:3)$ has been ignored.

Recall that $\varphi_1(4)=r_1^o+\Delta r_1$, where Δr_i is the estimation noise.

$$(\varphi_1(4)-\Delta\varphi_1(4))^2=(\mathbf{u}^o-\mathbf{s}_1)^T(\mathbf{u}^o-\mathbf{s}_1) \tag{2.42}$$

Expanding the left side and ignoring $\Delta\varphi_1(4)^2$

$$2\varphi_1(4)\Delta\varphi_1(4)=\varphi_1(4)^2-(\mathbf{u}^o-\mathbf{s}_1)^T(\mathbf{u}^o-\mathbf{s}_1) \tag{2.43}$$

We express (2.41) and (2.43) in matrix form

$$\boldsymbol{\epsilon}_2=\mathbf{B}_2\Delta\boldsymbol{\varphi}_1=\mathbf{h}_2-\mathbf{G}_2\boldsymbol{\varphi}_2 \tag{2.44}$$

where

$$\mathbf{B}_2=2\begin{bmatrix} diag(\mathbf{u}^o-\mathbf{s}_1) & \\ & r_1^o \end{bmatrix} \tag{2.45}$$

$$\mathbf{h}_2=\begin{bmatrix} (\boldsymbol{\varphi}_1(1:3)-\mathbf{s}_1)\odot(\boldsymbol{\varphi}_1(1:3)-\mathbf{s}_1) \\ \varphi_1(4)^2 \end{bmatrix} \tag{2.46}$$

$$\mathbf{G}_2=\begin{bmatrix} 1 & 0 & 0 \\ 0 & 1 & 0 \\ 0 & 0 & 1 \\ 1 & 1 & 1 \end{bmatrix} \tag{2.47}$$

The WLS solution for stage 2 is

$$\boldsymbol{\varphi}_2=(\mathbf{G}_2^T\mathbf{W}_2\mathbf{G}_2)^{-1}\mathbf{G}_2^T\mathbf{W}_2\mathbf{h}_2 \tag{2.48}$$

The covariance matrix of φ_2 is

$$cov(\boldsymbol{\varphi}_2)=(\mathbf{G}_2^T\mathbf{W}_2\mathbf{G}_2)^{-1} \tag{2.49}$$

where the weighting matrix is $\mathbf{W}_2=E[\boldsymbol{\epsilon}_2\boldsymbol{\epsilon}_2^T]^{-1}=[\mathbf{B}_2 cov(\boldsymbol{\varphi}_1)\mathbf{B}_2^T]^{-1}$.

The source location estimate $\mathbf{u}=[x,y,z]^T$ can be obtained from $\boldsymbol{\varphi}_2$

$$\mathbf{u}=\mathbf{P}[\sqrt{\boldsymbol{\varphi}_2(1)},\sqrt{\boldsymbol{\varphi}_2(2)},\sqrt{\boldsymbol{\varphi}_2(3)}]^T+\mathbf{s}_1 \tag{2.50}$$

where

$$\mathbf{P} = diag[sgn(\boldsymbol{\varphi}_1(1) - x_1), sgn(\boldsymbol{\varphi}_1(2) - y_1), sgn(\boldsymbol{\varphi}_1(3) - z_1)]. \tag{2.51}$$

According to (2.50), subtracting both sides by $\mathbf{s}_1$, squaring and taking differential,

$$\Delta\mathbf{u} = \mathbf{B}_3^{-1}\Delta\boldsymbol{\varphi}_2 \tag{2.52}$$

where

$$\mathbf{B}_3 = 2\begin{bmatrix} x^o - x_1 & & \\ & y^o - y_1 & \\ & & z^o - z_1 \end{bmatrix} \tag{2.53}$$

The covariance matrix of the final source position estimator is

$$cov(\mathbf{u}) = \mathbf{B}_3^{-1} cov(\boldsymbol{\varphi}_2)\mathbf{B}_3^{-T} \tag{2.54}$$

2.5 Summary

In this chapter, we introduce the basic idea of CRLB, which is a benchmark of optimal variance for any unbiased estimator. Taylor series[4] and Chan and Ho's method[3], the two source localization method, are also introduced in this chapter. Taylor series needs initial guess and only converge to the local minimum solution and Chan and Ho's method needs small noise condition.

Chapter 3

Cramer-Rao lower Bound(CRLB)

Cramer-Rao lower Bound(CRLB) provides a lower bound on the variance of any unbiased estimator. It gives optimal variance and alerts us it is impossible to find an unbiased estimator whose variance is less than the bound.

In this chapter, we will construct mathematic models for manifold sensor uncertainties, clock-bias error and the presence of the two kinds of uncertainties. Cramer-Rao lower Bound of the source location estimate under manifold sensor uncertainties, clock-bias error and the both kind of error will be derived according to the mathematic models.

3.1 CRLB Due to Measurement noise only

We will derive CRLB for TDOA source localization when the noise appear in TDOA measurements only.

Let $\mathbf{u}^o = [x^o, y^o, z^o]^T$ to be the source location. Sensor positions are represented by $\mathbf{S} = [\mathbf{s}_1^T, \ldots, \mathbf{s}_M^T]^T$ where $\mathbf{s}_i = [x_i, y_i, z_i]^T$ for i=*1*, ..., M is the sensor position of the i^{th} sensor.

The r_i^o is the range from source to the i^{th} sensor. If we choose sensor 1 as reference and denote range difference of r_i^o and r_1^o as $r_{i1}^o = r_i^o - r_1^o$, the TDOA measurement sensor i and sensor 1 is

$$r_{i1} = r_{i1}^o + n_{i1} \tag{3.1}$$

where n_{i1} is the measurement noise that is assumed as zero mean Gaussian. Let us collect *(M-1)* TDOA measurements as $\mathbf{r} = [r_{21}, r_{31}, \ldots, r_{M1}]^T$. The pdf of r parameterized on $\mathbf{u}^o$ is

$$p(\mathbf{r}; \mathbf{u}^o) = (\frac{1}{\sqrt{2\pi}})^{M-1} \frac{1}{|\mathbf{Q}_r|^{\frac{1}{2}}} \exp\{-\frac{1}{2}(\mathbf{r} - \mathbf{r}^o)^T \mathbf{Q}_r^{-1}(\mathbf{r} - \mathbf{r}^o)\} \tag{3.2}$$

where $\mathbf{Q}_r$ is the covariance matrix of measurement noise and $\mathbf{r}^o = [r_{21}^o, r_{31}^o, \ldots, r_{M1}^o]^T$.

As mentioned in Chapter 2, if the pdf satisfies,

$$E\left[\frac{\partial lnp(\mathbf{r};\mathbf{u}^o)}{\partial \mathbf{u}^o}\right] = 0 \tag{3.3}$$

Then the variance of any unbiased estimator $\mathbf{u}$ of $\mathbf{u}^o$ must satisfy

$$CRLB(\mathbf{u}) \geq \left(-E\left[\frac{\partial^2 lnp(\mathbf{r};\mathbf{u}^o)}{\partial \mathbf{u}^o \partial \mathbf{u}^{oT}}\right]\right)^{-1} \tag{3.4}$$

To obtain CRLB, first we calculate $lnp(\mathbf{r}; \mathbf{u})$

$$lnp(\mathbf{r}; \mathbf{u}^o) = -\frac{M-1}{2} ln(2\pi) - \frac{1}{2} ln|\mathbf{Q}_r| - \frac{1}{2}(\mathbf{r} - \mathbf{r}^o)^T \mathbf{Q}_r^{-1}(\mathbf{r} - \mathbf{r}^o) \tag{3.5}$$

The expectation of first order derivative of $lnp(\mathbf{r}; \mathbf{u}^o)$ is

$$E\left[\frac{\partial lnp(\mathbf{r};\mathbf{u}^o)}{\partial \mathbf{u}^o}\right] = E\left[-\frac{1}{2}(\frac{\partial \mathbf{r}^o}{\partial \mathbf{u}^o})^T \mathbf{Q}_r^{-1}(\mathbf{r} - \mathbf{r}^o) - \frac{1}{2}(\mathbf{r} - \mathbf{r}^o)^T \mathbf{Q}_r^{-1}(\frac{\partial \mathbf{r}^o}{\partial \mathbf{u}^o})\right] = 0 \tag{3.6}$$

So that (3.3) is satisfied.

$$cov(\mathbf{u}) \geq \left(-E\left[\frac{\partial^2 lnp(\mathbf{r};\mathbf{u})}{\partial \mathbf{u}^o \partial \mathbf{u}^{oT}}\right]\right)^{-1} \tag{3.7}$$

where

$$E\left[\frac{\partial^2 lnp(\mathbf{r};\mathbf{u})}{\partial \mathbf{u}^o \partial \mathbf{u}^{oT}}\right] = (\frac{\partial \mathbf{r}^o}{\partial \mathbf{u}^o})^T \mathbf{Q}_r^{-1}(\frac{\partial \mathbf{r}^o}{\partial \mathbf{u}^o}) \tag{3.8}$$

and

$$\frac{\partial \mathbf{r}^o}{\partial \mathbf{u}^o} = \left[\frac{(\mathbf{u}-\mathbf{s}_2)}{r_2^o} - \frac{(\mathbf{u}^o-\mathbf{s}_1)}{r_1^o}, \ldots, \frac{(\mathbf{u}^o-\mathbf{s}_M)}{r_M^o} - \frac{(\mathbf{u}^o-\mathbf{s}_1)}{r_1^o}\right]^T \tag{3.9}$$

3.2 CRLB for TDOA Source Localization in the Presence of Measurement noise and Manifold Sensor Uncertainties

In this section, we will discuss mathematic model of TDOA Source Localization in the presence of Manifold Sensor Uncertainties in addition to measurement noise. CRLB for TDOA source

localization will be obtained based on that model.

In the case of sensor manifold error, the position error of different sensors are related to each other. Let p be a random vector of length L where $L \leq 3M$. Then we model the sensor position vector as

$$\begin{aligned} \mathbf{s} &= \mathbf{s}^o + \mathbf{V}\mathbf{p} && (3.10) \\ &= \begin{bmatrix} \mathbf{s}_1^o \\ \vdots \\ \mathbf{s}_M^o \end{bmatrix} + \begin{bmatrix} \mathbf{V}_1 \\ \vdots \\ \mathbf{V}_M \end{bmatrix}_{3M \times L} \mathbf{p}_{L \times 1} && (3.11) \end{aligned}$$

where $\mathbf{V} = [\mathbf{V}_1^T, \ldots, \mathbf{V}_M^T]^T$ is a known matrix. $\mathbf{v}_i$ is transformation matrix which shows the relation between random vector $\mathbf{p}$ and the position uncertainties of the i^{th} sensor. If $\mathbf{V}$ is a $3M \times 3M$ identity matrix and $\mathbf{p}$ is a $3M \times 1$ random vector, the manifold sensor position uncertainties become independent uncertainties. f is assumed to be zero mean Gaussian.

We take both measurement noise and sensor position manifold uncertainties into account in deriving the CRLB. The unknown source position is $\mathbf{u}^o = [x^o, y^o, z^o]^T$, the measurement vector is $\mathbf{x} = [\mathbf{r}^T, \mathbf{p}^T]^T$ and the unknown parameter vector is $\boldsymbol{\theta}^o = [\mathbf{u}^{oT}, \mathbf{p}^T]^T$.

The pdf of $\mathbf{x}$ can be written as

$$\begin{aligned} \mathbf{p}(\mathbf{x};\boldsymbol{\theta}) &= (\frac{1}{\sqrt{2\pi}})^{M-1} \frac{1}{|\mathbf{Q}_r|^{\frac{1}{2}}} \exp\{-\frac{1}{2}(\mathbf{r}-\mathbf{r}^o)^T \mathbf{Q}_r^{-1}(\mathbf{r}-\mathbf{r}^o)\} \\ &\cdot(\frac{1}{\sqrt{2\pi}})^{L} \frac{1}{|\mathbf{Q}_p|^{\frac{1}{2}}} \exp\{-\frac{1}{2}\mathbf{p}^T \mathbf{Q}_r^{-1}\mathbf{p}\} \end{aligned} \quad (3.12)$$

Thus

$$lnp(\mathbf{x};\boldsymbol{\theta}) = -\frac{M-1}{2}ln(2\pi) - \frac{1}{2}ln|\mathbf{Q}_r| - \frac{1}{2}(\mathbf{r}-\mathbf{r}^o)^T\mathbf{Q}_r^{-1}(\mathbf{r}-\mathbf{r}^o) - \frac{L}{2}ln(2\pi) - \frac{1}{2}ln|\mathbf{Q}_p| - \frac{1}{2}\mathbf{p}^T\mathbf{Q}_r^{-1}\mathbf{p} \quad (3.13)$$

The expectation of first order derivative of nature logarithm of the pdf is

$$\begin{aligned} E\left[\frac{\partial lnp(\mathbf{x};\boldsymbol{\theta})}{\partial \boldsymbol{\theta}}\right] &= E\begin{bmatrix} \frac{\partial lnp(\mathbf{x};\boldsymbol{\theta})}{\partial \mathbf{u}^o} \\ \frac{\partial lnp(\mathbf{x};\boldsymbol{\theta})}{\partial \mathbf{p}} \end{bmatrix} \\ &= E\begin{bmatrix} -(\frac{\partial \mathbf{r}^o}{\partial \mathbf{u}^o})^T \mathbf{Q}_r^{-1}(\mathbf{r}-\mathbf{r}^o) \\ -\mathbf{Q}_p^{-1}\mathbf{p} \end{bmatrix} = 0 \end{aligned} \quad (3.14)$$

and (3.3) is satisfied. Thus the CRLB of $\boldsymbol{\theta}$ is

$$cov(\boldsymbol{\theta}) \geq \left(-E\left[\frac{\partial^2 ln\mathbf{p}(\mathbf{x};\boldsymbol{\theta})}{\partial\boldsymbol{\theta}\partial\boldsymbol{\theta}^T} \right] \right)^{-1} \tag{3.15}$$

where

$$E\left[\frac{\partial^2 lnp(\mathbf{x};\boldsymbol{\theta})}{\partial\boldsymbol{\theta}\partial\boldsymbol{\theta}^T} \right] = E\begin{bmatrix} \frac{\partial^2 lnp(\mathbf{x};\boldsymbol{\theta})}{\partial\mathbf{u}^o\partial\mathbf{u}^{oT}} & \frac{\partial^2 lnp(\mathbf{x};\boldsymbol{\theta})}{\partial\mathbf{u}^o\partial\mathbf{p}^T} \\ \frac{\partial^2 lnp(\mathbf{x};\boldsymbol{\theta})}{\partial\mathbf{p}\partial\mathbf{u}^{oT}} & \frac{\partial^2 lnp(\mathbf{x};\boldsymbol{\theta})}{\partial\mathbf{p}\partial\mathbf{p}^T} \end{bmatrix} \tag{3.16}$$

The partial derivatives in (3.16) are

$$E\left[\frac{\partial^2 ln\mathbf{p}(\mathbf{x};\boldsymbol{\theta})}{\partial\mathbf{u}^o\partial\mathbf{u}^{oT}} \right] = (\frac{\partial\mathbf{r}^o}{\partial\mathbf{u}})^T\mathbf{Q}_r^{-1}(\frac{\partial\mathbf{r}^o}{\partial\mathbf{u}}) \tag{3.17}$$

$$E\left[\frac{\partial^2 ln\mathbf{p}(\mathbf{x};\boldsymbol{\theta})}{\partial\mathbf{u}^o\partial\mathbf{p}^T} \right] = (\frac{\partial\mathbf{r}^o}{\partial\mathbf{u}^o})^T\mathbf{Q}_r^{-1}(\frac{\partial\mathbf{r}^o}{\partial\mathbf{p}}) \tag{3.18}$$

$$E\left[\frac{\partial^2 ln\mathbf{p}(\mathbf{x};\boldsymbol{\theta})}{\partial\mathbf{p}\partial\mathbf{u}^{oT}} \right] = (\frac{\partial\mathbf{r}^o}{\partial\mathbf{p}})^T\mathbf{Q}_r^{-1}(\frac{\partial\mathbf{r}^o}{\partial\mathbf{u}^o}) \tag{3.19}$$

$$E\left[\frac{\partial^2 ln\mathbf{p}(\mathbf{x};\boldsymbol{\theta})}{\partial\mathbf{p}\partial\mathbf{p}^T} \right] = (\frac{\partial\mathbf{r}^o}{\partial\mathbf{p}})^T\mathbf{Q}_r^{-1}(\frac{\partial\mathbf{r}^o}{\partial\mathbf{p}}) + \mathbf{Q}_p \tag{3.20}$$

where $\mathbf{Q}_r$ is covariance matrix of measurement noise vector $\mathbf{n}$ and $\mathbf{Q}_p$ is the covariance of random vector $\mathbf{p}$.

$$\frac{\partial\mathbf{r}^o}{\partial\mathbf{u}} = \left[\frac{(\mathbf{u}^o-\mathbf{s}_2)}{r_2^o} - \frac{(\mathbf{u}^o-\mathbf{s}_1)}{r_1^o}, \ldots, \frac{(\mathbf{u}^o-\mathbf{s}_M)}{r_M^o} - \frac{(\mathbf{u}^o-\mathbf{s}_1)}{r_1^o} \right]^T \tag{3.21}$$

$$\frac{\partial\mathbf{r}^o}{\partial\mathbf{p}} = \left[\left(\frac{(\mathbf{u}^o-\mathbf{s}_2)^T\mathbf{V}_2}{r_2^o} - \frac{(\mathbf{u}^o-\mathbf{s}_1)^T\mathbf{V}_1}{r_1^o} \right)^T, \ldots, \left(\frac{(\mathbf{u}^o-\mathbf{s}_M)^T\mathbf{V}_M}{r_M^o} - \frac{(\mathbf{u}^o-\mathbf{s}_1)^T\mathbf{V}_1}{r_1^o} \right)^T \right]^T \tag{3.22}$$

In this study, we are interested only in CRLB of the source position u. It is the upper 3×3 block of $CRLB(\boldsymbol{\theta})$ Denote the four block matrix in (3.16) as

$$E\left[\frac{\partial^2 ln\mathbf{p}(\mathbf{x};\boldsymbol{\theta})}{\partial\boldsymbol{\theta}\partial\boldsymbol{\theta}^T} \right] \quad \begin{bmatrix} E\left[\frac{\partial^2 ln\mathbf{p}(\mathbf{x};\boldsymbol{\theta})}{\partial\mathbf{u}^o\partial\mathbf{u}^{oT}} \right] & E\left[\frac{\partial^2 ln\mathbf{p}(\mathbf{x};\boldsymbol{\theta})}{\partial\mathbf{u}^o\partial\mathbf{p}^T} \right] \\ E\left[\frac{\partial^2 ln\mathbf{p}(\mathbf{x};\boldsymbol{\theta})}{\partial\mathbf{p}\partial\mathbf{u}^{oT}} \right] & E\left[\frac{\partial^2 ln\mathbf{p}(\mathbf{x};\boldsymbol{\theta})}{\partial\mathbf{p}\partial\mathbf{p}^T} \right] \end{bmatrix} \tag{3.23}$$

$$= \begin{bmatrix} \mathbf{X} & \mathbf{Y} \\ \mathbf{Y}^T & \mathbf{Z} \end{bmatrix} \tag{3.24}$$

According to the inverse of block matrix, X^{-1} is

$$CRLB(\mathbf{u}) = (\mathbf{X} - \mathbf{Y}\mathbf{Z}^{-1}\mathbf{X}^T)^{-1} \tag{3.25}$$

$$= \mathbf{X}^{-1} + \mathbf{X}^{-1}\mathbf{Y}(\mathbf{Z} - \mathbf{Y}^T\mathbf{X}^{-1}\mathbf{Y})^{-1}\mathbf{Y}^T\mathbf{X}^{-1} \tag{3.26}$$

In this section, CRLB in presence of manifold sensor position uncertainties in TDOA localization system is derived. It provide a benchmark for the performance of a estimator for the source location when the measurement noise and manifold sensor position uncertainties are presented.

3.3 CRLB for TDOA Source Localization in the Presence of Measurement Error and Clock-bias Uncertainties

In this section, we first derive mathematic model of TDOA source localization in the presence of clock-bias error. The CRLB of the source localization in the presence of clock-bias error will be obtained using that model.

The unknown source position is $\mathbf{u}^o = [x^o, y^o, z^o]^T$ and the known sensor position is $\mathbf{s}_i = [x_i, y_i, z_i]^T$.

Let us further assume that the sensor array can be decomposed into N sub-arrays. Within each sub-array the sensors are synchronized with the same clocks. However, the clocks among different sub-arrays are not synchronized and have clock bias $\delta_j, j = 2, 3, \ldots, N$ with respect to the first sub-array. Let us choose the first sensor as reference for TDOA measurements.

The TDOA measurements

$$\begin{aligned} r_{i1} &= \| \mathbf{u}^o - \mathbf{s}_i \| - \| \mathbf{u}^o - \mathbf{s}_1 \| + n_{i1}, i = 2, \ldots, m_1 \\ r_{i1} &= \| \mathbf{u}^o - \mathbf{s}_i \| - \| \mathbf{u}^o - \mathbf{s}_1 \| + \boldsymbol{\delta}_2^o + n_{i1}, i = m_1 + 1, \ldots, m_2 \\ &\cdots \\ r_{i1} &= \| \mathbf{u}^o - \mathbf{s}_i \| - \| \mathbf{u}^o - \mathbf{s}_1 \| + \boldsymbol{\delta}_N^o + n_{i1}, i = m_{N-1} + 1, \ldots, m_N \end{aligned} \tag{3.27}$$

where $\boldsymbol{\delta} = [\delta_2, \ldots, \delta_N]^T$ is the clock-bias vector. we shall assume in this study δ is deterministic and not random. $\{\mathbf{s}_1, \ldots, \mathbf{s}_{m_1}\}$, $\{\mathbf{s}_{m_1+1}, \ldots, \mathbf{s}_{m_2}\}$, $\ldots$, $\{\mathbf{s}_{m_{n-1}+1}, \ldots, \mathbf{s}_{m_n}\}$ are different sub-arrays.

We can write the TDOA measurements in vector form as

$$\mathbf{r} = \mathbf{r}^o + \mathbf{n} + \mathbf{F}\boldsymbol{\delta}^o \tag{3.28}$$

where $\mathbf{r} = [r_{21}, \ldots, r_{M_N,1}]^T$, $\mathbf{n} = [n_{21}, \ldots, n_{M_N,1}]^T$ and

$$\mathbf{F} = \begin{bmatrix} \overbrace{0, \ldots, 0}^{m_1-1}, \overbrace{1, \ldots, 1}^{m_2-m_1}, 0, \ldots, 0 \\ 0, \ldots, 0, 1, \ldots, 1, 0, \ldots, 0 \\ \cdots \\ \overbrace{0, \ldots, \ldots, \ldots, 0}^{m_{N-1}+1}, \overbrace{1, \ldots, 1}^{m_N-m_{N-1}} \end{bmatrix}^T \tag{3.29}$$

Denote the unknown parameter vector be $\boldsymbol{\theta}^o = [\mathbf{u}^o, \boldsymbol{\delta}^o]^T$ and the measurement vector be $\mathbf{x} = \mathbf{r}$, the pdf in the presence of measurement noise and clock-bias error is

$$p(\mathbf{x}; \boldsymbol{\theta}^o) = (\frac{1}{\sqrt{2\pi}})^{M-1} \frac{1}{|\mathbf{Q}_r|^{\frac{1}{2}}} \exp\{-\frac{1}{2}(\mathbf{r} - \mathbf{r}^o - \mathbf{F}\boldsymbol{\delta}^o)^T \mathbf{Q}_r^{-1}(\mathbf{r} - \mathbf{r}^o - \mathbf{F}\boldsymbol{\delta}^o)\} \tag{3.30}$$

The natural logarithm of the pdf is

$$lnp(\mathbf{x}; \theta) = -\frac{M-1}{2} ln(2\pi) - \frac{1}{2} ln|\mathbf{Q}_r| - \frac{1}{2}(\mathbf{r} - \mathbf{r}^o - \mathbf{F}\boldsymbol{\delta}^o)^T \mathbf{Q}_r^{-1}(\mathbf{r} - \mathbf{r}^o - \mathbf{F}\boldsymbol{\delta}^o) \tag{3.31}$$

Taking expectation of the nature logarithm of the PDF,

$$\begin{aligned} E\left[\frac{\partial lnp(\mathbf{x};\boldsymbol{\theta})}{\partial \boldsymbol{\theta}}\right] &= E\begin{bmatrix} \frac{\partial lnp(\mathbf{x};\boldsymbol{\theta})}{\partial \mathbf{u}^o} \\ \frac{\partial lnp(\mathbf{x};\boldsymbol{\theta})}{\partial \boldsymbol{\delta}^o} \end{bmatrix} \\ &= E\begin{bmatrix} -(\frac{\partial \mathbf{r}^o}{\partial \mathbf{u}^o})^T \mathbf{Q}_r^{-1}(\mathbf{r} - \mathbf{r}^o - \mathbf{F}\boldsymbol{\delta}^o) \\ -\mathbf{F}^T \mathbf{Q}_r^{-1}(\mathbf{r} - \mathbf{r}^o - \mathbf{F}\boldsymbol{\delta}^o) \end{bmatrix} \qquad (3.32) \\ &= 0 \qquad (3.33) \end{aligned}$$

and (3.3) is satisfied.

$$CRLB(\boldsymbol{\theta}^o) \geq \left(-E\left[\frac{\partial^2 lnp(\mathbf{x};\boldsymbol{\theta})}{\partial \boldsymbol{\theta} \partial \boldsymbol{\theta}^T}\right]\right)^{-1} \tag{3.34}$$

where

$$E\left[\frac{\partial^2 lnp(\mathbf{x};\boldsymbol{\theta})}{\partial \boldsymbol{\theta} \partial \boldsymbol{\theta}^T}\right] = E\begin{bmatrix} \frac{\partial^2 lnp(\mathbf{x};\boldsymbol{\theta})}{\partial \mathbf{u}^o \partial \mathbf{u}^{oT}} & \frac{\partial^2 lnp(\mathbf{x};\boldsymbol{\theta})}{\partial \mathbf{u} \partial \boldsymbol{\delta}^{oT}} \\ \frac{\partial^2 lnp(\mathbf{x};\boldsymbol{\theta})}{\partial \boldsymbol{\delta}^o \partial \mathbf{u}^{oT}} & \frac{\partial^2 lnp(\mathbf{x};\boldsymbol{\theta})}{\partial \boldsymbol{\delta}^o \partial \boldsymbol{\delta}^{oT}} \end{bmatrix} \tag{3.35}$$

The partial derivatives in (3.35) are

$$E\left[\frac{\partial^2 lnp(\mathbf{x};\boldsymbol{\theta})}{\partial \mathbf{u}^o \partial \mathbf{u}^{oT}}\right] = (\frac{\partial \mathbf{r}^o}{\partial \mathbf{u}^o})^T \mathbf{Q}_r^{-1} (\frac{\partial \mathbf{r}^o}{\partial \mathbf{u}^o}) \tag{3.36}$$

$$E\left[\frac{\partial^2 lnp(\mathbf{x};\boldsymbol{\theta})}{\partial \mathbf{u}^o \partial \boldsymbol{\delta}^{oT}}\right] = (\frac{\partial \mathbf{r}^o}{\partial \mathbf{u}^o})^T \mathbf{Q}_r^{-1} \mathbf{F} \tag{3.37}$$

$$E\left[\frac{\partial^2 lnp(\mathbf{x};\boldsymbol{\theta})}{\partial \boldsymbol{\delta}^o \partial \mathbf{u}^{oT}}\right] = \mathbf{F}^T \mathbf{Q}_r^{-1} (\frac{\partial \mathbf{r}^o}{\partial \mathbf{u}^o}) \tag{3.38}$$

$$E\left[\frac{\partial^2 lnp(\mathbf{x};\boldsymbol{\theta})}{\partial \boldsymbol{\delta}^o \partial \boldsymbol{\delta}^{oT}}\right] = \mathbf{F}^T \mathbf{Q}_r^{-1} \mathbf{F} \tag{3.39}$$

where $\mathbf{Q}_r$ is covariance matrix of measurement noise vector $\mathbf{n}$, and

$$\frac{\partial \mathbf{r}^o}{\partial \mathbf{u}^o} = \left[\frac{(\mathbf{u}-\mathbf{s}_2)}{r_2^o} - \frac{(\mathbf{u}-\mathbf{s}_1)}{r_1^o}, \ldots, \frac{(\mathbf{u}-\mathbf{s}_M)}{r_M^o} - \frac{(\mathbf{u}-\mathbf{s}_1)}{r_1^o}\right]^T. \tag{3.40}$$

We are interested in the source position $\mathbf{u}^o$. The CRLB of the source position $\mathbf{u}$ is the upper left 3×3 block of $CRLB(\boldsymbol{\theta}^o)$. Denote

$$E\left[\frac{\partial^2 ln\mathbf{p}(\mathbf{x};\boldsymbol{\theta})}{\partial\boldsymbol{\theta}\partial\boldsymbol{\theta}^T}\right] = \begin{bmatrix} E\left[\frac{\partial^2 ln\mathbf{p}(\mathbf{x};\boldsymbol{\theta})}{\partial\mathbf{u}^o\partial\mathbf{u}^{oT}}\right] & E\left[\frac{\partial^2 ln\mathbf{p}(\mathbf{x};\boldsymbol{\theta})}{\partial\mathbf{u}^o\partial\boldsymbol{\delta}^{oT}}\right] \\ E\left[\frac{\partial^2 ln\mathbf{p}(\mathbf{x};\boldsymbol{\theta})}{\partial\boldsymbol{\delta}^o\partial\mathbf{u}^{oT}}\right] & E\left[\frac{\partial^2 ln\mathbf{p}(\mathbf{x};\boldsymbol{\theta})}{\partial\boldsymbol{\delta}^o\partial\boldsymbol{\delta}^{oT}}\right] \end{bmatrix} \tag{3.41}$$

$$= \begin{bmatrix} \mathbf{X} & \mathbf{Y} \\ \mathbf{Y}^T & \mathbf{Z} \end{bmatrix} \tag{3.42}$$

According to the block matrix inversion formular, $CRLB(\mathbf{u}^o)$

$$CRLB(\mathbf{u}^o) = (\mathbf{X} - \mathbf{Y}\mathbf{Z}^{-1}\mathbf{X}^T)^{-1} \tag{3.43}$$

$$= \mathbf{X}^{-1} + \mathbf{X}^{-1}\mathbf{Y}(\mathbf{Z} - \mathbf{Y}^T\mathbf{X}^{-1}\mathbf{Y})^{-1}\mathbf{Y}^T\mathbf{X}^{-1} \tag{3.44}$$

In this section, the CRLB for the TDOA source localization problem which contains clock-bias error is derived. It provides the minimum achievable variance of an estimator for source location in the presence of measurement noise and clock-bias error.

3.4 CRLB for TDOA Source Localization in the Presence of Combination of manifold and Clock-bias Uncertainties

In this section, we shall consider the presence of all three kinds of errors in estimating the source position. We shall started by construct a mathematic model for the measurement and sensor positions. Then,we will derive the CRLB using the models.

The measurement vector is $\mathbf{x} = [\mathbf{r}^T, \mathbf{p}^T]^T$ and the unknown parameter vector is $\boldsymbol{\theta}^o = [\mathbf{u}^{oT}, \mathbf{p}^T, \boldsymbol{\delta}^{oT}]^T$. Following Section 3.2, the sensor position vector is modeled as

$$\mathbf{s} = \mathbf{s}^o + \mathbf{V}\mathbf{p} \tag{3.45}$$

$$= \begin{bmatrix} \mathbf{s}_1^o \\ \vdots \\ \mathbf{s}_M^o \end{bmatrix} + \begin{bmatrix} \mathbf{V}_1 \\ \vdots \\ \mathbf{V}_M \end{bmatrix}_{3M\times L} \mathbf{p}_{L\times 1} \tag{3.46}$$

where $\mathbf{p}$ is a zero-mean Gaussian random vector, $\mathbf{V} = [\mathbf{V}_1^T, \ldots, \mathbf{V}_M^T]^T$ and $\mathbf{V}_i$ is transformation matrix which shows the relation between random vector $\mathbf{p}$ and the position uncertainties of i^{th} sensor.

From Section 3.3, TDOA measurements are

$$\begin{aligned} r_{i1} &= \| \mathbf{u}^o - \mathbf{s}_i \| - \| \mathbf{u}^o - \mathbf{s}_1 \| + n_{i1}, i = 1, \ldots, m_1 \\ r_{i1} &= \| \mathbf{u}^o - \mathbf{s}_i \| - \| \mathbf{u}^o - \mathbf{s}_1 \| + \boldsymbol{\delta}_2^o + n_{i1}, i = m_1 + 1, \ldots, m_2 \\ r_{i1} &= \| \mathbf{u}^o - \mathbf{s}_i \| - \| \mathbf{u}^o - \mathbf{s}_1 \| + \boldsymbol{\delta}_N^o + n_{i1}, i = m_{N-1} + 1, \ldots, m_N \end{aligned} \tag{3.47}$$

Or in vector form,

$$\mathbf{r} = \mathbf{r}^o + \mathbf{n} + \mathbf{F}\boldsymbol{\delta}^o \tag{3.48}$$

where $\mathbf{r} = [r_{21}, \ldots, r_{M_N,1}]$ and

$$\mathbf{F} = \begin{bmatrix} \overbrace{0, \ldots, 0}^{m_1-1}, \overbrace{1, \ldots, 1}^{m_2-m_1}, 0, \ldots, 0 \\ 0, \ldots, 0, 1, \ldots, 1, 0, \ldots, 0 \\ \cdots \\ \overbrace{0, \ldots, \ldots, \ldots, 0}^{m_{N-1}+1}, \overbrace{1, \ldots, 1}^{m_N - m_{N-1}} \end{bmatrix}^T \tag{3.49}$$

where $\boldsymbol{\delta}^o = [\delta_2^o, \ldots, \delta_N^o]^T$ is the clock-bias.

The pdf of $\mathbf{x}$ is

$$\begin{aligned} p(\mathbf{x}; \boldsymbol{\theta}^o) &= (\frac{1}{\sqrt{2\pi}})^{M-1} \frac{1}{|\mathbf{Q}_r|^{\frac{1}{2}}} \exp\{-\frac{1}{2}(\mathbf{r} - \mathbf{r}^o - \mathbf{F}\boldsymbol{\delta}^o)^T \mathbf{Q}_r^{-1} (\mathbf{r} - \mathbf{r}^o - \mathbf{F}\boldsymbol{\delta}^o)\} \\ &\cdot (\frac{1}{\sqrt{2\pi}})^L \frac{1}{|\mathbf{Q}_p|^{\frac{1}{2}}} \exp\{-\frac{1}{2}\mathbf{p}^T \mathbf{Q}_p^{-1} \mathbf{p}\} \end{aligned} \tag{3.50}$$

Thus, the nature logarithm of $p(x; \theta)$

$$\begin{aligned} ln\mathbf{p}(\mathbf{x}; \boldsymbol{\theta}) &= -\frac{M-1}{2} ln(2\pi) - \frac{1}{2} ln|\mathbf{Q}_r| - \frac{1}{2}(\mathbf{r} - \mathbf{r}^o - \mathbf{F}\boldsymbol{\delta}^o)^T \mathbf{Q}_r^{-1} (\mathbf{r} - \mathbf{r}^o - \mathbf{F}\boldsymbol{\delta}^o) \\ &- \frac{L}{2} ln(2\pi) - \frac{1}{2} ln|\mathbf{Q}_p| - \frac{1}{2}\mathbf{p}^T \mathbf{Q}_p^{-1} \mathbf{p} \end{aligned} \tag{3.51}$$

Expectation of first order derivative of nature logarithm of the PDF is

$$\begin{aligned} E\left[\frac{\partial lnp(\mathbf{x};\boldsymbol{\theta}^o)}{\partial \boldsymbol{\theta}^o}\right] &= E\begin{bmatrix} \frac{\partial lnp(\mathbf{x};\boldsymbol{\theta}^o)}{\partial \mathbf{u}^o} \\ \frac{\partial lnp(\mathbf{x};\boldsymbol{\theta}^o)}{\partial \mathbf{p}} \\ \frac{\partial lnp(\mathbf{x};\boldsymbol{\theta}^o)}{\partial \boldsymbol{\delta}^o} \end{bmatrix} \\ &= E\begin{bmatrix} -(\frac{\partial \mathbf{r}^o}{\partial \mathbf{u}^o})^T\mathbf{Q}_r^{-1}(\mathbf{r}-\mathbf{r}^o-\mathbf{F}\boldsymbol{\delta}^o) \\ -\mathbf{Q}_p^{-1}\mathbf{p} \\ -\mathbf{F}^T\mathbf{Q}_r^{-1}(\mathbf{r}-\mathbf{r}^o-\mathbf{F}\boldsymbol{\delta}^o) \end{bmatrix} \\ &= \mathbf{0} \end{aligned} \tag{3.52}$$

and (3.3) is satisfied. Thus

$$CRLB(\boldsymbol{\theta}^o) \geq \left(-E\left[\frac{\partial^2 lnp(\mathbf{x};\boldsymbol{\theta}^o)}{\partial \boldsymbol{\theta}^o \partial \boldsymbol{\theta}^{oT}}\right]\right)^{-1} \tag{3.53}$$

where

$$E\left[\frac{\partial^2 lnp(\mathbf{x};\boldsymbol{\theta}^o)}{\partial \boldsymbol{\theta}^o \partial \boldsymbol{\theta}^{oT}}\right] = E\begin{bmatrix} \frac{\partial^2 lnp(\mathbf{x};\boldsymbol{\theta}^o)}{\partial \mathbf{u}^o \partial \mathbf{u}^{oT}} & \frac{\partial^2 lnp(\mathbf{x};\boldsymbol{\theta}^o)}{\partial \mathbf{u}^o \partial \mathbf{p}^T} & \frac{\partial^2 lnp(\mathbf{x};\boldsymbol{\theta}^o)}{\partial \mathbf{u}^o \partial \delta^{oT}} \\ \frac{\partial^2 lnp(\mathbf{x};\boldsymbol{\theta}^o)}{\partial \mathbf{p} \partial \mathbf{u}^{oT}} & \frac{\partial^2 lnp(\mathbf{x};\boldsymbol{\theta}^o)}{\partial \mathbf{p} \partial \mathbf{p}^T} & \frac{\partial^2 lnp(\mathbf{x};\boldsymbol{\theta}^o)}{\partial \mathbf{p} \partial \boldsymbol{\delta}^{oT}} \\ \frac{\partial^2 lnp(\mathbf{x};\boldsymbol{\theta}^o)}{\partial \boldsymbol{\delta}^o \partial \mathbf{u}^{oT}} & \frac{\partial^2 lnp(\mathbf{x};\boldsymbol{\theta}^o)}{\partial \boldsymbol{\delta}^o \partial \mathbf{p}^T} & \frac{\partial^2 lnp(\mathbf{x};\boldsymbol{\theta}^o)}{\partial \boldsymbol{\delta}^o \partial \boldsymbol{\delta}^{oT}} \end{bmatrix} \tag{3.54}$$

The partial derivatives in (3.54) are

$$E\left[\frac{\partial^2 lnp(\mathbf{x};\boldsymbol{\theta})}{\partial \mathbf{u}^o \partial \mathbf{u}^{oT}}\right] = (\frac{\partial \mathbf{r}^o}{\partial \mathbf{u}^o})^T\mathbf{Q}_r^{-1}(\frac{\partial \mathbf{r}^o}{\partial \mathbf{u}^o}) \tag{3.55}$$

$$E\left[\frac{\partial^2 lnp(\mathbf{x};\boldsymbol{\theta})}{\partial \mathbf{u}^o \partial \mathbf{p}^T}\right] = (\frac{\partial \mathbf{r}^o}{\partial \mathbf{u}^o})^T\mathbf{Q}_r^{-1}(\frac{\partial \mathbf{r}^o}{\partial \mathbf{p}}) \tag{3.56}$$

$$E\left[\frac{\partial^2 lnp(\mathbf{x};\boldsymbol{\theta})}{\partial \mathbf{p} \partial \mathbf{u}^{oT}}\right] = (\frac{\partial \mathbf{r}^o}{\partial \mathbf{p}})^T\mathbf{Q}_r^{-1}(\frac{\partial \mathbf{r}^o}{\partial \mathbf{u}^o}) \tag{3.57}$$

$$E\left[\frac{\partial^2 lnp(\mathbf{x};\boldsymbol{\theta})}{\partial \mathbf{p} \partial \mathbf{p}^T}\right] = (\frac{\partial \mathbf{r}^o}{\partial \mathbf{p}})^T\mathbf{Q}_r^{-1}(\frac{\partial \mathbf{r}^o}{\partial \mathbf{p}}) + \mathbf{Q}_p \tag{3.58}$$

$$E\left[\frac{\partial^2 lnp(\mathbf{x};\boldsymbol{\theta})}{\partial \mathbf{u}^o \partial \boldsymbol{\delta}^{oT}}\right] = (\frac{\partial \mathbf{r}^o}{\partial \mathbf{u}})^T\mathbf{Q}_r^{-1}\mathbf{F} \tag{3.59}$$

$$E\left[\frac{\partial^2 lnp(\mathbf{x};\boldsymbol{\theta})}{\partial \boldsymbol{\delta}^o \partial \mathbf{u}^{oT}}\right] = \mathbf{F}^T\mathbf{Q}_r^{-1}(\frac{\partial \mathbf{r}^o}{\partial \mathbf{u}^o}) \tag{3.60}$$

$$E\left[\frac{\partial^2 lnp(\mathbf{x};\boldsymbol{\theta})}{\partial \boldsymbol{\delta}^o \partial \boldsymbol{\delta}^{oT}}\right] = \mathbf{F}^T\mathbf{Q}_r^{-1}\mathbf{F} \tag{3.61}$$

where $\mathbf{Q}_r$ is covariance matrix of measurement noise vector $\mathbf{n}$, $\mathbf{Q}_p$ is the covariance of random vector $\mathbf{p}$

$$\frac{\partial \mathbf{r}^o}{\partial \mathbf{u}} = \left[\frac{(\mathbf{u}-\mathbf{s}_2)}{r_2^o} - \frac{(\mathbf{u}-\mathbf{s}_1)}{r_1^o}, \ldots, \frac{(\mathbf{u}-\mathbf{s}_M)}{r_M^o} - \frac{(\mathbf{u}-\mathbf{s}_1)}{r_1^o}\right]^T \tag{3.62}$$

$$\frac{\partial \mathbf{r}^o}{\partial \mathbf{p}} = \left[\left(\frac{(\mathbf{u}-\mathbf{s}_2)^T\mathbf{V}_2}{r_2^o} - \frac{(\mathbf{u}-\mathbf{s}_1)^T\mathbf{V}_1}{\mathbf{r}_1^o}\right)^T, \ldots, \left(\frac{(\mathbf{u}-\mathbf{s}_M)^T\mathbf{V}_M}{r_M^o} - \frac{(\mathbf{u}-\mathbf{s}_1)^T\mathbf{V}_1}{r_1^o}\right)^T\right]^T. \tag{3.63}$$

The CRLB of $\mathbf{u}^o$ is the upper left 3×3 block of $CRLB(\boldsymbol{\theta}^o)$ Denote

$$E\left[\frac{\partial^2 ln\mathbf{p}(\mathbf{x};\boldsymbol{\theta})}{\partial\boldsymbol{\theta}\partial\boldsymbol{\theta}^T}\right] = \begin{bmatrix} E\left[\frac{\partial^2 ln\mathbf{p}(\mathbf{x};\boldsymbol{\theta}^o)}{\partial\ \mathbf{u}^o\partial\mathbf{u}^{oT}}\right] & E\left[\frac{\partial^2 ln\mathbf{p}(\mathbf{x};\boldsymbol{\theta}^o)}{\partial\mathbf{u}^o\partial\mathbf{p}^T}\right] & E\left[\frac{\partial^2 ln\mathbf{p}(\mathbf{x};\boldsymbol{\theta}^o)}{\partial\mathbf{u}^o\partial\boldsymbol{\delta}^{oT}}\right] \\ E\left[\frac{\partial^2 ln\mathbf{p}(\mathbf{x};\boldsymbol{\theta}^o)}{\partial\mathbf{p}\partial\mathbf{u}^{oT}}\right] & E\left[\frac{\partial^2 ln\mathbf{p}(\mathbf{x};\boldsymbol{\theta}^o)}{\partial\mathbf{p}\partial\mathbf{p}^T}\right] & E\left[\frac{\partial^2 ln\mathbf{p}(\mathbf{x};\boldsymbol{\theta}^o)}{\partial\mathbf{p}\partial\boldsymbol{\delta}^{oT}}\right] \\ E\left[\frac{\partial^2 ln\mathbf{p}(\mathbf{x};\boldsymbol{\theta}^o)}{\partial\boldsymbol{\delta}^o\partial\mathbf{u}^{oT}}\right] & E\left[\frac{\partial^2 ln\mathbf{p}(\mathbf{x};\boldsymbol{\theta}^o)}{\partial\boldsymbol{\delta}^o\partial\mathbf{p}^T}\right] & E\left[\frac{\partial^2 ln\mathbf{p}(\mathbf{x};\boldsymbol{\theta}^o)}{\partial\boldsymbol{\delta}^o\partial\boldsymbol{\delta}^{oT}}\right] \end{bmatrix} \tag{3.64}$$

$$= \begin{bmatrix} \mathbf{X}_{11} & \mathbf{X}_{12} & \mathbf{X}_{13} & \}3 \\ \mathbf{X}_{12}^T & \mathbf{X}_{22} & \mathbf{X}_{23} & \}L \\ \underbrace{\mathbf{X}_{13}^T} & \underbrace{\mathbf{X}_{23}^T} & \underbrace{\mathbf{X}_{33}} & \}N \\ 3 & L & N & \end{bmatrix} \tag{3.65}$$

Using the inversion formula, the upper left $(L+3) \times (L+3)$ block of the $CRLB(\boldsymbol{\theta}^o)$ is

$$\left[\begin{bmatrix} \mathbf{X}_{11} & \mathbf{X}_{12} \\ \mathbf{X}_{12}^T & \mathbf{X}_{22} \end{bmatrix} - \begin{bmatrix} \mathbf{X}_{13} \\ \mathbf{X}_{23} \end{bmatrix} \mathbf{X}_{33}^{-1} \begin{bmatrix} \mathbf{X}_{13}^T & X_{23}^T \end{bmatrix}\right]^{-1} \tag{3.66}$$

$$= \begin{bmatrix} \mathbf{X}_{11} - \mathbf{X}_{13}\mathbf{X}_{33}^{-1}\mathbf{X}_{13}^T & \mathbf{X}_{12} - \mathbf{X}_{13}\mathbf{X}_{33}^{-1}\mathbf{X}_{23}^T \\ \mathbf{X}_{12}^T - \mathbf{X}_{23}\mathbf{X}_{33}^{-1}\mathbf{X}_{13}^T & \mathbf{X}_{22} - \mathbf{X}_{23}\mathbf{X}33^{-1}\mathbf{X}_{23}^T \end{bmatrix}^{-1} \tag{3.67}$$

Thus, the upper left 3×3 block of (3.66) is

$$\begin{aligned} CRLB(\mathbf{u}^o)^{-1} &= (\mathbf{X}_{11} - \mathbf{X}_{13}\mathbf{X}_{33}^{-1}\mathbf{X}_{13}^T) \\ &\quad -(\mathbf{X}_{12} - \mathbf{X}_{13}\mathbf{X}_{33}^{-1}\mathbf{X}_{23}^T)(\mathbf{X}_{22} - \mathbf{X}_{23}\mathbf{X}_{33}^{-1}\mathbf{X}_{23}^T)^{-1}(\mathbf{X}_{12}^T - \mathbf{X}_{23}\mathbf{X}_{33}^{-1}\mathbf{X}_{13}^T) \end{aligned} \tag{3.68}$$

Substituting (3.55)-(3.61) into (3.68), give the CRLB of the source position when the observation noise, manifold sensor position uncertainties and clock-bias error are present.

3.5 Summary

In this chapter, we derive four CRLB. The first one is the CRLB only in presence of measurement noise. Then we derive the CRLB in the presence of measurement noise and sensor position manifold uncertainties, the CRLB in the presence of measurement noise and clock-bias error, and the CRLB when all the three kind of noise exist.

Chapter 4

A New Estimator and Performance Analysis of Source Localization in the Presence of Manifold Sensor Position Uncertainties

In this chapter, we will develop an estimator for source localization when measurement noise and sensor position manifold uncertainties are present and analysis its performance. This estimator has closed-form solution and is obtained based on the two stage approach from Chan and Ho's closed-form algorithm. The simulation result of the proposed algorithm will be given. In the last part of this chapter, we will prove the theoretically the performance of the proposed algorithm reaches the CRLB.

4.1 Mathematic Derivation

Denote $\mathbf{u}^o = [x^o, y^o, z^o]^T$ as unknown source location and $\mathbf{s}_i^o$ as the unknown sensor position of i^{th} sensor, $i = 1, \ldots, M$. $\mathbf{s}_i$ is the known noisy sensor position of the i^{th} sensor, where $\mathbf{s}_i = \mathbf{s}_i^o + \Delta\mathbf{s}_i$ and $\Delta\mathbf{s}_i$ is the sensor position error. We shall model $\Delta\mathbf{s}_i = \mathbf{V}_i\mathbf{p}$, where $\mathbf{p}$ is a random vector with length L and $\mathbf{V}_i$ is the transformation matrix relates the random vector $\mathbf{p}$ and the position uncertainties of the i^{th} sensor. Thus

$$\mathbf{s}_i = \mathbf{s}_i^o + \mathbf{V}_i\mathbf{p} \tag{4.1}$$

Denote $\mathbf{s} = [\mathbf{s}_1^T, \ldots, \mathbf{s}_M^T]^T$ and $\mathbf{V} = [\mathbf{V}_1^T, \ldots, \mathbf{V}_M^T]^T$, then

$$\mathbf{S} = \mathbf{S}^o + \mathbf{V}\mathbf{p} \tag{4.2}$$

From the emitted source signal in reaching the sensors, we have M-1 TDOA r_{i1} measurements

$$r_{i1} = r_{i1}^o + n_{i1}, i = 2, 3, \ldots, M \tag{4.3}$$

where r_{i1} is the true TDOA and n_{i1} is the noise that is zero mean Gaussian. Sensor $\mathbf{s}_1$ is the reference sensor in computing TDOAs.

The true range from source to the i^{th} sensor is

$$r_i^o = \|\mathbf{u}^o - \mathbf{s}_i^o\| = \sqrt{(x^o - x_i^o)^2 + (y^o - y_i^o)^2 + (z^o - z_i^o)^2} \tag{4.4}$$

Stage 1:

Without loss of generality, true TDOA measurement is equal to

$$r_{i1}^o = r_i^o - r_1^o, i = 2, 3, \ldots, M, \tag{4.5}$$

or

$$r_{i1}^o + r_1^o = r_i^o, i = 2, 3, \ldots, M. \tag{4.6}$$

For the i^{th} sensor, we substituting (4.4) into (4.6) and after squaring

$$r_{i1}^{o2} + 2r_{i1}^o r_1^o + 2(\mathbf{s}_i^o - \mathbf{s}_1^o)^T\mathbf{u}^o + \mathbf{s}_1^{oT}\mathbf{s}_1^o - \mathbf{s}_i^{oT}\mathbf{s}_i^o = 0 \tag{4.7}$$

Expressing $r_{i1}^o = r_{i1} - n_{i1}$ and $\mathbf{s}_i^o = \mathbf{s}_i + \mathbf{V}_i\mathbf{p}$, we have

$$\begin{aligned} &r_{i1}^2 - 2r_{i1}n_{i1} + n_{i1}^2 + 2r_{i1}r_1^o - 2r_1^o n_{i1} + 2(\mathbf{s}_i - \mathbf{V}_i\mathbf{p} - \mathbf{s}_1 + \mathbf{V}_1\mathbf{p})^T\mathbf{u}^o \\ &+(\mathbf{s}_1 - \mathbf{V}_1\mathbf{p})^T(\mathbf{s}_1 - \mathbf{V}_1\mathbf{p}) - (\mathbf{s}_i - \mathbf{V}_i\mathbf{p})^T(\mathbf{s}_i - \mathbf{V}_i\mathbf{p}) = 0. \end{aligned} \tag{4.8}$$

Ignoring the 2^{nd} order noise terms and rearranging

$$\begin{aligned} & 2r_i^o n_{i1} + 2(\mathbf{u}^o - \mathbf{s}_i)^T \mathbf{V}_i \mathbf{p} - 2(\mathbf{u}^o - \mathbf{s}_1)^T \mathbf{V}_1 \mathbf{p} \\ & = r_{i1}^2 - \mathbf{s}_i^T \mathbf{s}_i + \mathbf{s}_1^T \mathbf{s}_1 + 2(\mathbf{s}_i - \mathbf{s}_1)^T \mathbf{u}^o + 2r_{i1} r_1^o \end{aligned} \tag{4.9}$$

Because r_1^o is the true value, it depends on the true position of $\mathbf{s}_1$. We can express it as

$$r_1^o = \|\mathbf{u}^o - \mathbf{s}_1^o\| = \|\mathbf{u}^o - \mathbf{s}_1 + \Delta\mathbf{s}_1\| \approx \widetilde{r}_1^o + \boldsymbol{\rho}_{\mathbf{u}^o,\mathbf{s}_1}^T \mathbf{V}_1 \mathbf{p} \tag{4.10}$$

where $\widetilde{r}_1^o = \|\mathbf{u}^o - \mathbf{s}_1\|$ and $\boldsymbol{\rho}_{\mathbf{u}^o,\mathbf{s}_1} \approx \frac{(\mathbf{u}^o - \mathbf{s}_1)}{\|\mathbf{u}^o - \mathbf{s}_1\|}$ represents the unit vector from $\mathbf{s}_1$ to $\mathbf{u}^o$. (4.9) now becomes

$$\begin{aligned} & 2r_i^o n_{i1} + 2(\mathbf{u}^o - \mathbf{s}_i)^T \mathbf{V}_i \mathbf{p} - 2(\mathbf{u}^o - \mathbf{s}_1 + r_{i1}\boldsymbol{\rho}_{\mathbf{u}^o,\mathbf{s}_1})^T \mathbf{V}_1 \mathbf{p} \\ & = r_{i1}^2 - \mathbf{s}_i^T \mathbf{s}_i + \mathbf{s}_1^T \mathbf{s}_1 + 2(\mathbf{s}_i - \mathbf{s}_1)^T \mathbf{u}^o + 2r_{i1} \widetilde{r}_1^o \end{aligned} \tag{4.11}$$

The unknown vector is $\boldsymbol{\varphi}_1^o = \begin{bmatrix} \mathbf{u}^{oT} & \widetilde{r}_1^o \end{bmatrix}^T$. In matrix form, we can express (4.11) as

$$\boldsymbol{\epsilon}_1 = \mathbf{B}_1 \mathbf{n} + \mathbf{D}\mathbf{p} = \mathbf{h}_1 - \mathbf{G}_1 \boldsymbol{\varphi}_1^o \tag{4.12}$$

where

$$\mathbf{B}_1 = 2 \begin{bmatrix} r_2^o & & & \\ & r_3^o & & \\ & & \ddots & \\ & & & r_M^o \end{bmatrix} \tag{4.13}$$

$$\mathbf{D} = 2 \begin{bmatrix} (\mathbf{u}^o - \mathbf{s}_2)^T \mathbf{V}_2 - (\mathbf{u}^o - \mathbf{s}_1 + r_{21}\boldsymbol{\rho}_{\mathbf{u}^o,\mathbf{s}_1})^T \mathbf{V}_1 \\ \vdots \\ (\mathbf{u}^o - \mathbf{s}_M)^T \mathbf{V}_2 - (\mathbf{u}^o - \mathbf{s}_1 + r_{M1}\boldsymbol{\rho}_{\mathbf{u}^o,\mathbf{s}_1})^T \mathbf{V}_M \end{bmatrix} \tag{4.14}$$

$$\mathbf{h}_1 = \begin{bmatrix} r_{21}^2 - \mathbf{s}_2^T \mathbf{s}_2 + \mathbf{s}_1^T \mathbf{s}_1 \\ \vdots \\ r_{M1}^2 - \mathbf{s}_M^T \mathbf{s}_M + \mathbf{s}_1^T \mathbf{s}_1 \end{bmatrix} \tag{4.15}$$

$$\mathbf{G}_1 = -2 \begin{bmatrix} (\mathbf{s}_2 - \mathbf{s}_1)^T & r_{21} \\ \vdots & \\ (\mathbf{s}_M - \mathbf{s}_1)^T & r_{M1} \end{bmatrix} \tag{4.16}$$

and $\mathbf{n} = [n_{21}, \ldots, n_{M1}]^T$ is the noise vector.

In this case, weighted least-square (WLS) technique can be applied to estimate $\boldsymbol{\varphi}_1$ and the result is

$$\boldsymbol{\varphi}_1 = (\mathbf{G}_1^T \mathbf{W}_1 \mathbf{G}_1)^{-1} \mathbf{G}_1^T \mathbf{W}_1 \mathbf{h}_1 \tag{4.17}$$

The covariance matrix of $\boldsymbol{\varphi}_1$ is

$$cov(\boldsymbol{\varphi}_1) = (\mathbf{G}_1^T \mathbf{W}_1 \mathbf{G}_1)^{-1} \tag{4.18}$$

The weighting matrix $\mathbf{W}_1$ is calculated using

$$\mathbf{W}_1 = E[\boldsymbol{\epsilon}_1 \boldsymbol{\epsilon}_1^T]^{-1} = (\mathbf{B}_1 \mathbf{Q} \mathbf{B}_1^T + \mathbf{D} \mathbf{Q}_p \mathbf{D}^T)^{-1} \tag{4.19}$$

where $\mathbf{Q}$ is the covariance matrix of $\mathbf{n}$ and $\mathbf{Q_p}$ is the covariance matrix of $\mathbf{p}$.

Stage 2:

Stage 2 follows stage 2 in Chan and Ho's method[3], we refine the estimation of the source location using $\widetilde{r}_1$ in $\boldsymbol{\varphi}_1$. Let $\boldsymbol{\varphi}_2^o = [(x^o - x_1)^2, (y^o - y_1)^2, (z^o - z_1)^2]^T$

$$(\mathbf{u}^o - \mathbf{s}_1) \odot (\mathbf{u}^o - \mathbf{s}_1) = \boldsymbol{\varphi}_2^o \tag{4.20}$$

Since $\boldsymbol{\varphi}_1(1:3)$ is an estimator of $\mathbf{u}^o$, ie $\boldsymbol{\varphi}_1(1:3) = \mathbf{u}^o + \Delta\boldsymbol{\varphi}_1(1:3)$, where $\Delta\varphi_1(1:3)$ is the estimation noise. Thus replacing $\mathbf{u}^o$ in (4.20) by $\boldsymbol{\varphi}_1(1:3) - \Delta\boldsymbol{\varphi}_1(1:3)$

$$(\boldsymbol{\varphi}_1(1:3)^o - \mathbf{s}_1) \odot (\boldsymbol{\varphi}_1(1:3)^o - \mathbf{s}_1) - 2(\boldsymbol{\varphi}_1(1:3)^o - \mathbf{s}_1) \odot \Delta\boldsymbol{\varphi}_1(1:3)^o = (\mathbf{u}^o - \mathbf{s}_1) \odot (\mathbf{u}^o - \mathbf{s}_1) \tag{4.21}$$

or

$$2(\boldsymbol{\varphi}_1(1:3) - \mathbf{s}_1) \odot \Delta\boldsymbol{\varphi}_1(1:3) = (\boldsymbol{\varphi}_1(1:3) - s_1) \odot (\boldsymbol{\varphi}_1(1:3) - s_1) - (\mathbf{u}^o - \mathbf{s}_1) \odot (\mathbf{u}^o - \mathbf{s}_1) \tag{4.22}$$

where the second order noise $\Delta\boldsymbol{\varphi}_1(1:3) \odot \Delta\boldsymbol{\varphi}_1(1:3)$ has been ignored.

Recall that $\varphi_1(4) = r_1^o + \Delta r_1$, where Δr_i is the estimation noise.

$$(\varphi_1(4) - \Delta\varphi_1(4))^2 = (\mathbf{u}^o - \mathbf{s}_1)^T (\mathbf{u}^o - \mathbf{s}_1) \tag{4.23}$$

Expanding the left side and ignoring $\Delta\varphi_1(4)^2$

$$2\varphi_1(4)\Delta\varphi_1(4) = \varphi_1(4)^2 - (\mathbf{u}^o - \mathbf{s}_1)^T (\mathbf{u}^o - \mathbf{s}_1) \tag{4.24}$$

We express (4.22) and (4.24) in matrix form

$$\boldsymbol{\epsilon}_2 = \mathbf{B}_2 \Delta\boldsymbol{\varphi}_1 = \mathbf{h}_2 - \mathbf{G}_2 \boldsymbol{\varphi}_2 \tag{4.25}$$

where

$$\mathbf{B}_2 = 2\begin{bmatrix} diag(\mathbf{u}^o - \mathbf{s}_1) & \\ & r_1^o \end{bmatrix} \tag{4.26}$$

$$\mathbf{h}_2 = \begin{bmatrix} (\boldsymbol{\varphi}_1(1:3) - \mathbf{s}_1) \odot (\boldsymbol{\varphi}_1(1:3) - \mathbf{s}_1) \\ \varphi_1(4)^2 \end{bmatrix} \tag{4.27}$$

$$\mathbf{G}_2 = \begin{bmatrix} 1 & 0 & 0 \\ 0 & 1 & 0 \\ 0 & 0 & 1 \\ 1 & 1 & 1 \end{bmatrix} \tag{4.28}$$

The WLS solution for stage 2 is

$$\boldsymbol{\varphi}_2 = (\mathbf{G}_2^T \mathbf{W}_2 \mathbf{G}_2)^{-1} \mathbf{G}_2^T \mathbf{W}_2 \mathbf{h}_2 \tag{4.29}$$

The covariance matrix of $\boldsymbol{\varphi}_2$ is

$$cov(\boldsymbol{\varphi}_2) = (\mathbf{G}_2^T \mathbf{W}_2 \mathbf{G}_2)^{-1} \tag{4.30}$$

where the weighting matrix is $\mathbf{W}_2 = E[\boldsymbol{\epsilon}_2 \boldsymbol{\epsilon}_2^T]^{-1} = [\mathbf{B}_2 cov(\boldsymbol{\varphi}_1) \mathbf{B}_2^T]^{-1}$.

The source location estimate $\mathbf{u} = [x, y, z]^T$ can be obtained from $\boldsymbol{\varphi}_2$

$$\mathbf{u} = \mathbf{P}[\sqrt{\boldsymbol{\varphi}_2(1)}, \sqrt{\boldsymbol{\varphi}_2(2)}, \sqrt{\boldsymbol{\varphi}_2(3)}]^T + \mathbf{s}_1 \tag{4.31}$$

where

$$\mathbf{P} = diag[sgn(\boldsymbol{\varphi}_1(1) - x_1), sgn(\boldsymbol{\varphi}_1(2) - y_1), sgn(\boldsymbol{\varphi}_1(3) - z_1)]. \tag{4.32}$$

According to (4.31), subtracting both sides by $\mathbf{s}_1$, squaring and taking differential,

$$\Delta \mathbf{u} = \mathbf{B}_3^{-1} \Delta \boldsymbol{\varphi}_2 \tag{4.33}$$

where

$$\mathbf{B}_3 = 2\begin{bmatrix} x^o - x_1 & & \\ & y^o - y_1 & \\ & & z^o - z_1 \end{bmatrix} \tag{4.34}$$

The covariance matrix of the final source position estimator is

$$cov(\mathbf{u}) = \mathbf{B}_3^{-1} cov(\boldsymbol{\varphi}_2) \mathbf{B}_3^{-T} \tag{4.35}$$

x_i	y_i	z_i
300	100	150
400	150	100
300	500	200
350	200	100
-100	-100	-100
200	-300	-200

Table 4.1: True Sensor Position

4.2 Simulation

The weighting matrix $\mathbf{W}_1$ in first stage is depend on the unknown true source and sensor positions. In practice, We set $\mathbf{W}_1$ to $\mathbf{Q}$ at first. After we have an initial estimate of the source location, we use it to obtain $\mathbf{W}_1$. Then, we make use of the updated $\mathbf{W}_1$ to obtain more accurate estimation of $\boldsymbol{\varphi}_1$. We repeat the stage 1 computation several times, to obtain more accurate result. In our implementation, the number of times to repeat is set to 3.

The TDOA measurements are obtained according to $\mathbf{r} = \mathbf{r}^o + \mathbf{n}$ where $\mathbf{r}$ is the TDOA measurements with noise, $\mathbf{r}^o$ is the true TDOA values and $\mathbf{n}$ is the noise vector. In simulation, $\mathbf{r}^o$ is calculated by $r^o_{i1} = \|\mathbf{u}^o - \mathbf{s}_i\| - \|\mathbf{u}^o - \mathbf{s}_1\|$ and the covariance matrix of $\mathbf{n}$ is $\mathbf{Q}$.

Besides measurement noise, sensor position manifold uncertainties in the simulation are given by $\mathbf{s} = \mathbf{s}^o + \mathbf{V}\mathbf{p}$. The covariance matrix of $\mathbf{p}$ is $\mathbf{Q}_p$. $\mathbf{V} = [\mathbf{V}_1^T, \ldots, \mathbf{V}_M^T]^T$ where v_i is 3×3 identity matrix.

In the simulation, we compare mse(mean-square error) with CRLB. It is obtained according to $mse = \frac{\sum_{k=1}^{K}(\mathbf{u}^o - \mathbf{u}^{(k)})^T(\mathbf{u}^o - \mathbf{u}^{(k)})}{K}$, where K is the number of ensemble runs of the proposed solution. We set K to 5000.

Table 4.1 is the sensor positions used in the simulations. Figure 4.1 is the distribution of the sensors.

Figure 4.2 is the simulation result for a near-field source at $\mathbf{u}^o = [600, 550, 650]^T$. Measurement noise matrix $\mathbf{Q}$ is set to $c^2\sigma^2$ in the diagonal elements and $0.5c^2\sigma^2$ otherwise. $\mathbf{Q}_p$, which is the covariance matrix of $\mathbf{p}$, is set to a $L \times L$ identity matrix with the noise power of $c^2\sigma^2$. The

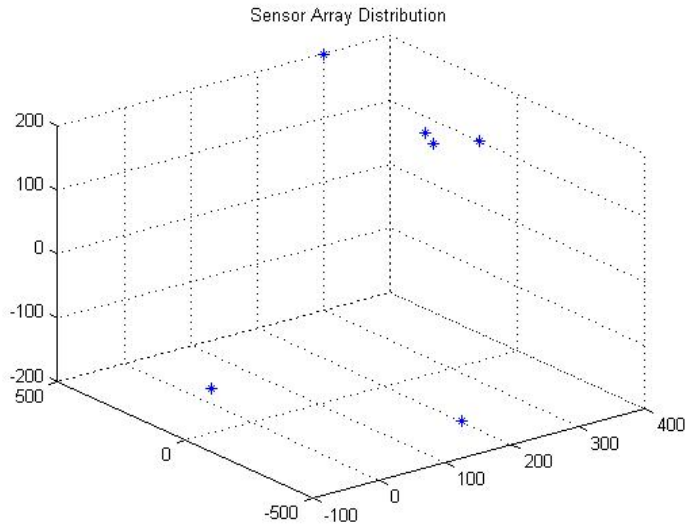

Figure 4.1: Sensor Array Distribution

CRLB of source localization in the presence of manifold sensor position error is higher than the CRLB of source localization which has accurate sensor positions. According to this simulation, mean-square error of the source location estimate reaches CRLB when σ is small.

Figure 4.3 is the simulation result for a near-field source $u^o = [600, 550, 650]^T$. The measurement noise matrix $\mathbf{Q}$ is set to $c^2\sigma^2$ in the diagonal elements and $0.5c^2\sigma^2$ otherwise. $\mathbf{Q}_p$ is set to 0.1 times $L \times L$ identity matrix. At the beginning when σ^2 is small, the performance of source localization in the presence of manifold sensor position error is mainly effected by the sensor manifold uncertainties because sensor manifold uncertainties is much larger than measurement noise at first. As the measurement noise power increases, the measurement noise power becomes much larger than the noise power of manifold sensor uncertainties and it dominates the performance. In addition, the CRLB in the presence manifold sensor uncertainties becomes close to the CRLB in absence of sensor manifold error. From this simulation, mean-square error of source localization reaches CRLB when the measurement noise power is small.

Figure 4.4 is the simulation result for a near-field source at $\mathbf{u}^o = [600, 550, 650]^T$. The Measurement noise matrix $\mathbf{Q}$ is fixed to 1 in the diagonal elements and 0.5 otherwise times 0.1. $\mathbf{Q}_p$ is set to a $L \times L$ identity matrix times the noise power of $c^2\sigma^2$. Because the measurement noise power is fixed, The CRLB of the source location estimate in presence of measurement noise only is a horizontal line. When the power of the sensor position manifold error is small, the two CRLBs

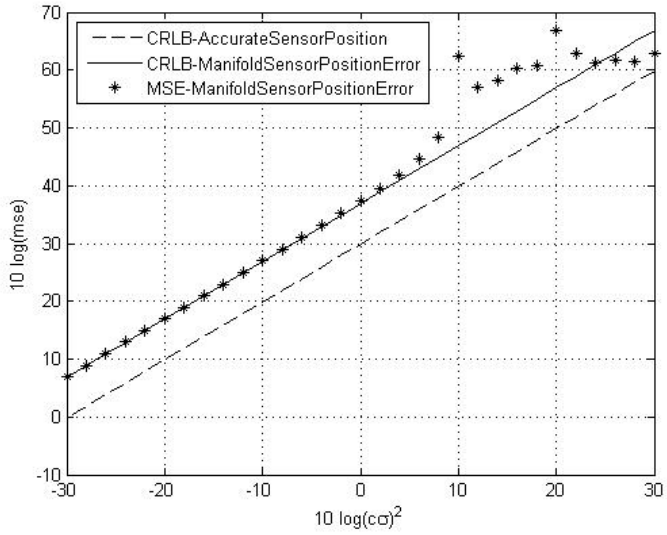

Figure 4.2: Near-field source localization in the presence of manifold sensor position uncertainties

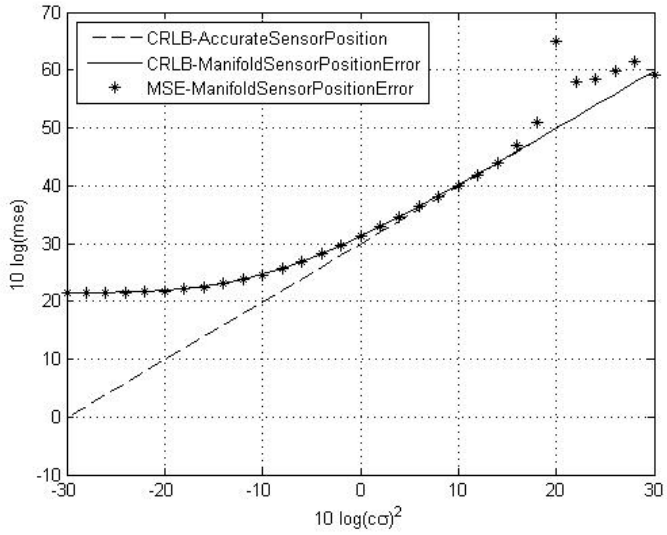

Figure 4.3: Near-field source localization in the presence of manifold sensor position uncertainties -fix $\mathbf{Q}_p$

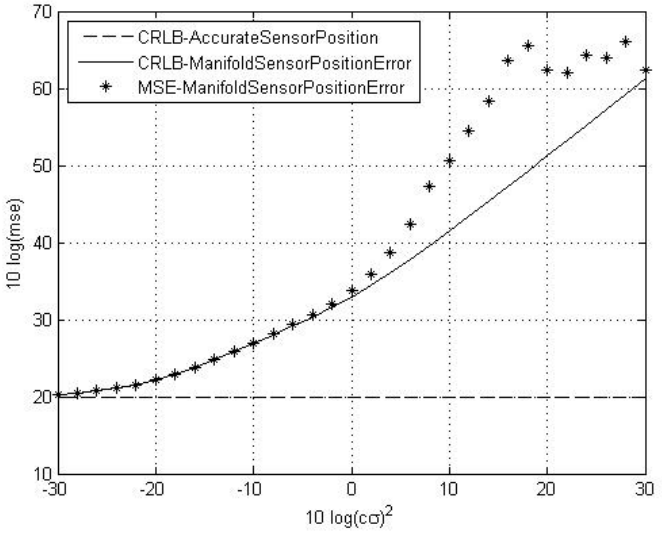

Figure 4.4: Near-field source localization in the presence of manifold sensor position uncertainties -fix $\mathbf{Q}$

with and without sensor position manifold error are close to each other. When the power of sensor position manifold error become much larger than the fixed measurement noise power, the CRLB of source localization in presence of manifold uncertainties is higher than the one without manifold uncertainties. The mean-square error of the source location estimate reaches the CRLB when the sensor position manifold error is small.

Figure 4.5 is the simulation result for the distant source at $u^o = [2000, 2500, 3000]^T$. The measurement noise matrix $\mathbf{Q}$ is set to $c^2\sigma^2$ in the diagonal elements and $0.5c^2\sigma^2$ otherwise. $\mathbf{Q_p}$, which is the covariance matrix of $\mathbf{p}$, is set to a $L \times L$ identity matrix with the noise power of $c^2\sigma^2$. Comparing to the near-field source localization in Figure 4.2, the mean-square error diverges from CRLB earlier for the distant source. However, the mean-square error remains to reach the corresponding CRLB if the noise is small enough.

Figure 4.3 is the simulation result for a far-field source $\mathbf{u}^o = [2000, 2500, 3000]^T$. The measurement noise matrix $\mathbf{Q}$ is set to $c^2\sigma^2$ in the diagonal elements and $0.5c^2\sigma^2$ otherwise. $\mathbf{Q_p}$ is set to a 0.1 times an $L \times L$ identity matrix. At the beginning when σ^2 is small, the performance of source localization in the presence of manifold sensor position error is dominated by the sensor manifold uncertainties because it is much larger than the measurement noise. As the measurement noise power increases, the measurement noise power dominates the localization

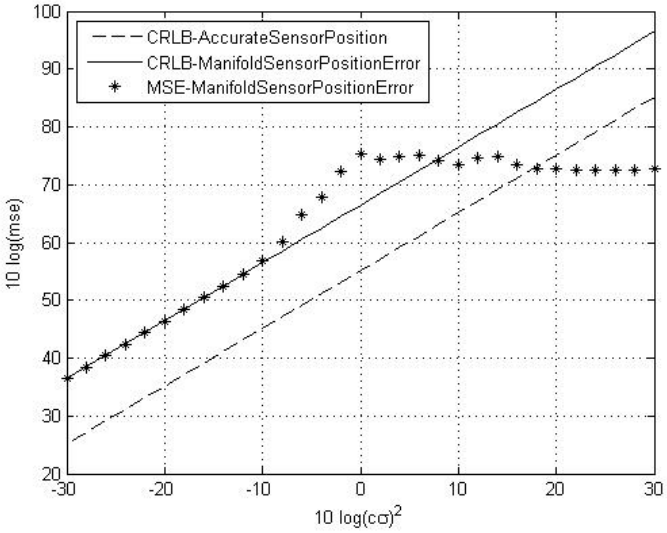

Figure 4.5: Distant source localization in the presence of manifold sensor position uncertainties

performance. In addition, the CRLB in the presence manifold sensor uncertainties becomes close to the CRLB in absence of sensor manifold error. From this simulation, the mean-square error of source localization reaches the CRLB when the measurement noise power is small, but the performance diverges earlier from the bound than that of the near-field case.

Figure 4.7 is the simulation result for the distant source $\mathbf{u}^o = [2000, 2500, 3000]^T$. The measurement noise power is fixed. $\mathbf{Q}$ is fixed to 0.1 times 1 in the diagonal elements and 0.5 otherwise. $\mathbf{Q}_p$ is set to a $L \times L$ identity matrix times the noise power of $c^2\sigma^2$. The CRLB of the source location estimate in presence of measurement noise only is a horizontal line as σ^2 increase. When the power of sensor position manifold error is small, the two CRLBs of with and without sensor position manifold error are close to each other. When the power of sensor position manifold error becomes much larger than the fixed measurement noise power, CRLB of source localization in presence of manifold uncertainties is higher than the one without manifold uncertainties. The mean-square error of source localization reaches CRLB when the sensor position manifold error is small, but the performance diverges from the bound earlier than the near-field case.

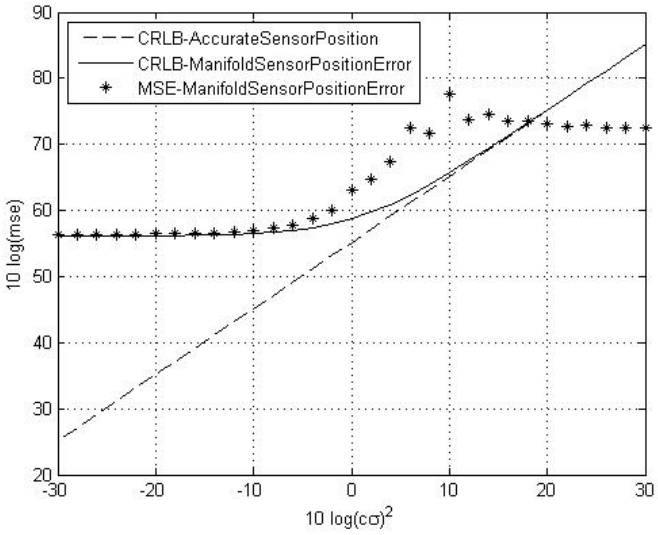

Figure 4.6: Distant source localization in the presence of manifold sensor position uncertainties -fix $\mathbf{Q_p}$

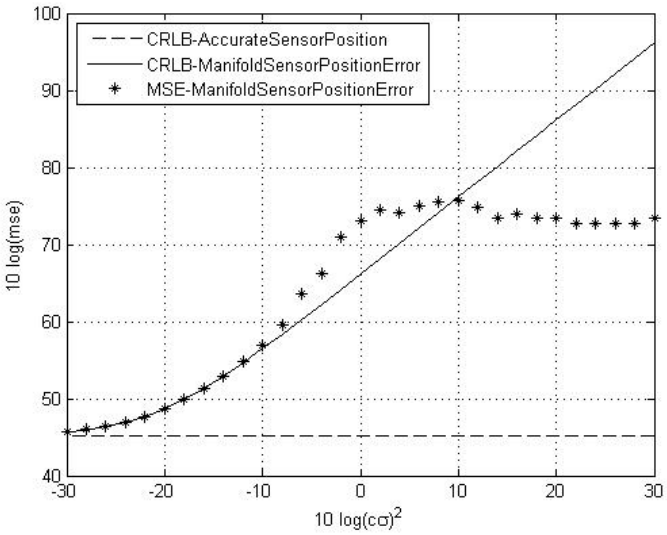

Figure 4.7: Distant source localization in the presence of manifold sensor position uncertainties -fix $\mathbf{Q}$

4.3 Mathematic Proof of Optimum Performance of the Proposed Estimator for Source Localization in the Presence of Sensor Position Manifold Uncertainties

In this section, we will prove that the Mean-square Error of the proposed estimator achieves the CRLB performance. The CRLB of source localization in the presence of sensor position manifold error has been given in Chapter 3. Now, we evaluate the covariance of the source location estimate from the proposed estimator.

$$\begin{aligned} cov(\mathbf{u})^{-1} &= \mathbf{B}_3^T cov(\boldsymbol{\varphi}_2)^{-1}\mathbf{B}_3 \\ &= \mathbf{B}_3^T\mathbf{G}_2^T\mathbf{B}_2^{-1}\mathbf{G}_1^T\mathbf{B}_1^{-T}(\mathbf{Q}+\mathbf{B}_1^{-1}\mathbf{D}\mathbf{Q}_p\mathbf{D}^T\mathbf{B}_1^{-T})^{-1}\mathbf{B}_1^{-1}\mathbf{G}_1\mathbf{B}_2^{-1}\mathbf{G}_2\mathbf{B}_3 \end{aligned} \quad (4.36)$$

Let

$$\begin{cases} \mathbf{G}_3 = \mathbf{B}_1^{-1}\mathbf{G}_1\mathbf{B}_2^{-1}\mathbf{G}_2\mathbf{B}_3 \\ \mathbf{G}_4 = \mathbf{B}_1^{-1}\mathbf{D} \end{cases}, \quad (4.37)$$

After using matrix inversion Lemma, we have

$$\begin{aligned} cov(\mathbf{u})^{-1} &= \mathbf{G}_3^T(\mathbf{Q}+\mathbf{G}_4\mathbf{Q}_p\mathbf{G}_4^T)^{-1}\mathbf{G}_3 \\ &= \mathbf{G}_3^T\mathbf{Q}^{-1}\mathbf{G}_3 - \mathbf{G}_3^T\mathbf{Q}^{-1}\mathbf{G}_4(\mathbf{Q}_\mathbf{p}^{-1}+\mathbf{G}_4^T\mathbf{Q}^{-1}\mathbf{G}_4)\mathbf{G}_4^T\mathbf{Q}^{-1}\mathbf{G}_3 \end{aligned} \quad (4.38)$$

Substituting (4.13), (4.16), (4.26), (4.28) and (4.34), $\mathbf{G}_3$ becomes

$$\begin{aligned} \mathbf{G}_3 &= \mathbf{B}_1^{-1}\mathbf{G}_1\mathbf{B}_2^{-1}\mathbf{G}_2\mathbf{B}_3 \\ &= -\begin{bmatrix} \frac{x_2-x_1}{r_2^o}+\frac{r_{21}(x^o-x_1)}{r_2^o\widetilde{r}_1^o} & \frac{y_2-y_1}{r_2^o}+\frac{r_{21}(y^o-y_1)}{r_2^o\widetilde{r}_1^o} & \frac{z_2-z_1}{r_2^o}+\frac{r_{21}(z^o-z_1)}{r_2^o\widetilde{r}_1^o} \\ \vdots & \vdots & \vdots \\ \frac{x_M-x_1}{r_M^o}+\frac{r_{M1}(x^o-x_1)}{r_M^o\widetilde{r}_1^o} & \frac{y_M-y_1}{r_M^o}+\frac{r_{M1}(y^o-y_1)}{r_M^o\widetilde{r}_1^o} & \frac{z_M-z_1}{r_M^o}+\frac{r_{M1}(z^o-z_1)}{r_M^o\widetilde{r}_1^o} \end{bmatrix} \\ &= -\begin{bmatrix} \frac{(\mathbf{s}_2-\mathbf{s}_1)^T}{r_j^o}+\frac{r_{21}(\mathbf{u}^o-\mathbf{s}_1)^T}{r_2^o\widetilde{r}_1^o} \\ \vdots \\ \frac{(\mathbf{s}_M-\mathbf{s}_1)^T}{r_M^o}+\frac{r_{M1}(\mathbf{u}^o-\mathbf{s}_1)^T}{r_M^o\widetilde{r}_1^o} \end{bmatrix} \end{aligned} \quad (4.39)$$

where we assume $\mathbf{B}_2^o \Delta\boldsymbol{\varphi} \approx \mathbf{0}$ is valid. The $(j-1)^{th}$ row of $\mathbf{G}_3$ is

$$\begin{aligned} -\left(\frac{(\mathbf{s}_j-\mathbf{s}_1)^T}{r_j^o}+\frac{r_{j1}(\mathbf{u}^o-\mathbf{s}_1)^T}{r_j^o\widetilde{r}_1^o}\right) &= -\left(\frac{(\mathbf{s}_j^o-\mathbf{s}_1^o+\mathbf{V}_j\mathbf{p}-\mathbf{V}_1\mathbf{p})^T}{r_j^o}+\frac{(r_{j1}^o+n_{j1})(\mathbf{u}^o-\mathbf{s}_1^o-\mathbf{V}_1\mathbf{p})^T}{r_j^o(r_1^o-\boldsymbol{\rho}_{\mathbf{u}^o,\mathbf{s}_1}^T\mathbf{V}_1\mathbf{p})}\right) \\ &= -\left(\frac{(\mathbf{s}_j^o-\mathbf{s}_1^o)^T}{r_j^o}+\frac{r_{j1}^o(\mathbf{u}^o-\mathbf{s}_1^o)^T}{r_j^o r_1^o}\right)(if\ C_1\ and\ C_2\ are\ satisfied) \\ &= \frac{(\mathbf{u}^o-\mathbf{s}_j^o)^T}{r_j^o}-\frac{(\mathbf{u}^o-\mathbf{s}_1^o)^T}{r_1^o} \end{aligned}$$

and hence

$$\mathbf{G}_3 = \frac{\partial \mathbf{r}^o}{\partial \mathbf{u}^o} \tag{4.40}$$

where,

$$\begin{cases} C_1 : \frac{n_{j1}}{r_j^o} = 0, j = 2, \ldots, M \\ C_2 : \frac{\|\mathbf{V}_j\mathbf{p}\|}{r_j^o} = 0, j = 1, \ldots, M \end{cases} \tag{4.41}$$

Substituting (4.14) and (4.13) into $\mathbf{G}_4$

$$\begin{aligned} \mathbf{G}_4 &= \mathbf{B}_1^{-1}\mathbf{D} \\ &= \begin{bmatrix} \frac{(\mathbf{u}^o-\mathbf{s}_2)^T\mathbf{V}_2-(\mathbf{u}^o-\mathbf{s}_1+r_{21}\boldsymbol{\rho}_{\mathbf{u}^o,\mathbf{s}_1})^T\mathbf{V}_1}{r_2^o} \\ \vdots \\ \frac{(\mathbf{u}^o-\mathbf{s}_M)^T\mathbf{V}_M-(\mathbf{u}^o-\mathbf{s}_1+r_{M1}\boldsymbol{\rho}_{\mathbf{u}^o,\mathbf{s}_1})^T\mathbf{V}_1}{r_M^o} \end{bmatrix} \end{aligned} \tag{4.42}$$

The $(j-1)^{th}$ row of $\mathbf{G}_4$ is

$$\begin{aligned} & \frac{(\mathbf{u}^o-\mathbf{s}_j^o-\Delta\mathbf{s}_j)^T\mathbf{V}_j-(\mathbf{u}^o-\mathbf{s}_1^o-\Delta\mathbf{s}_1+r_{j1}\boldsymbol{\rho}_{\mathbf{u}^o,\mathbf{s}_1})^T\mathbf{V}_1}{r_j^o} \\ = & \frac{(\mathbf{u}^o-\mathbf{s}_j^o-\Delta\mathbf{s}_j)^T\mathbf{V}_j-(\mathbf{u}^o-\mathbf{s}_1^o-\Delta\mathbf{s}_1+(r_{j1}^o+n_{i1})\frac{(\mathbf{u}^o-\mathbf{s}_1)}{\widetilde{r}_1^o})\mathbf{V}_1}{r_j^o} \\ = & \frac{(\mathbf{u}^o-\mathbf{s}_j^o)^T\mathbf{V}_j-(\mathbf{u}^o-\mathbf{s}_1^o+r_{j1}^o\frac{(\mathbf{u}^o-\mathbf{s}_1^o)}{r_1^o})\mathbf{V}_1}{r_j^o}(if\ C_1\ and\ C_2\ are\ satisfied) \\ = & \frac{(\mathbf{u}^o-\mathbf{s}_j^o)^T\mathbf{V}_j}{r_j^o}-\frac{(\mathbf{u}^o-\mathbf{s}_1^o)^T\mathbf{V}_i}{r_1^o} \end{aligned}$$

and hence

$$\mathbf{G}_4 = \frac{\partial \mathbf{r}^o}{\partial \mathbf{p}} \tag{4.43}$$

Covariance Matrix of $\mathbf{u}$ is,

$$\begin{aligned} cov(\mathbf{u}) = & (\frac{\partial \mathbf{r}}{\partial \mathbf{u}})^T\mathbf{Q}^{-1}(\frac{\partial \mathbf{r}}{\partial \mathbf{u}})-(\frac{\partial \mathbf{r}}{\partial \mathbf{u}})^T\mathbf{Q}^{-1}(\frac{\partial \mathbf{r}}{\partial \mathbf{p}})\left(\mathbf{Q}_p^{-1}+(\frac{\partial \mathbf{r}}{\partial \mathbf{p}})^T\mathbf{Q}^{-1}(\frac{\partial \mathbf{r}}{\partial \mathbf{p}})\right)^{-1}(\frac{\partial \mathbf{r}}{\partial \mathbf{p}})^T\mathbf{Q}^{-1}(\frac{\partial \mathbf{r}}{\partial \mathbf{u}}) \\ & = CRLB(\mathbf{u}^o) \end{aligned} \tag{4.44}$$

Hence the performance of the proposed estimator reaches CRLB performance when the condition (C_1) and (C_2) are satisfied.

4.4 Summary

In this Chapter, we proposed an algorithm of the source localization problem in the presence of measurement noise and sensor position manifold uncertainties. Then, simulation result shows that the proposed method reached the CRLB performance for both near-field and distant source in small error region. In the final part of the chapter, the proposed method has been provn that its performance reaches CRLB theoretically.

Chapter 5

A New Estimator and Performance Analysis of Source Localization in the Presence of Clock-bias Error

In this chapter, we will develop an algorithm for source localization in the presence of measurement noise and clock-bias error. This algorithm is a closed-form method based on Chan and Ho's closed-form solution. The simulation result of the proposed algorithm and the theoretical proof that the proposed algorithm reaches CRLB will be given in this chapter.

5.1 Mathematic Derivation

In this section, we will derive a algorithm of source localization when the measurement noise and clock-bias error exist.

The unknown source position is $\mathbf{u}^o = [x^o, y^o, z^o]^T$ and the known sensor position is $\mathbf{s}_i = [x_i, y_i, z_i]^T$. Let us further assume that the sensor array can be decomposed into N sub-arrays and the i^{th} sub-array has $(m_i - m_{i-1})$ elements, $i = 1, 2, \ldots, N$. Here, m_0 is zero and the total

number of sensor is $M = m_N$. Within each sub-array the sensors are synchronized with the same clocks. However, the clocks among different sub-arrays are not synchronized and have clock bias $\delta_j, j = 2, 3, \ldots, N$ with respect to the first sub-array. Let us choose the first sensor of the first sub-array as reference for TDOA measurements.

From the emitted source signal, we have $m_N - 1$ TDOA r_{i1} measurements.

$$r_{i1} = \| \mathbf{u}^o - \mathbf{s}_i \| - \| \mathbf{u}^o - \mathbf{s}_1 \| + n_{i1}, i = 2, \ldots, m_1$$

$$r_{i1} = \| \mathbf{u}^o - \mathbf{s}_i \| - \| \mathbf{u}^o - \mathbf{s}_1 \| + \delta_2^o + n_{i1}, i = m_1 + 1, \ldots, m_2 \tag{5.1}$$

$$\ldots$$

$$r_{i1} = \| \mathbf{u}^o - \mathbf{s}_i \| - \| \mathbf{u}^o - \mathbf{s}_1 \| + \delta_N^o + n_{i1}, i = m_{N-1} + 1, \ldots, m_N$$

where $\boldsymbol{\delta}^o = [\delta_2^o, \ldots, \delta_N^o]^T$ is the clock-bias vector. We shall assume in this study δ is deterministic and not random. $\{\mathbf{s}_1, \ldots, \mathbf{s}_{m_1}\}$, $\{\mathbf{s}_{m_1+1}, \ldots, \mathbf{s}_{m_2}\}$, $\ldots$, $\{\mathbf{s}_{m_{N-1}+1}, \ldots, \mathbf{s}_{m_N}\}$ are different sub-arrays.

Although different sub-arrays have clock bias between each other, sensors within a sub-array are synchronized.

Hence, we can convert the $m_N - 1$ measurements in (5.1) to the following $m_N - N$ TDOA values:

$$r_{i,m_{j-1}+1} = r_{i,1} - r_{m_{j-1}+1,1}, \begin{cases} i = m_{j-1} + 2, \ldots, m_j \\ j = 1, 2, \ldots, N \end{cases} \tag{5.2}$$

where sensor $m_{j-1} + 1$ in the j^{th} sub-array is used as a reference for the TDOAs within the sub-array. The above $m_N - N$ TDOA values are free of clock bias. The proposed algorithm is derived based on (5.2).

Stage 1:

If the i^{th} sensor is in the j^{th} sub-array, we have

$$r_i^o = r_{m_{j-1}+1}^o + r_{i,m_{j-1}+1}^o \tag{5.3}$$

Taking square of both side and expanding,

$$r_{i,m_{j-1}+1}^{o2} + 2 r_{i,m_{j-1}+1}^o r_{m_{j-1}+1}^o = \mathbf{s}_i^T \mathbf{s}_i - \mathbf{s}_{m_{j-1}+1}^T \mathbf{s}_{m_{j-1}+1} - 2(\mathbf{s}_i - \mathbf{s}_{m_{j-1}+1})^T \mathbf{u}^o \tag{5.4}$$

Let $n_{i,m_{j-1}+1}$ be noise of $r_{i,m_{j-1}+1}$, which is related to the noise in the original TDOA noise $n_{i,m_{j-1}+1} = n_{i,1} - n_{m_{j-1}+1,1}$. we can represent $r_{i,m_{j-1}+1}$ as

$$r^o_{i,m_{j-1}+1} = r_{i,m_{j-1}+1} - n_{i,m_{j-1}+1} \tag{5.5}$$

Hence, (5.4) can be expressed as

$$2r^o_i n_{i,m_{j-1}+1} = r^2_{i,m_{j-1}+1} - \mathbf{s}_i^T\mathbf{s}_i + \mathbf{s}^T_{m_{j-1}+1}\mathbf{s}_{m_{j-1}+1} + 2(\mathbf{s}_i - \mathbf{s}_{m_{j-1}+1})^T\mathbf{u}^o + 2r_{i,m_{j-1}+1}r^o_{m_{j-1}+1} \tag{5.6}$$

For all N sub-arrays, we have $m_N - N$ equations:

$$\begin{cases} 2r^o_2 n_{21} = r^2_{21} - \mathbf{s}_2^T\mathbf{s}_2 + \mathbf{s}_1^T\mathbf{s}_1 + 2(\mathbf{s}_2 - \mathbf{s}_1)^T\mathbf{u}^o + 2r_{21}r^o_1 \\ \vdots \\ 2r^o_i n_{i,m_{j-1}+1} = r^2_{i,m_{j-1}+1} - \mathbf{s}_i^T\mathbf{s}_i + \mathbf{s}^T_{m_{j-1}+1}\mathbf{s}_{m_{j-1}+1} + 2(\mathbf{s}_i - \mathbf{s}_{m_{j-1}+1})^T\mathbf{u}^o \\ +2r_{i,m_{j-1}+1}r^o_{m_{j-1}+1} \\ \vdots \\ 2r^o_{m_N} n_{m_N,m_{N-1}+1} = r^2_{m_N,m_{N-1}+1} - \mathbf{s}^T_{m_N}\mathbf{s}_{m_N} + \mathbf{s}^T_{m_{N-1}+1}\mathbf{s}_{m_{N-1}+1} \\ +2(\mathbf{s}_{m_N} - \mathbf{s}_{m_{N-1}+1})^T\mathbf{u}^o + 2r_{m_N,m_{N-1}+1}r^o_{m_{N-1}+1} \end{cases} \tag{5.7}$$

Let the unknown vector be $\boldsymbol{\varphi}^o_1 = [\mathbf{u}^{oT}, r^o_1, r^o_{m_1+1}, \ldots, r^o_{m_{N-1}+1}]^T$, where $r_{m_{j-1}+1},\ j = 1, 2, \ldots, N$ are nuisance variables. Expressing (5.7) in matrix form,

$$\boldsymbol{\epsilon}_1 = \mathbf{B}_1\mathbf{n}_a = \mathbf{h}_1 - \mathbf{G}_1\boldsymbol{\varphi}^o_1 \tag{5.8}$$

where

$$\mathbf{B}_1 = 2\begin{bmatrix} r^o_2 & & & & & & \\ & \ddots & & & & & \\ & & r^o_{m_1} & & & & \\ & & & \ddots & & & \\ & & & & r^o_{m_{N-1}+2} & & \\ & & & & & \ddots & \\ & & & & & & r^o_{m_N} \end{bmatrix}_{(m_N-N)\times(m_N-N)} \tag{5.9}$$

$$\mathbf{h}_1 = \begin{bmatrix} r_{21}^2 - \mathbf{s}_2^T\mathbf{s}_2 + \mathbf{s}_1^T\mathbf{s}_1 \\ \vdots \\ r_{m_1,1}^2 - \mathbf{s}_{m_1}^T\mathbf{s}_{m_1} + \mathbf{s}_1^T\mathbf{s}_1 \\ \vdots \\ r_{m_{N-1}+2,m_{N-1}+1}^2 - \mathbf{s}_{m_{N-1}+2}^T\mathbf{s}_{m_{N-1}+2} + \mathbf{s}_{m_{N-1}+1}^T\mathbf{s}_{m_{N-1}+1} \\ \vdots \\ r_{m_N,m_{N-1}+1}^2 - \mathbf{s}_{m_N}^T\mathbf{s}_{m_N} + \mathbf{s}_{m_{N-1}+1}^T\mathbf{s}_{m_{N-1}+1} \end{bmatrix}_{(m_N-N)\times 1)} \tag{5.10}$$

$$\mathbf{G}_1 = -2\begin{bmatrix} (\mathbf{s}_2 - \mathbf{s}_1)^T & r_{21} & 0 & \dots & 0 \\ \vdots & \vdots & \vdots & \ddots & \vdots \\ (\mathbf{s}_{m_1} - \mathbf{s}_1)^T & r_{m_1,1} & 0 & \dots & 0 \\ \vdots & \vdots & & \vdots & \\ (\mathbf{s}_{m_{N-1}+2} - \mathbf{s}_{m_{N-1}+1})^T & 0 & \dots & 0 & r_{m_{N-1}+2,m_{N-1}+1} \\ \vdots & \vdots & \ddots & \vdots & \vdots \\ (\mathbf{s}_{m_N} - \mathbf{s}_{m_{N-1}+1})^T & 0 & \dots & 0 & r_{m_N,m_{N-1}+1} \end{bmatrix}_{(m_N-N)\times(N+3)} \tag{5.11}$$

and $\mathbf{n}_a$ is the noise vector of the modified TDOA measurements in (5.2),

$$\mathbf{n}_a = \begin{bmatrix} n_{21} & \dots & n_{m_1,1} & n_{m_1+2,m_1+1} & \dots & n_{m_2,m_1+1} \dots & n_{m_{N-1}+2,m_{N-1}+1} & \dots & n_{m_N,m_{N-1}+1} \end{bmatrix}^T. \tag{5.12}$$

It is related to the TDOA measurement noise vector $\mathbf{n}$ through

$$\mathbf{n}_a = \mathbf{A}\mathbf{n} \tag{5.13}$$

where

$$\mathbf{A} = \begin{bmatrix} \mathbf{D}_1 & & & \\ & \mathbf{D}_2 & & \\ & & \ddots & \\ & & & \mathbf{D}_N \end{bmatrix} \tag{5.14}$$

is a block diagonal matrix whose first block is

$$\mathbf{D}_1 = \mathbf{I}_{m_1-1\times m_1-1}$$

and the i^{th} block is

$$\mathbf{D}_i = \begin{bmatrix} -\mathbf{1}_{(m_j-m_{j-1}-1)\times 1} & \mathbf{I}_{(m_j-m_{j-1}-1)\times(m_j-m_{j-1}-1)} \end{bmatrix}$$

The covariance matrix of $\mathbf{n}_a$ is

$$\begin{aligned} cov(\mathbf{n}_a) &= E\left[\mathbf{n}_a\mathbf{n}_a^T\right] \\ &= E\left[\mathbf{An}(\mathbf{An})^T\right] \\ &= \mathbf{A}E\left[\mathbf{nn}^T\right]\mathbf{A}^T \\ &= \mathbf{AQA}^T \qquad (5.15) \\ &= \mathbf{Q}_a \qquad (5.16) \end{aligned}$$

The weighted least-square (WLS) technique can be applied to estimate $\boldsymbol{\varphi}_1$ and the result is

$$\boldsymbol{\varphi}_1 = (\mathbf{G}_1^T\mathbf{W}_1\mathbf{G}_1)^{-1}\mathbf{G}_1^T\mathbf{W}_1\mathbf{h}_1 \qquad (5.17)$$

and the covariance matrix of $\boldsymbol{\varphi}_1$ is

$$cov(\boldsymbol{\varphi}_1) = (\mathbf{G}_1^T\mathbf{W}_1\mathbf{G}_1)^{-1}. \qquad (5.18)$$

The weighting matrix $\mathbf{W}_1$ is calculated using

$$\mathbf{W}_1 = E[\boldsymbol{\epsilon}_1\boldsymbol{\epsilon}_1^T]^{-1} = (\mathbf{B}_1^T\mathbf{Q}_a\mathbf{B}_1)^{-1}. \qquad (5.19)$$

Stage 2:

In stage 2, we refine the source location estimate in $\boldsymbol{\varphi}_1(1:3)$ using $r_1^o,\ r_{m_1+1}^o,\ \ldots,\ r_{m_{N-1}+1}$. Let $\boldsymbol{\varphi}_2^o = [x^{o2}, y^{o2}, z^{o2}]^T$. Since $\boldsymbol{\varphi}_1(1:3)$ is an estimator of $\mathbf{u}^o$, $\boldsymbol{\varphi}_1(1:3) = \mathbf{u}^o + \Delta\boldsymbol{\varphi}_1(1:3)$, where $\Delta\boldsymbol{\varphi}_1(1:3)$ is the estimation noise. Thus

$$(\boldsymbol{\varphi}_1(1:3)^o - \Delta\boldsymbol{\varphi}_1(1:3)) \odot (\boldsymbol{\varphi}_1(1:3)^o - \Delta\boldsymbol{\varphi}_1(1:3)) = \mathbf{u}^o \odot \mathbf{u}^o \qquad (5.20)$$

$$\boldsymbol{\varphi}_1(1:3)^o \odot \boldsymbol{\varphi}_1(1:3)^o - 2\boldsymbol{\varphi}_1(1:3)^o \odot \Delta\boldsymbol{\varphi}_1(1:3)^o = \mathbf{u}^o \odot \mathbf{u}^o \qquad (5.21)$$

or

$$2\boldsymbol{\varphi}_1(1:3) \odot \Delta\boldsymbol{\varphi}_1(1:3) \approx \boldsymbol{\varphi}_1(1:3) \odot \boldsymbol{\varphi}_1(1:3) - \mathbf{u}^o \odot \mathbf{u}^o. \qquad (5.22)$$

Recall that $\boldsymbol{\varphi}_1(j+3) = r_{m_{j-1}+1}^o + \Delta r_{m_{j-1}+1}, j = 1, \ldots, N$, where $\Delta r_{m_{j-1}+1}$ is the estimation noise. Hence

$$(\boldsymbol{\varphi}_1(j+3) - \Delta\boldsymbol{\varphi}_1(j+3))^2 = (\mathbf{u}^o - \mathbf{s}_{m_{j-1}+1})^T(\mathbf{u}^o - \mathbf{s}_{m_{j-1}+1}) \qquad (5.23)$$

Expanding (5.23) and substituting $\mathbf{u}^o = \boldsymbol{\varphi}_1(1:3) - \Delta\boldsymbol{\varphi}_1(1:3)$ we have

$$2\mathbf{s}_{m_{j-1}+1}^T\Delta\boldsymbol{\varphi}_1(1:3)+2\boldsymbol{\varphi}_1(j+3)\Delta\boldsymbol{\varphi}_1(j+3) = \boldsymbol{\varphi}_1(j+3)^2+2\mathbf{s}_{m_{j-1}+1}^T\boldsymbol{\varphi}_1(1:3)-\mathbf{s}_{m_{j-1}+1}^T\mathbf{s}_{m_{j-1}+1}-\mathbf{u}^{oT}\mathbf{u}^o \tag{5.24}$$

Over all j from 1 to N, we obtain

$$\begin{cases} 2\mathbf{s}_1^T\Delta\boldsymbol{\varphi}_1(1:3) + 2\boldsymbol{\varphi}_1(4)\Delta\boldsymbol{\varphi}_1(4) = \boldsymbol{\varphi}_1(4)^2 + 2\mathbf{s}_1^T\boldsymbol{\varphi}_1(1:3) - \mathbf{s}_1^T\mathbf{s}_1 - \mathbf{u}^{oT}\mathbf{u}^o \\ \vdots \\ 2\mathbf{s}_{m_{N-1}+1}^T\Delta\boldsymbol{\varphi}_1(1:3) + 2\boldsymbol{\varphi}_1(N+3)\Delta\boldsymbol{\varphi}_1(N+3) \\ = \boldsymbol{\varphi}_1(N+3)^2 + 2\mathbf{s}_{m_{N-1}+1}^T\boldsymbol{\varphi}_1(1:3) - \mathbf{s}_{m_{N-1}+1}^T\mathbf{s}_{m_{N-1}+1} - \mathbf{u}^{oT}\mathbf{u}^o \end{cases}. \tag{5.25}$$

We can express (5.22) and (5.25) in matrix form as

$$\boldsymbol{\epsilon}_2 = \mathbf{B}_2\Delta\boldsymbol{\varphi}_1 = \mathbf{h}_2 - \mathbf{G}_2\boldsymbol{\varphi}_2 \tag{5.26}$$

where

$$\mathbf{B}_2 = 2\begin{bmatrix} diag(\boldsymbol{\varphi}_1(1:3)) & & \\ \mathbf{s}_1^T & \boldsymbol{\varphi}_1(4) & \\ \vdots & & \ddots \\ \mathbf{s}_{m_{N-1}+1}^T & & \boldsymbol{\varphi}_1(N+3) \end{bmatrix} \tag{5.27}$$

$$\mathbf{h}_2 = \begin{bmatrix} \boldsymbol{\varphi}_1(1:3) \odot \boldsymbol{\varphi}_1(1:3) \\ \boldsymbol{\varphi}_1(4)^2 + 2\mathbf{s}_1^T\boldsymbol{\varphi}_1(1:3) - \mathbf{s}_1^T\mathbf{s}_1 \\ \vdots \\ \boldsymbol{\varphi}_1(N+3)^2 + 2\mathbf{s}_{m_{N-1}+1}^T\boldsymbol{\varphi}_1(1:3) - \mathbf{s}_{m_{N-1}+1}^T\mathbf{s}_{m_{N-1}+1} \end{bmatrix} \tag{5.28}$$

$$\mathbf{G}_2 = \begin{bmatrix} 1 & 0 & 0 \\ 0 & 1 & 0 \\ 0 & 0 & 1 \\ 1 & 1 & 1 \\ & \vdots & \\ 1 & 1 & 1 \end{bmatrix} \tag{5.29}$$

The WLS solution for stage 2 is

$$\boldsymbol{\varphi}_2 = (\mathbf{G}_2^T\mathbf{W}_2\mathbf{G}_2)^{-1}\mathbf{G}_2^T\mathbf{W}_2\mathbf{h}_2. \tag{5.30}$$

The weighting matrix is $\mathbf{W}_2 = E[\boldsymbol{\epsilon}_2\boldsymbol{\epsilon}_2^T]^{-1} = [\mathbf{B}_2 cov(\boldsymbol{\varphi}_1)\mathbf{B}_2^T]^{-1} = \mathbf{B}_2^{-T}(\mathbf{G}_1^T\mathbf{W}_1\mathbf{G}_1)\mathbf{B}_2^{-1}$, where (5.18) has been used.

The covariance matrix of $\boldsymbol{\varphi}_2$ is

$$cov(\boldsymbol{\varphi}_2) = (\mathbf{G}_2^T\mathbf{W}_2\mathbf{G}_2)^{-1} \tag{5.31}$$

The source location estimate $\mathbf{u} = [x, y, z]^T$ can be obtained from $\boldsymbol{\varphi}_2$ using

$$\mathbf{u} = \mathbf{P}[\sqrt{\boldsymbol{\varphi}_2(1)}, \sqrt{\boldsymbol{\varphi}_2(2)}, \sqrt{\boldsymbol{\varphi}_2(3)}]^T \tag{5.32}$$

where

$$\mathbf{P} = diag[sgn(\boldsymbol{\varphi}_1(1)), sgn(\boldsymbol{\varphi}_1(2)), sgn(\boldsymbol{\varphi}_1(3))]. \tag{5.33}$$

According to (5.32), squaring and taking differential,

$$\Delta\mathbf{u} = \mathbf{B}_3^{-1}\Delta\boldsymbol{\varphi}_2 \tag{5.34}$$

where

$$\mathbf{B}_3 = 2\begin{bmatrix} x^o & & \\ & y^o & \\ & & z^o \end{bmatrix}. \tag{5.35}$$

The covariance matrix of the final source position estimator is

$$cov(\mathbf{u}) = \mathbf{B}_3^{-1} cov(\boldsymbol{\varphi}_2)\mathbf{B}_3^{-T}. \tag{5.36}$$

5.2 Simulation

The weighting matrix $\mathbf{W}_1$ is dependent on the unknown true source position. In our simulation, we first initialize it to $\mathbf{Q}_a = \mathbf{AQA}^T$, which is the covariance matrix of the transformed noise vector $\mathbf{n}_a = \mathbf{An}$. Then we have an initial estimate of the source localization by applying (5.17) and use it to update $\mathbf{W}_1$. Using the new $\mathbf{W}_1$, we can have a more accurate result of $\boldsymbol{\varphi}_1$. In our simulation, the number of times to repeat the computation of $\boldsymbol{\varphi}1$ and the update of $\mathbf{W}_1$ is set to 2.

In the simulation a total of 12 sensors is used. Table 5.1 gives the sensor positions used in simulation. Figure 5.1 is the geometric distribution of the sensors.

x_i	30	40	30	350	100	200	200	500	300	-400	300	400
y_i	10	15	50	200	-100	200	100	400	400	200	500	400
z_i	15	10	20	100	100	300	-150	400	-200	300	-400	200

Table 5.1: True Sensor Positions

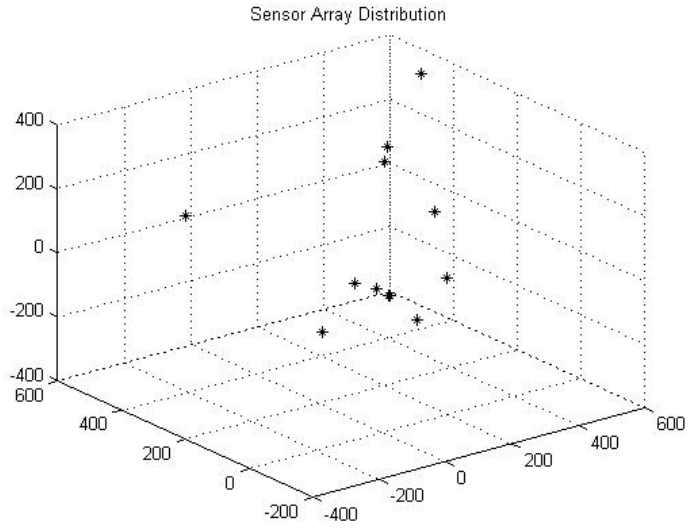

Figure 5.1: Distribution of sensors

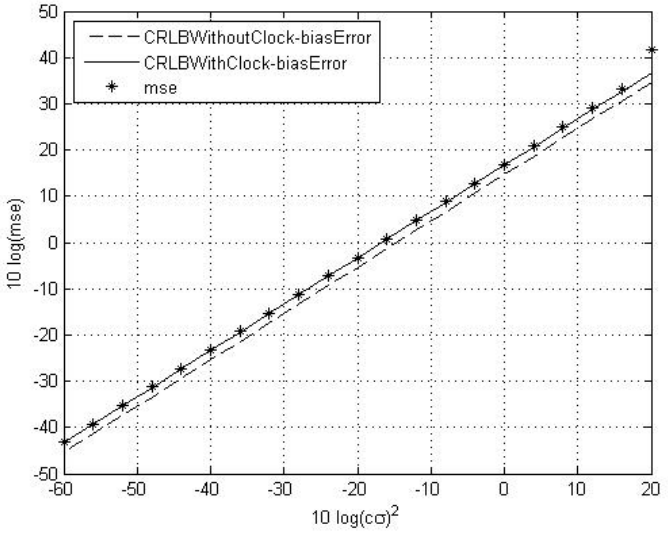

Figure 5.2: Near-field source localization in the presence of two clock offsets

The TDOA measurements are obtained according to $\mathbf{r} = \mathbf{r}^o + \mathbf{n}$ where $\mathbf{r}$ is the TDOA measurements with noise, $\mathbf{r}^o$ is the true TDOA values and $\mathbf{n}$ is the noise vector. In simulation, $\mathbf{r}^o$ is calculated by $r_{i1}^o = \|\mathbf{u}^o - \mathbf{s}_i\| - \|\mathbf{u}^o - \mathbf{s}_1\|$ and $\mathbf{Q}$ is the the covariance matrix of $\mathbf{n}$.

Besides measurement noise, we have clock-bias error in the simulation. All the sensors can be divided into several sub-arrays. Within one sub-array, the sensors are synchronized. However, the clocks among different sub-arrays are not synchronized. The clock bias δ_i are generated randomly in each ensemble run.

In the simulation, we compare mse(mean-square error) with CRLB. It is obtained according to $mse = \frac{\sum_{k=1}^{K}(\mathbf{u}^o - \mathbf{u}^{(K)})^T(\mathbf{u}^o - \mathbf{u}^{(K)})}{K}$, where K is the number of ensemble run of the proposed solution and $u^{(K)}$ is the source location estimate of the proposed algorithm at ensemble run K. We set K to 5000.

Figure 5.2 is the simulation result for a near-field source of $\mathbf{u}^o = [600, 550, 650]^T$. The measurement noise matrix $\mathbf{Q}$ is set to $c^2\sigma^2$ in the diagonal elements and $0.5c^2\sigma^2$ otherwise. We have 3 sub-arrays in this simulation and Table 5.2 shows the sensor positions of the three sub-arrays. From the figure, the CRLB with the clock-bias error is higher than the CRLB in the absence of the clock-bias error. The accuracy of source localization decreases because clock-bias error is introduced. The performance of the proposed estimator reach the CRLB when the noise power is small.

	Sub-array 1			Sub-array 2						Sub-array 3		
x_i	30	40	30	350	100	200	200	500	300	-400	300	400
y_i	10	15	50	200	-100	200	100	400	400	200	500	400
z_i	15	10	20	100	100	300	-150	400	-200	300	-400	200

Table 5.2: Sensor positions of the 3 sub-arrays

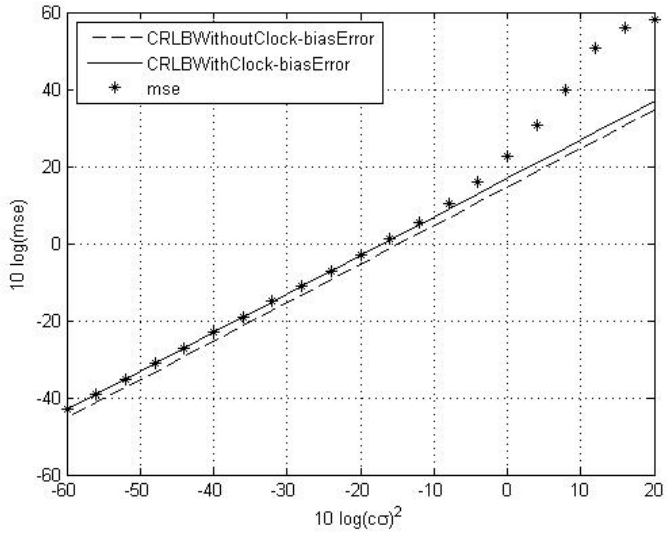

Figure 5.3: Near-field source localization in the presence of three clock offsets

Figure 5.3 is the simulation where we have three clock bias values. The source is a near-field source at $\mathbf{u}^o = [600, 550, 650]^T$. The measurement noise matrix $\mathbf{Q}$ is set to $c^2\sigma^2$ in the diagonal elements and $0.5c^2\sigma^2$ otherwise.Table 5.3 is the grouping of the sensors in the sub-arrays. From the figure, CRLB in the presence the clock-bias error is higher than the CRLB in the absence of the clock-bias error. The performance of the estimator reaches the CRLB when the noise power is small. However, having three clock offsets has performance diverging from the CRLB earlier compare to the case in Figure 5.3 where there are only two clock bias offsets.

Figure 5.4 is the simulation result for the distant source $\mathbf{u}^o = [2000, 2500, 3000]^T$. The measurement noise matrix $\mathbf{Q}$ is set to $c^2\sigma^2$ in the diagonal elements and $0.5c^2\sigma^2$ otherwise. Table 5.2 is the sensor positions of the 3 sub-arrays. From the figure, we observe the CRLB with the clock-bias error is higher than the CRLB in the absence of the clock-bias error.The mean square error of the distant source in Figure 5.4 diverges from the CRLB earlier of the near-field source.

	Sub-array 1			Sub-array 2			Sub-array 3			Sub-array 4		
x_i	30	40	30	350	100	200	200	500	300	-400	300	400
y_i	10	15	50	200	-100	200	100	400	400	200	500	400
z_i	15	10	20	100	100	300	-150	400	-200	300	-400	200

Table 5.3: Sensor position of 4 sub-arrays

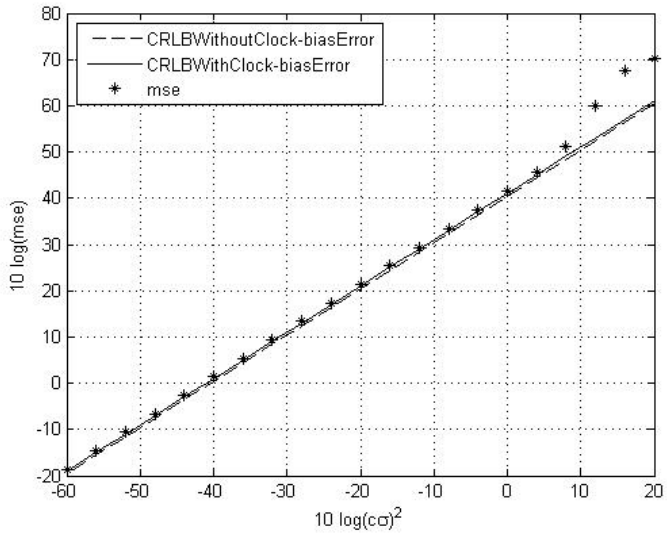

Figure 5.4: Distant source localization in the clock-bias error of two clock offsets

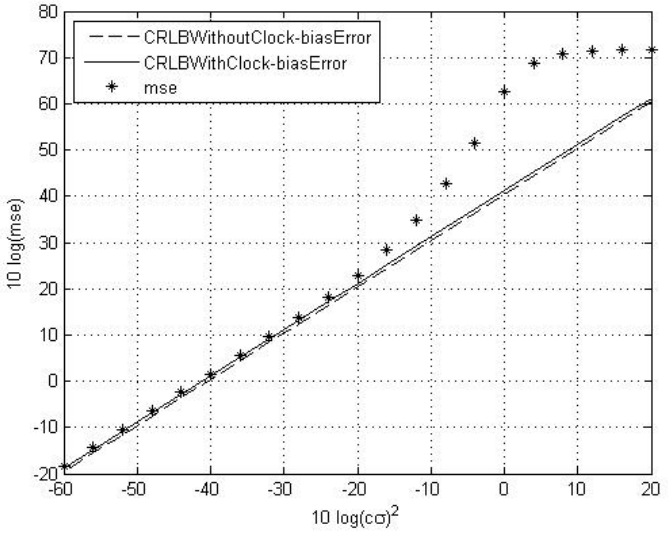

Figure 5.5: Distant source localization in the clock-bias error of three clock offsets

Nevertheless the performance of the estimator reaches the CRLB when the noise power is small.

Figure 5.5 is the simulation for the distant source at $\mathbf{u}^o = [2000, 2500, 3000]^T$ with three clock bias offsets. The measurement noise matrix $\mathbf{Q}$ is set to $c^2\sigma^2$ in the diagonal elements and $0.5c^2\sigma^2$ otherwise. Table 5.3 gives the sensor positions of the simulation. From Figure 5.5, the CRLB in the presence the clock-bias error is higher than the CRLB in the absence of the clock-bias error. The performance of the estimator reaches the CRLB when the noise power is small. However, mean square error of three clock bias offsets diverges from the CRLB earlier than that when we have only two clock bias. In addition, mean square error of far-field source diverges earlier than the mean square error of the near-field source.

5.3 Mathematic Proof of Optimum Performance of the Proposed Estimator for Source Localization in the Presence of Clock-bias Error

In this section, we will prove the mean square error of the proposed estimator achieve the CRLB performance. The CRLB of the source localization in the presence of clock-bias error has been

given in chapter 3. We will evaluate the covariance of the proposed estimator and compare it with the CRLB

$$\begin{aligned} cov(\mathbf{u})^{-1} &= \mathbf{B}_3^T cov(\boldsymbol{\varphi}_2)^{-1}\mathbf{B}_3 \\ &= \mathbf{B}_3^T\mathbf{G}_2^T\mathbf{B}_2^{-T}\mathbf{G}_1^T\mathbf{B}_1^{-T}(\mathbf{A}\mathbf{Q}\mathbf{A}^T)^{-1}\mathbf{B}_1^{-1}\mathbf{G}_1\mathbf{B}_2^{-1}\mathbf{G}_2\mathbf{B}_3 \end{aligned} \tag{5.37}$$

Under the situation in which $\mathbf{B}_2^{o-1}\Delta\boldsymbol{\varphi} \approx \mathbf{0}$, $\mathbf{B}_2 \approx \mathbf{B}_2^o$, where $\mathbf{B}_2$ is defined in (5.27) and $\mathbf{B}_2^o$ is $\mathbf{B}_2$ with all the noisy quantities replaced by the true value. Applying the block matrix inversion lemma on $\mathbf{B}_2^o$ gives

$$\mathbf{B}_2^{-1} \approx \frac{1}{2}\begin{bmatrix} [diag(\mathbf{u}^o)]^{-1} & \mathbf{O} \\ -\begin{bmatrix} \frac{\mathbf{s}_1^T}{r_1^o} \\ \vdots \\ \frac{\mathbf{s}_{m_{N-1}+1}^T}{r_{m_{N-1}+1}^o} \end{bmatrix}[diag(\mathbf{u}^o)]^{-1} & \begin{bmatrix} \frac{1}{r_1^o} & & \\ & \ddots & \\ & & \frac{1}{r_{m_{N-1}+1}^o} \end{bmatrix} \end{bmatrix} \tag{5.38}$$

Substituting (5.9),(5.11),(5.29) and (5.35), we have

$$\begin{aligned} &\mathbf{B}_1^{-1}\mathbf{G}_1\mathbf{B}_2^{-1}\mathbf{G}_2\mathbf{B}_3 \\ = \quad - &\begin{bmatrix} \frac{(\mathbf{s}_2-\mathbf{s}_1)^T}{r_2^o} + \frac{r_{21}(\mathbf{u}^o-\mathbf{s}_1)^T}{r_2^o r_1^o} \\ \vdots \\ \frac{(\mathbf{s}_{m_1}-\mathbf{s}_1)^T}{r_{m_1}^o} + \frac{r_{m_1,1}(\mathbf{u}^o-\mathbf{s}_1)^T}{r_{m_1}^o r_1^o} \\ \vdots \\ \frac{(\mathbf{s}_{m_{N-1}+2}-\mathbf{s}_{m_{N-1}+1})^T}{r_{m_{N-1}+2}^o} + \frac{r_{m_{N-1}+2,m_{N-1}+1}(\mathbf{u}^o-\mathbf{s}_{N-1+1})^T}{r_{m_{N-1}+2}^o r_{m_{N-1}+1}^o} \\ \vdots \\ \frac{(\mathbf{s}_{m_N}-\mathbf{s}_{m_{N-1}+1})^T}{r_{m_N}^o} + \frac{r_{m_N,m_{N-1}+1}(\mathbf{u}^o-\mathbf{s}_{m_{N-1}+1})^T}{r_{m_N}^o r_{m_{N-1}+1}^o} \end{bmatrix} \end{aligned} \tag{5.39}$$

If the measurement noise is small enough compare to the distance between the source and sensors, the condition $C_1: \frac{n_{j1}}{r_j^o} \approx 0, j = 2, \ldots, M$ is satisfied. As a result,

$$
\begin{aligned}
& \mathbf{B}_1^{-1}\mathbf{G}_1\mathbf{B}_2^{-1}\mathbf{G}_2\mathbf{B}_3 \\
= \quad & -\begin{bmatrix}
\frac{(\mathbf{s}_2-\mathbf{s}_1)^T}{r_2^o} + \frac{r_{21}^o(\mathbf{u}^o-\mathbf{s}_1)^T}{r_2^o r_1^o} \\
\vdots \\
\frac{(\mathbf{s}_{m_1}-\mathbf{s}_1)^T}{r_{m_1}^o} + \frac{r_{m_1,1}^o(\mathbf{u}^o-\mathbf{s}_1)^T}{r_{m_1}^o r_1^o} \\
\vdots \\
\frac{(\mathbf{s}_{m_{N-1}+2}-\mathbf{s}_{m_{N-1}+1})^T}{r_{m_{N-1}+2}^o} + \frac{r_{m_{N-1}+2,m_{N-1}+1}^o(\mathbf{u}^o-\mathbf{s}_{m_{N-1}+1})^T}{r_{m_{N-1}+2}^o r_{m_{N-1}+1}^o} \\
\vdots \\
\frac{(\mathbf{s}_{m_N}-\mathbf{s}_{m_{N-1}+1})^T}{r_{m_N}^o} + \frac{r_{m_N,m_{N-1}+1}^o(\mathbf{u}^o-\mathbf{s}_{m_{N-1}+1})^T}{r_{m_N}^o r_{m_{N-1}+1}^o}
\end{bmatrix} \\
= \quad & \begin{bmatrix}
\frac{(\mathbf{u}^o-\mathbf{s}_2^o)^T}{r_2^o} - \frac{(\mathbf{u}^o-\mathbf{s}_1^o)^T}{r_1^o} \\
\vdots \\
\frac{(\mathbf{u}^o-\mathbf{s}_{m_1}^o)^T}{r_{m_1}^o} - \frac{(\mathbf{u}^o-\mathbf{s}_1^o)^T}{r_1^o} \\
\vdots \\
\frac{(\mathbf{u}^o-\mathbf{s}_{m_{N-1}+2}^o)^T}{r_{m_{N-1}+2}^o} - \frac{(\mathbf{u}^o-\mathbf{s}_{m_{N-1}+1}^o)^T}{r_{m_{N-1}+1}^o} \\
\vdots \\
\frac{(\mathbf{u}^o-\mathbf{s}_{m_N}^o)^T}{r_{m_N}^o} - \frac{(\mathbf{u}^o-\mathbf{s}_{m_{N-1}+1}^o)^T}{r_{m_{N-1}+1}^o}
\end{bmatrix} \\
= \quad & \begin{bmatrix}
\frac{\partial r_{21}^o}{\partial \mathbf{u}^o} \\
\vdots \\
\frac{\partial r_{m_1,1}^o}{\partial \mathbf{u}^o} \\
\vdots \\
\frac{\partial r_{m_{N-1}+2,m_{N-1}+1}^o}{\partial \mathbf{u}^o} \\
\vdots \\
\frac{\partial r_{m_N,m_{N-1}+1}^o}{\partial \mathbf{u}^o}
\end{bmatrix} \\
= \quad & \mathbf{A}\frac{\partial \mathbf{r}^o}{\partial \mathbf{u}^o}
\end{aligned}
\tag{5.40}
$$

where $\mathbf{r}^o = [r_{21}^o, \ldots, r_{m_N,1}^o]^T$.

Substituting (5.40) into (5.37), we have

$$
cov(\mathbf{u})^{-1} = (\frac{\partial \mathbf{r}^o}{\partial \mathbf{u}^o})^T \mathbf{A}^T (\mathbf{A}\mathbf{Q}\mathbf{A}^T)^{-1}\mathbf{A}\frac{\partial \mathbf{r}^o}{\partial \mathbf{u}^o}. \tag{5.41}
$$

From Chapter 3, the CRLB of the proposed estimator is

$$CRLB(\mathbf{u}^o)^{-1} = (\frac{\partial \mathbf{r}^o}{\partial \mathbf{u}^o})^T \left[\mathbf{Q}^{-1} - \mathbf{Q}^{-1}\mathbf{F}(\mathbf{F}^T\mathbf{Q}^{-1}\mathbf{F})^{-1}\mathbf{F}^T\mathbf{Q}^{-1}\right] \frac{\partial \mathbf{r}^o}{\partial \mathbf{u}^o}. \tag{5.42}$$

If we denote $\widetilde{\mathbf{A}} = \mathbf{Q}^{\frac{1}{2}}\mathbf{A}^T$ and $\widetilde{\mathbf{F}} = \mathbf{Q}^{-\frac{1}{2}}\mathbf{F}$,

$$\mathbf{A}^T(\mathbf{A}\mathbf{Q}\mathbf{A}^T)^{-1}\mathbf{A} = \mathbf{Q}^{-\frac{1}{2}}\widetilde{\mathbf{A}}(\widetilde{\mathbf{A}}^T\widetilde{\mathbf{A}})^{-1}\widetilde{\mathbf{A}}^T\mathbf{Q}^{-\frac{1}{2}} \tag{5.43}$$

and

$$\mathbf{Q}^{-1} - \mathbf{Q}^{-1}\mathbf{F}(\mathbf{F}^T\mathbf{Q}^{-1}\mathbf{F})^{-1}\mathbf{F}^T\mathbf{Q}^{-1} = \mathbf{Q}^{-\frac{1}{2}}\left[\mathbf{I} - \widetilde{\mathbf{F}}(\widetilde{\mathbf{F}}^T\widetilde{\mathbf{F}})^{-1}\widetilde{\mathbf{F}}^T\right]\mathbf{Q}^{-\frac{1}{2}} \tag{5.44}$$

where $\mathbf{I}$ is a $(m_N - 1) \times (m_N - 1)$ identity matrix.

Note that $\widetilde{\mathbf{A}}(\widetilde{\mathbf{A}}^T\widetilde{\mathbf{A}})^{-1}\widetilde{\mathbf{A}}^T$ is the projection matrix onto the subspace defined by the columns of $\widetilde{\mathbf{A}}$.

$\widetilde{\mathbf{F}}(\widetilde{\mathbf{F}}^T\widetilde{\mathbf{F}})^{-1}\widetilde{\mathbf{F}}^T$ is the projection matrix onto the subspace defined by the columns of $\widetilde{\mathbf{F}}$.

$$\begin{aligned}\widetilde{\mathbf{A}}^T\widetilde{\mathbf{F}} &= \mathbf{A}\mathbf{Q}^{\frac{1}{2}}\mathbf{Q}^{-\frac{1}{2}}\mathbf{F} \\ &= \mathbf{A}\mathbf{F} \\ &= \mathbf{O}\end{aligned} \tag{5.45}$$

where the definition of A in (5.14) and that of F (3.29) have been used. (5.45) indicates that the columns of $\widetilde{\mathbf{A}}$ and that of $\widetilde{\mathbf{F}}$ are orthogonal to each other. Also, the columns of them together span the entire space of dimension $m_N - 1$. Thus $\widetilde{\mathbf{A}}^T$ and $\widetilde{\mathbf{F}}$ are orthogonal. We have

$$\widetilde{\mathbf{A}}(\widetilde{\mathbf{A}}^T\widetilde{\mathbf{A}})^{-1}\widetilde{\mathbf{A}}^T = \mathbf{I} - \widetilde{\mathbf{F}}(\widetilde{\mathbf{F}}^T\widetilde{\mathbf{F}})^{-1}\widetilde{\mathbf{F}}^T \tag{5.46}$$

as a result, using (5.43), (5.44) and 5.46

$$(\frac{\partial \mathbf{r}^o}{\partial \mathbf{u}^o})^T\mathbf{A}^T(\mathbf{A}\mathbf{Q}\mathbf{A}^T)^{-1}\mathbf{A}\frac{\partial \mathbf{r}^o}{\partial \mathbf{u}^o} = (\frac{\partial \mathbf{r}^o}{\partial \mathbf{u}^o})^T \left[\mathbf{Q}^{-1} - \mathbf{Q}^{-1}\mathbf{F}(\mathbf{F}^T\mathbf{Q}^{-1}\mathbf{F})^{-1}\mathbf{F}^T\mathbf{Q}^{-1}\right] \frac{\partial \mathbf{r}^o}{\partial \mathbf{u}^o} \tag{5.47}$$

In other word,

$$cov(\mathbf{u})^{-1} = CRLB(\mathbf{u})^{-1} \tag{5.48}$$

Or,

$$cov(\mathbf{u}) = CRLB(\mathbf{u}) \tag{5.49}$$

When the condition C_1 is satisfied.

5.4 Summary

In this chapter, we proposed an estimator of the source localization problem in the presence of measurement noise and clock unknown but fixed offset. Then, simulation results shows that the proposed method reached the CRLB performance for both near-field and distant sources in small error region. In the final part of the chapter, the performance of the proposed method in reaching CRLB has been proved theoretically under the small noise condition.

Chapter 6

Source Location Estimator and Performance Analysis in the Presence of Measurement Noise, Sensor Position Manifold Uncertainties and Clock-bias Error

In this chapter, we will develop an estimator for source localization in the presence of measurement noise, sensor position manifold uncertainties and clock-bias error. The proposed algorithm is a closed-form method based on Chan and Ho's closed-form solution. The simulation result of the proposed algorithm and the theoretical proof that the proposed algorithm reaches CRLB will be given in this chapter.

6.1 Mathematic Derivation

In this section, we will derive a algorithm of source localization when the measurement noise, sensor position manifold uncertainties and clock-bias error are all present.

The unknown source position is $\mathbf{u}^o = [x^o, y^o, z^o]^T$ and the unknown true sensor position of i^{th} sensor is $\mathbf{s}_i^o = [x_i^o, y_i^o, z_i^o]^T,\ i = 1,\ \ldots,\ M.$ $\mathbf{s}_i$ is the known noisy sensor position of the i^{th} sensor, where $\mathbf{s}_i = \mathbf{s}_i^o + \Delta\mathbf{s}_i$ and $\Delta\mathbf{s}_i$ is the sensor position error. We shall represent $\Delta\mathbf{s}_i = \mathbf{V}_i\mathbf{p}$, where $\mathbf{p}$ is a random vector with length L and $\mathbf{V}_i$ is the transformation matrix that relates the random vector $\mathbf{p}$ and the position uncertainties of the i^{th} sensor.

Thus

$$\mathbf{s}_i = \mathbf{s}_i^o + \mathbf{V}_i\mathbf{p} \tag{6.1}$$

Denoting $\mathbf{s} = [\mathbf{s}_1^T, \ldots, \mathbf{s}_M^T]^T$ and $\mathbf{V} = [\mathbf{V}_1^T, \ldots, \mathbf{V}_M^T]^T$, then

$$\mathbf{s} = \mathbf{s}^o + \mathbf{V}\mathbf{p} \tag{6.2}$$

Let us further assume that the sensor array can be decomposed into N sub-arrays and the i^{th} sub-array has $(m_i - m_{i-1})$ elements, $i = 1, 2, \ldots, N$. Here, m_0 is zero and the total number of sensors is $M = m_N$. Within each sub-array the sensors are synchronized with the same clocks. However, the clocks among different sub-arrays are not synchronized and have clock bias $\delta_j, j = 2, 3, \ldots, N$ with respect to the first sub-array. Let us choose the first sensor of the first sub-array as reference for TDOA measurements.

From the emitted source signal, we have $m_N - 1$ TDOA measurements r_{i1}.

$$\begin{aligned}
r_{i1} &= \| \mathbf{u}^o - \mathbf{s}_i \| - \| \mathbf{u}^o - \mathbf{s}_1 \| + n_{i1}, i = 2, \ldots, m_1 \\
r_{i1} &= \| \mathbf{u}^o - \mathbf{s}_i \| - \| \mathbf{u}^o - \mathbf{s}_1 \| + \delta_2^o + n_{i1}, i = m_1 + 1, \ldots, m_2 \\
&\ldots \\
r_{i1} &= \| \mathbf{u}^o - \mathbf{s}_i \| - \| \mathbf{u}^o - \mathbf{s}_1 \| + \delta_N^o + n_{i1}, i = m_{N-1} + 1, \ldots, m_N
\end{aligned} \tag{6.3}$$

where $\boldsymbol{\delta}^o = [\delta_2^o, \ldots, \delta_N^o]^T$ is the clock-bias vector. we shall assume in this study $\boldsymbol{\delta}$ is deterministic and not random. $\{\mathbf{s}_1, \ldots, \mathbf{s}_{m_1}\}$, $\{\mathbf{s}_{m_1+1}, \ldots, \mathbf{s}_{m_2}\}$, $\ldots$, $\{\mathbf{s}_{m_{N-1}+1}, \ldots, \mathbf{s}_{m_N}\}$ are different sub-arrays.

Although different sub-arrays have clock bias between each other, the sensors within a sub-array

are synchronized.

We can convert the $m_N - 1$ measurements in (6.3) to the following $m_N - N$ TDOA values:

$$r_{i,m_{j-1}+1} = r_{i,1} - r_{m_{j-1}+1,1}, \begin{cases} i = m_{j-1}+2, \ldots, m_j \\ j = 1, 2, \ldots, N \end{cases} \tag{6.4}$$

where sensor $m_{j-1}+1$ in the j^{th} sub-array is used as a reference for the TDOAs within the sub-array. The above $m_N - N$ TDOA values are free of clock bias.

Stage 1:

If the i^{th} sensor is in the j^{th} sub-array, we have

$$r_i^o = r_{m_{j-1}+1}^o + r_{i,m_{j-1}+1}^o. \tag{6.5}$$

Taking square of both side and expanding,

$$r_{i,m_{j-1}+1}^{o2} + 2r_{i,m_{j-1}+1}^o r_{m_{j-1}+1}^o + 2(\mathbf{s}_i^o - \mathbf{s}_{m_{j-1}+1}^o)^T \mathbf{u}^o + \mathbf{s}_{m_{j-1}+1}^{oT} \mathbf{s}_{m_{j-1}+1}^o - \mathbf{s}_i^{oT} \mathbf{s}_i^o = 0 \tag{6.6}$$

Expressing $r_{i,m_{j-1}+1}^o = r_{i,m_{j-1}+1} - n_{i,m_{j-1}+1}$ and $\mathbf{s}_i^o = \mathbf{s}_i - \mathbf{V}_i \mathbf{p}$, where, $n_{i,m_{j-1}+1}$ is the noise of $r_{i,m_{j-1}+1}$, which is related to the original TDOA noise as $n_{i,m_{j-1}+1} = n_{i,1} - n_{m_{j-1}+1,1}$, we have

$$\begin{aligned} &2r_i^o n_{i,m_{j-1}+1} + 2(\mathbf{u}^o - \mathbf{s}_i)^T \mathbf{V}_i \mathbf{p} - 2(\mathbf{u}^o - \mathbf{s}_{m_{j-1}+1})^T \mathbf{V}_{m_{j-1}+1} \mathbf{p} \\ &= r_{i,m_{j-1}+1}^2 - \mathbf{s}_i^T \mathbf{s}_i + \mathbf{s}_{m_{j-1}+1}^T \mathbf{s}_{m_{j-1}+1} + 2(\mathbf{s}_i - \mathbf{s}_{m_{j-1}+1})^T \mathbf{u}^o + 2r_{i,m_{j-1}+1} r_{m_{j-1}+1}^o \end{aligned} \tag{6.7}$$

Because $r_{m_{j-1}+1}^o$ is the true value, it depends on the true positions of $\mathbf{s}_{m_{j-1}+1}$. Expressing

$$r_{m_{j-1}+1}^o = \|\mathbf{u}^o - \mathbf{s}_{m_{j-1}+1}^o\| = \|\mathbf{u}^o - \mathbf{s}_{m_{j-1}+1} + \Delta\mathbf{s}_{m_{j-1}+1}\| \approx \widetilde{r}_{m_{j-1}+1}^o + \boldsymbol{\rho}_{\mathbf{u}^o, \mathbf{s}_{m_{j-1}+1}}^T \mathbf{V}_{m_{j-1}+1} \mathbf{p} \tag{6.8}$$

where $\widetilde{r}_{m_{j-1}+1}^o = \|\mathbf{u}^o - \mathbf{s}_{m_{j-1}+1}\|$ and $\boldsymbol{\rho}_{\mathbf{u}^o, \mathbf{s}_{m_{j-1}+1}} \approx \frac{(\mathbf{u}^o - \mathbf{s}_{m_{j-1}+1})}{\|\mathbf{u}^o - \mathbf{s}_{m_{j-1}+1}\|}$ represents the unit vector from $\mathbf{s}_1$ to $\mathbf{u}^o$,

$$\begin{aligned} &2r_i^o n_{i,m_{j-1}+1} + 2(\mathbf{u}^o - \mathbf{s}_i)^T \mathbf{V}_i \mathbf{p} - 2(\mathbf{u}^o - \mathbf{s}_{m_{j-1}+1} + r_{i,m_{j-1}+1} \boldsymbol{\rho}_{\mathbf{u}^o, \mathbf{s}_{m_{j-1}+1}})^T \mathbf{V}_{m_{j-1}+1} \mathbf{p} \\ &= r_{i,m_{j-1}+1}^2 - \mathbf{s}_i^T \mathbf{s}_i + \mathbf{s}_{m_{j-1}+1}^T \mathbf{s}_{m_{j-1}+1} + 2(\mathbf{s}_i - \mathbf{s}_{m_{j-1}+1})^T \mathbf{u}^o + 2r_{i,m_{j-1}+1} \widetilde{r}_{m_{j-1}+1}^o \end{aligned} \tag{6.9}$$

For all sensors, we have $m_N - N$ equations.

$$\begin{cases} 2r_2^o n_{21} + 2(\mathbf{u}^o - \mathbf{s}_2)^T \mathbf{V}_2 \mathbf{p} - 2(\mathbf{u}^o - \mathbf{s}_1 + r_{21}\boldsymbol{\rho}_{\mathbf{u}^o,\mathbf{s}_1})^T \mathbf{V}_1 \mathbf{p} \\ = r_{21}^2 - \mathbf{s}_2^T \mathbf{s}_2 + \mathbf{s}_1^T \mathbf{s}_1 + 2(\mathbf{s}_2 - \mathbf{s}_1)^T \mathbf{u}^o + 2r_{21}\widetilde{r}_1^o \\ \vdots \\ 2r_i^o n_{i,m_{j-1}+1} + 2(\mathbf{u}^o - \mathbf{s}_i)^T \mathbf{V}_i \mathbf{p} - 2(\mathbf{u}^o - \mathbf{s}_{m_{j-1}+1} + r_{i,m_{j-1}+1}\boldsymbol{\rho}_{\mathbf{u}^o,\mathbf{s}_{m_{j-1}+1}})^T \mathbf{V}_{m_{j-1}+1} \mathbf{p} \\ = r_{i,m_{j-1}+1}^2 - \mathbf{s}_i^T \mathbf{s}_i + \mathbf{s}_{m_{j-1}+1}^T \mathbf{s}_{m_{j-1}+1} + 2(\mathbf{s}_i - \mathbf{s}_{m_{j-1}+1})^T \mathbf{u}^o + 2r_{i,m_{j-1}+1}\widetilde{r}_{m_{j-1}+1}^o \\ \vdots \\ 2r_{m_N}^o n_{m_N,m_{N-1}+1} + 2(\mathbf{u}^o - \mathbf{s}_{m_N})^T \mathbf{V}_{m_N} \mathbf{p} - 2(\mathbf{u}^o - \mathbf{s}_{m_{N-1}+1} + r_{m_N,m_{N-1}+1}\boldsymbol{\rho}_{\mathbf{u}^o,\mathbf{s}_{m_{N-1}+1}})^T \mathbf{V}_{m_{N-1}+1} \mathbf{p} \\ = r_{m_N,m_{N-1}+1}^2 - \mathbf{s}_{m_N}^T \mathbf{s}_{m_N} + \mathbf{s}_{m_{N-1}+1}^T \mathbf{s}_{m_{N-1}+1} + 2(\mathbf{s}_{m_N} - \mathbf{s}_{m_{N-1}+1})^T \mathbf{u}^o + 2r_{m_N,m_{N-1}+1}\widetilde{r}_{m_{N-1}+1}^o \end{cases} \tag{6.10}$$

Assume $\boldsymbol{\varphi}_1^o = [\mathbf{u}^{oT}, \widetilde{r}_1^o, \widetilde{r}_{m_1+1}^o, \ldots, \widetilde{r}_{m_{N-1}+1}^o]^T$. Express (6.10) in matrix form,

$$\boldsymbol{\epsilon}_1 = \mathbf{B}_1 \mathbf{n}_a + \mathbf{D}\mathbf{p} = \mathbf{h}_1 - \mathbf{G}_1 \boldsymbol{\varphi}_1^o \tag{6.11}$$

where

$$\mathbf{B}_1 = 2 \begin{bmatrix} r_2^o & & & & & & \\ & \ddots & & & & & \\ & & r_{m_1}^o & & & & \\ & & & \ddots & & & \\ & & & & r_{m_{N-1}+2}^o & & \\ & & & & & \ddots & \\ & & & & & & r_{m_N}^o \end{bmatrix}_{(N_m - N)\times(N_m - N)} \tag{6.12}$$

$$\mathbf{D} = 2\begin{bmatrix} (\mathbf{u}^o - \mathbf{s}_2)^T\mathbf{V}_2 - (\mathbf{u}^o - \mathbf{s}_1 + r_{21}\boldsymbol{\rho}_{\mathbf{u}^o,\mathbf{s}_1})^T\mathbf{V}_1 \\ \vdots \\ (\mathbf{u}^o - \mathbf{s}_{m_1})^T\mathbf{V}_{m_1} - (\mathbf{u}^o - \mathbf{s}_1 + r_{m_1,1}\boldsymbol{\rho}_{\mathbf{u}^o,\mathbf{s}_1})^T\mathbf{V}_1 \\ \vdots \\ (\mathbf{u}^o - \mathbf{s}_{m_{N-1}+2})^T\mathbf{V}_{m_{N-1}+2} - (\mathbf{u}^o - \mathbf{s}_{m_{N-1}+1} + r_{m_{N-1}+2,m_{N-1}+1}\boldsymbol{\rho}_{\mathbf{u}^o,\mathbf{s}_{m_{N-1}+1}})^T\mathbf{V}_{m_{N-1}+1} \\ \vdots \\ (\mathbf{u}^o - \mathbf{s}_{m_N})^T\mathbf{V}_{m_N} - (\mathbf{u}^o - \mathbf{s}_{m_{N-1}+1} + r_{m_N,m_{N-1}+1}\boldsymbol{\rho}_{\mathbf{u}^o,\mathbf{s}_{m_{N-1}+1}})^T\mathbf{V}_{m_{m_{N-1}+1}} \end{bmatrix}_{(N_m-N)\times 1} \tag{6.13}$$

$$\mathbf{h}_1 = \begin{bmatrix} r_{21}^2 - \mathbf{s}_2^T\mathbf{s}_2 + \mathbf{s}_1^T\mathbf{s}_1 \\ \vdots \\ r_{m_1,1}^2 - \mathbf{s}_{m_1}^T\mathbf{s}_{m_1} + \mathbf{s}_1^T\mathbf{s}_1 \\ \vdots \\ r_{m_{N-1}+2,m_{N-1}+1}^2 - \mathbf{s}_{m_{N-1}+2}^T\mathbf{s}_{m_{N-1}+2} + \mathbf{s}_{m_{N-1}+1}^T\mathbf{s}_{m_{N-1}+1} \\ \vdots \\ r_{m_N,m_{N-1}+1}^2 - \mathbf{s}_{m_N}^T\mathbf{s}_{m_N} + \mathbf{s}_{m_{N-1}+1}^T\mathbf{s}_{m_{N-1}+1} \end{bmatrix}_{(N_m-N)\times 1} \tag{6.14}$$

$$\mathbf{G}_1 = -2\begin{bmatrix} (\mathbf{s}_2 - \mathbf{s}_1)^T & r_{21} & 0 & \dots & 0 \\ \vdots & \vdots & \vdots & \ddots & \vdots \\ (\mathbf{s}_{m_1} - \mathbf{s}_1)^T & r_{m_1,1} & 0 & \dots & 0 \\ \vdots & \vdots & & \vdots & \\ (\mathbf{s}_{m_{N-1}+2} - \mathbf{s}_{m_{N-1}+1})^T & 0 & \dots & 0 & r_{m_{N-1}+2,m_{N-1}+1} \\ \vdots & \vdots & \ddots & \vdots & \vdots \\ (\mathbf{s}_{m_N} - \mathbf{s}_{m_{N-1}+1})^T & 0 & \dots & 0 & r_{m_N,m_{N-1}+1} \end{bmatrix}_{(N_m-N)\times(N+3)} \tag{6.15}$$

$\mathbf{n}_a$ is the noise vector of the modified TDOA measurements,

$$\mathbf{n}_a = \begin{bmatrix} n_{21} & \dots & n_{m_1,1} & n_{m_1+2,m_1+1} & \dots & n_{m_2,m_1+1} \dots & n_{m_{N-1}+2,m_{N-1}+1} & \dots & n_{m_N,m_{N-1}+1} \end{bmatrix}^T. \tag{6.16}$$

It is related to the TDOA measurement noise vector $\mathbf{n}$ through

$$\mathbf{n}_a = \mathbf{A}\mathbf{n} \tag{6.17}$$

where

$$\mathbf{A} = \begin{bmatrix} \mathbf{D}_1 & & & \\ & \mathbf{D}_2 & & \\ & & \ddots & \\ & & & \mathbf{D}_N \end{bmatrix} \tag{6.18}$$

is a block diagonal matrix whose first block is

$$\mathbf{D}_1 = \mathbf{I}_{(m_1-1)\times(m_1-1)}$$

and the i^{th} block is

$$\mathbf{D}_i = \begin{bmatrix} -\mathbf{1}_{(m_j-m_{j-1}-1)\times 1} & \mathbf{I}_{(m_j-m_{j-1}-1)\times(m_j-m_{j-1}-1)} \end{bmatrix}$$

The covariance matrix of $\mathbf{n}_a$ is

$$\begin{aligned} cov(\mathbf{n}_a) &= E\left[\mathbf{n}_a\mathbf{n}_a^T\right] \\ &= E\left[\mathbf{A}\mathbf{n}(\mathbf{A}\mathbf{n})^T\right] \\ &= \mathbf{A}E\left[\mathbf{n}\mathbf{n}^T\right]\mathbf{A}^T \\ &= \mathbf{A}\mathbf{Q}\mathbf{A}^T \qquad (6.19) \\ &= \mathbf{Q}_a. \qquad (6.20) \end{aligned}$$

The weighted least-square (WLS) technique can be applied to estimate $\boldsymbol{\varphi}_1(1:3)$ and the result is

$$\boldsymbol{\varphi}_1 = (\mathbf{G}_1^T\mathbf{W}_1\mathbf{G}_1)^{-1}\mathbf{G}_1^T\mathbf{W}_1\mathbf{h}_1 \tag{6.21}$$

and the covariance matrix of $\boldsymbol{\varphi}_1$ is

$$cov(\boldsymbol{\varphi}_1) = (\mathbf{G}_1^T\mathbf{W}_1\mathbf{G}_1)^{-1}. \tag{6.22}$$

The weighting matrix $\mathbf{W}_1$ is calculated using

$$\mathbf{W}_1 = E[\boldsymbol{\epsilon}_1\boldsymbol{\epsilon}_1^T]^{-1} = (\mathbf{B}_1\mathbf{Q}_a\mathbf{B}_1^T + \mathbf{D}\mathbf{Q}_p\mathbf{D}^T)^{-1}. \tag{6.23}$$

Stage 2:

In stage 2, we refine the source localization estimate in $\boldsymbol{\varphi}_1(1:3)$ using $\widetilde{r}_1^o,\ \widetilde{r}_{m_1+1}^o,\ \ldots,\ \widetilde{r}_{m_{N-1}+1}$. Let $\boldsymbol{\varphi}_2^o = [x^{o2}, y^{o2}, z^{o2}]^T$. Since $\boldsymbol{\varphi}_1(1:3)$ is an estimator of $\mathbf{u}^o$, $\boldsymbol{\varphi}_1(1:3) = \mathbf{u}^o + \Delta\boldsymbol{\varphi}_1(1:3)$, where $\Delta\boldsymbol{\varphi}_1(1:3)$ is the estimation noise. Thus

$$(\boldsymbol{\varphi}_1(1:3)^o - \Delta\boldsymbol{\varphi}_1(1:3)) \odot (\boldsymbol{\varphi}_1(1:3)^o - \Delta\boldsymbol{\varphi}_1(1:3)) = \mathbf{u}^o \odot \mathbf{u}^o \tag{6.24}$$

$$\boldsymbol{\varphi}_1(1:3)^o \odot \boldsymbol{\varphi}_1(1:3)^o - 2\boldsymbol{\varphi}_1(1:3)^o \odot \Delta\boldsymbol{\varphi}_1(1:3) \approx \mathbf{u}^o \odot \mathbf{u}^o \tag{6.25}$$

or

$$2\boldsymbol{\varphi}_1(1:3) \odot \Delta\boldsymbol{\varphi}_1(1:3) = \boldsymbol{\varphi}_1(1:3) \odot \boldsymbol{\varphi}_1(1:3) - \mathbf{u}^o \odot \mathbf{u}^o, \tag{6.26}$$

Where the second order noise terms is ignored. Recall that $\boldsymbol{\varphi}_1(j+3) = r^o_{m_{j-1}+1} + \Delta r_{m_{j-1}+1}, j = 1, \ldots, N$, where $\Delta r_{m_{j-1}+1}$ is the estimation noise. Hence

$$(\boldsymbol{\varphi}_1(j+3) - \Delta\boldsymbol{\varphi}_1(j+3))^2 = (\mathbf{u}^o - \mathbf{s}_{m_{j-1}+1})^T(\mathbf{u}^o - \mathbf{s}_{m_{j-1}+1}) \tag{6.27}$$

Expanding (6.27) and substituting $\mathbf{u}^o = \boldsymbol{\varphi}_1(1:3) - \Delta\boldsymbol{\varphi}_1(1:3)$ we have

$$2\mathbf{s}^T_{m_{j-1}+1}\Delta\boldsymbol{\varphi}_1(1:3) + 2\boldsymbol{\varphi}_1(j+3)\Delta\boldsymbol{\varphi}_1(j+3) = \boldsymbol{\varphi}_1(j+3)^2 + 2\mathbf{s}^T_{m_{j-1}+1}\boldsymbol{\varphi}_1(1:3) - \mathbf{s}^T_{m_{j-1}+1}\mathbf{s}_{m_{j-1}+1} - \mathbf{u}^{oT}\mathbf{u}^o. \tag{6.28}$$

Over all j from $1, \ldots, N$, we obtain

$$\begin{cases} 2\mathbf{s}_1^T\Delta\boldsymbol{\varphi}_1(1:3) + 2\boldsymbol{\varphi}_1(4)\Delta\boldsymbol{\varphi}_1(4) = \boldsymbol{\varphi}_1(4)^2 + 2\mathbf{s}_1^T\boldsymbol{\varphi}_1(1:3) - \mathbf{s}_1^T\mathbf{s}_1 - \mathbf{u}^{oT}\mathbf{u}^o \\ \vdots \\ 2\mathbf{s}^T_{m_{N-1}+1}\Delta\boldsymbol{\varphi}_1(1:3) + 2\boldsymbol{\varphi}_1(N+3)\Delta\boldsymbol{\varphi}_1(N+3) \\ = \boldsymbol{\varphi}_1(N+3)^2 + 2\mathbf{s}^T_{m_{N-1}+1}\boldsymbol{\varphi}_1(1:3) - \mathbf{s}^T_{m_{N-1}+1}\mathbf{s}_{m_{N-1}+1} - \mathbf{u}^{oT}\mathbf{u}^o \end{cases}. \tag{6.29}$$

We can express (6.26) and (6.29) in matrix form as

$$\boldsymbol{\epsilon}_2 = \mathbf{B}_2\Delta\boldsymbol{\varphi}_1 = \mathbf{h}_2 - \mathbf{G}_2\boldsymbol{\varphi}_2 \tag{6.30}$$

where

$$\mathbf{B}_2 = 2\begin{bmatrix} diag(\boldsymbol{\varphi}_1(1:3)) & & \\ \mathbf{s}_1^T & \boldsymbol{\varphi}_1(4) & \\ \vdots & & \ddots \\ \mathbf{s}^T_{m_{N-1}+1} & & \boldsymbol{\varphi}_1(N+3) \end{bmatrix} \tag{6.31}$$

$$\mathbf{h}_2 = \begin{bmatrix} \boldsymbol{\varphi}_1(1:3) \odot \boldsymbol{\varphi}_1(1:3) \\ \boldsymbol{\varphi}_1(4)^2 + 2\mathbf{s}_1^T\boldsymbol{\varphi}_1(1:3) - \mathbf{s}_1^T\mathbf{s}_1 \\ \vdots \\ \boldsymbol{\varphi}_1(N+3)^2 + 2\mathbf{s}_{m_{N-1}+1}^T\boldsymbol{\varphi}_1(1:3) - \mathbf{s}_{m_{N-1}+1}^T\mathbf{s}_{m_{N-1}+1} \end{bmatrix} \tag{6.32}$$

$$\mathbf{G}_2 = \begin{bmatrix} 1 & 0 & 0 \\ 0 & 1 & 0 \\ 0 & 0 & 1 \\ 1 & 1 & 1 \\ & \vdots & \\ 1 & 1 & 1 \end{bmatrix} \tag{6.33}$$

The WLS solution for Stage 2 is

$$\boldsymbol{\varphi}_2 = (\mathbf{G}_2^T\mathbf{W}_2\mathbf{G}_2)^{-1}\mathbf{G}_2^T\mathbf{W}_2\mathbf{h}_2. \tag{6.34}$$

The covariance matrix of $\boldsymbol{\varphi}_2$ is

$$cov(\boldsymbol{\varphi}_2) = (\mathbf{G}_2^T\mathbf{W}_2\mathbf{G}_2)^{-1} \tag{6.35}$$

where the weighting matrix is $\mathbf{W}_2 = E[\boldsymbol{\epsilon}_2\boldsymbol{\epsilon}_2^T]^{-1} = [\mathbf{B}_2 cov(\boldsymbol{\varphi}_1)\mathbf{B}_2^T]^{-1} = \mathbf{B}_2^{-T}(\mathbf{G}_1^T\mathbf{W}_1\mathbf{G}_1)\mathbf{B}_2^{-1}$.

The source location estimate $\mathbf{u} = [x, y, z]^T$ can be obtained from $\boldsymbol{\varphi}_2$ using

$$\mathbf{u} = \mathbf{P}[\sqrt{\boldsymbol{\varphi}_2(1)}, \sqrt{\boldsymbol{\varphi}_2(2)}, \sqrt{\boldsymbol{\varphi}_2(3)}]^T \tag{6.36}$$

where

$$\mathbf{P} = diag[sgn(\boldsymbol{\varphi}_1(1)), sgn(\boldsymbol{\varphi}_1(2)), sgn(\boldsymbol{\varphi}_1(3))]. \tag{6.37}$$

According to (6.36), squaring and taking differential give

$$\Delta\mathbf{u} = \mathbf{B}_3^{-1}\Delta\boldsymbol{\varphi}_2 \tag{6.38}$$

where

$$\mathbf{B}_3 = 2\begin{bmatrix} x^o & 0 & 0 \\ 0 & y^o & 0 \\ 0 & 0 & z^o \end{bmatrix}. \tag{6.39}$$

The covariance matrix of the final source position estimate is

$$cov(\mathbf{u}) = \mathbf{B}_3^{-1}cov(\boldsymbol{\varphi}_2)\mathbf{B}_3^{-T}. \tag{6.40}$$

x_i	30	40	30	350	100	200	200	500	300	-400	300	400
y_i	10	15	50	200	-100	200	100	400	400	200	500	400
z_i	15	10	20	100	100	300	-150	400	-200	300	-400	200

Table 6.1: True Sensor Positions

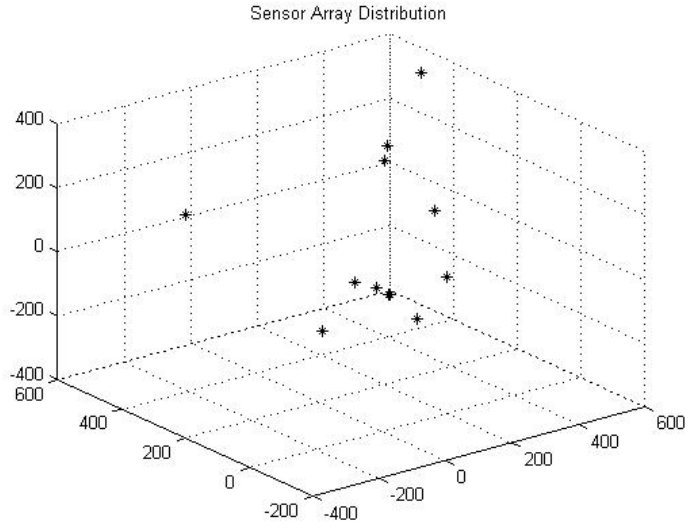

Figure 6.1: Distribution of sensors

6.2 Simulation

The weighting matrix $\mathbf{W}_1$ is dependent on the unknown true source position. In our simulation, we first initialize it to $\mathbf{Q}_a = \mathbf{AQA}$, which is the covariance matrix of the transformed noise vector $\mathbf{n}_a = \mathbf{An}$. Then we have an initial estimate of the source localization and use it to update $\mathbf{W}_1$. Using the new $\mathbf{W}_1$, we can have a more accurate result. In our simulation, the number of times to repeat the update of $\mathbf{W}_1$ and the computation of $\boldsymbol{\varphi}_1(1:3)$ is set to 2.

In this simulation a total of 12 sensors is used. Table 6.1 gives the sensor positions used in simulation. Figure 6.1 is the geometric distribution of the sensors.

The TDOA measurements are obtained according to $\mathbf{r} = \mathbf{r}^o + \mathbf{n}$ where $\mathbf{r}$ is the TDOA measurements, $\mathbf{r}^o$ is the true TDOA values and $\mathbf{n}$ is the noise vector. In the simulation, $\mathbf{r}^o$ is calculated by $r_{i1}^o = \|\mathbf{u}^o - \mathbf{s}_i\| - \|\mathbf{u}^o - \mathbf{s}_1\|$ and the covariance matrix of $\mathbf{n}$ is $\mathbf{Q}$.

Besides measurement noise, we have clock-bias error in the simulation. All the sensors can be divided into several sub-arrays. Within one sub-array, the sensors are synchronized. However,

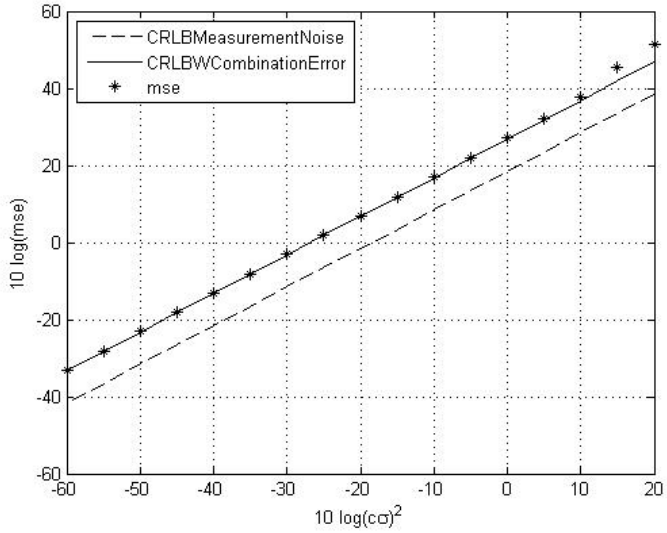

Figure 6.2: Near-field source localization in the presence of measurement noise, sensor position manifold uncertainties and clock-bias errors; the number of unknown clock offsets is 2

the clocks among different sub-arrays are not synchronized. The clock bias δ_i are generated randomly in each ensemble run.

Sensor position manifold uncertainties in the simulation are given by $\mathbf{s} = \mathbf{s}^o + \mathbf{V}\mathbf{p}$. The covariance matrix of $\mathbf{p}$ is $\mathbf{Q}_p$. We set sensor position uncertainties related to each other when sensor is from the same sub-array and independent when sensors are in different sub-arrays.

In the simulation, we compare mse(mean-square error) with the CRLB. It is obtained according to $mse = \frac{\sum_{k=1}^{K}(\mathbf{u}^o - \mathbf{u}^{(K)})^T(\mathbf{u}^o - \mathbf{u}^{(K)})}{K}$, where K is the number of ensemble runs of the proposed solution. We set K to 5000.

Figure 6.2 is the simulation result for a near-field source at $\mathbf{u}^o = [600, 550, 650]^T$. The measurement noise matrix $\mathbf{Q}$ is set to $c^2\sigma^2$ in the diagonal elements and $0.5c^2\sigma^2$ otherwise. $\mathbf{Q}_p$, is set to a $L \times L$ identity matrix with the noise power of $c^2\sigma^2$. We have two unknown clock offsets in sub-arrays 2 and 3 in this simulation and Table 6.2 shows the sensor positions of sub-arrays. From the figure, the CRLB with the sensor position manifold uncertainties and clock-bias error is higher than the CRLB with measurement noise only. The performance of the proposed estimator reaches the CRLB when the noise power is small.

Figure 6.3 shows the simulation when we have three unknown clock-bias values for a near-field source $\mathbf{u}^o = [600, 550, 650]^T$. The measurement noise matrix $\mathbf{Q}$ is set to $c^2\sigma^2$ in the diagonal

	Sub-array 1			Sub-array 2						Sub-array 3		
x_i	30	40	30	350	100	200	200	500	300	-400	300	400
y_i	10	15	50	200	-100	200	100	400	400	200	500	400
z_i	15	10	20	100	100	300	-150	400	-200	300	-400	200

Table 6.2: Sensor position of 3 sub-arrays

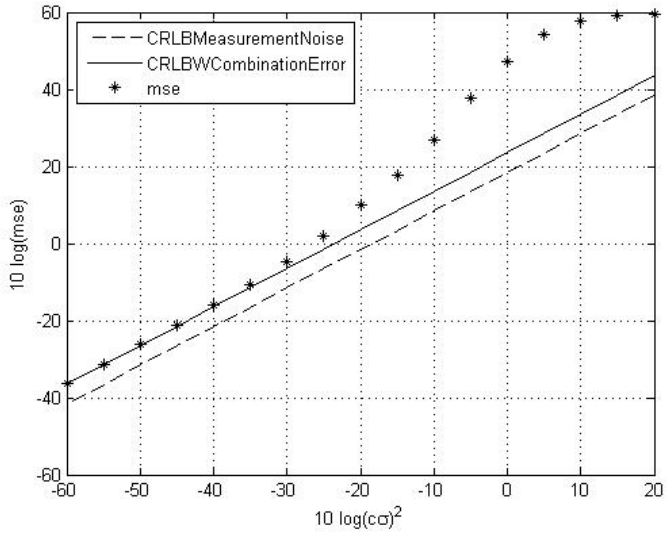

Figure 6.3: Near-field source localization in the presence of measurement noise, sensor position manifold uncertainties and clock-bias errors; the number of unknown clock offsets is 3

	Sub-array 1			Sub-array 2			Sub-array 3			Sub-array 4		
x_i	30	40	30	350	100	200	200	500	300	-400	300	400
y_i	10	15	50	200	-100	200	100	400	400	200	500	400
z_i	15	10	20	100	100	300	-150	400	-200	300	-400	200

Table 6.3: Sensor positions of 4 sub-arrays

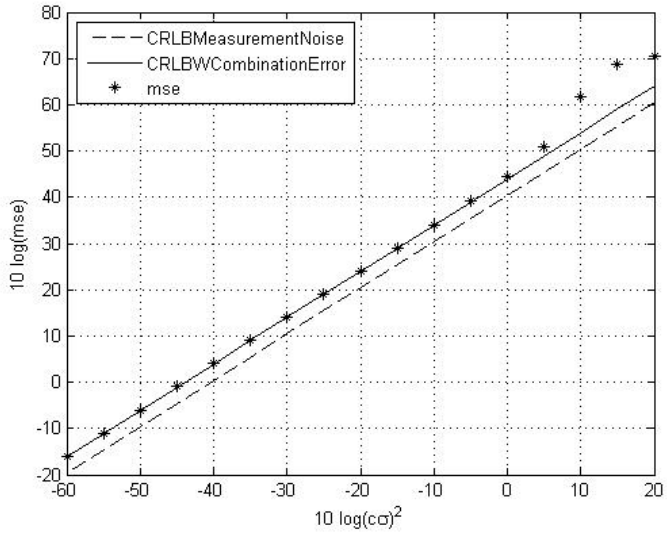

Figure 6.4: Distant source localization in the presence of measurement noise, sensor position manifold uncertainties and clock-bias errors; the number of unknown clock offsets is 2

elements and $0.5c^2\sigma^2$ otherwise. $\mathbf{Q}_p$, is set to a $L \times L$ identity matrix with the noise power of $c^2\sigma^2$. We have 4 sub-arrays in this simulation. Table 6.3 is the grouping of the sensors in the sub-arrays. From the figure, the CRLB in the presence of sensor position manifold uncertainties and clock-bias error is higher than the CRLB without them. The performance of the estimator reaches the CRLB when the noise power is small. However, having three clock offsets has performance diverging from the CRLB earlier compare to the Figure 6.2 where there are only two clock offsets.

Figure 6.4 is the simulation result for the distant source at $\mathbf{u}^o = [2000, 2500, 3000]^T$ with two clock bias offsets. The measurement noise matrix $\mathbf{Q}$ is set to $c^2\sigma^2$ in the diagonal elements and $0.5c^2\sigma^2$ otherwise. $\mathbf{Q}_p$, is set to a $L \times L$ identity matrix with the noise power of $c^2\sigma^2$. Table 6.2 shows the sensor position of the 3 sub-arrays in this simulation. From the figure, we can

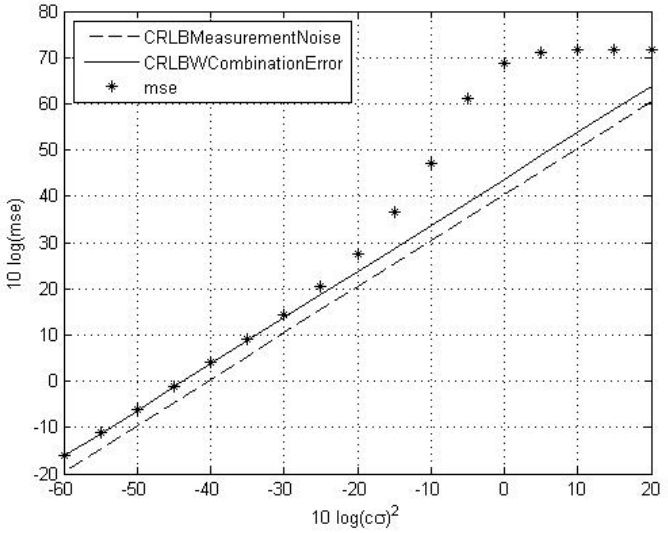

Figure 6.5: Distant source localization in the presence of measurement noise, sensor position manifold uncertainties and clock-bias errors; the number of unknown clock offsets is 3

observe that the CRLB with the sensor position manifold uncertainties and clock-bias error is higher than the CRLB in the absence of them. The mean square error of the distant source diverges from the CRLB earlier than the mean square error of near-field source by comparing Figure 6.4 and Figure 6.2. Nevertheless, the performance of the estimator reach CRLB when the noise power is small.

Figure 6.5 is the simulation for the distant source at $\mathbf{u}^o = [2000, 2500, 3000]^T$. The measurement noise matrix $\mathbf{Q}$ is set to $c^2\sigma^2$ in the diagonal elements and $0.5c^2\sigma^2$ otherwise. $\mathbf{Q}_p$, is set to a $L \times L$ identity matrix with the noise power of $c^2\sigma^2$. Table 6.3 shows gives the sensor position of the 4 sub-arrays. From Figure 6.5, the CRLB in the presence of sensor position manifold uncertainties is higher than the CRLB in the absence of them. The performance of the estimator reaches the CRLB when the noise power is small. However, the mean square error with three clock-bias offset diverges from the CRLB earlier. Compared to the case when we have two clock-bias offsets as shown in Figure 6.5. In addition, mean square error of the distant source diverges earlier than the mean square error of the near-field source.

6.3 Mathematic Proof of the Optimum Performance of the Proposed Estimator for Source Localization in the Presence of Sensor Position Manifold Uncertainties and Clock-bias Error

In this section, we shall prove the mean square error of the proposed estimator achieves the CRLB performance. The CRLB of the source localization in the presence of clock-bias error has been given in chapter 3. We will evaluate the covariance matrix of the proposed estimator and compare it with the CRLB.

$$\begin{aligned} cov(\mathbf{u})^{-1} &= \mathbf{B}_3^T cov(\boldsymbol{\varphi}_2)^{-1}\mathbf{B}_3 \\ &= \mathbf{B}_3^T\mathbf{G}_2^T\mathbf{B}_2^{-T}\mathbf{G}_1^T\mathbf{B}_1^{-T}(\mathbf{Q}_\mathbf{a}^T + \mathbf{B}_1^{-1}\mathbf{D}\mathbf{Q}_p\mathbf{D}^T\mathbf{B}_1^{-T})^{-1}\mathbf{B}_1^{-1}\mathbf{G}_1\mathbf{B}_2^{-1}\mathbf{G}_2\mathbf{B}_3 \end{aligned} \tag{6.41}$$

Denote

$$\begin{cases} \mathbf{G}_3 = \mathbf{B}_1^{-1}\mathbf{G}_1\mathbf{B}_2^{-1}\mathbf{G}_2\mathbf{B}_3 \\ \mathbf{G}_4 = \mathbf{B}_1^{-1}\mathbf{D} \end{cases} \tag{6.42}$$

We have

$$\begin{aligned} cov(\mathbf{u})^{-1} &= \mathbf{G}_3^T(\mathbf{Q}_a + \mathbf{G}_4\mathbf{Q}_\mathbf{p}\mathbf{G}_4^T)^{-1}\mathbf{G}_3 \\ &= \mathbf{G}_3^T\mathbf{Q}_a^{-1}\mathbf{G}_3 - \mathbf{G}_3^T\mathbf{Q}_a^{-1}\mathbf{G}_4(\mathbf{Q}_\mathbf{p}^{-1} + \mathbf{G}_4^T\mathbf{Q}_a^{-1}\mathbf{G}_4)\mathbf{G}_4^T\mathbf{Q}_a^{-1}\mathbf{G}_3 \end{aligned} \tag{6.43}$$

Under the situation in which $\mathbf{B}_2^{o-1}\Delta\boldsymbol{\varphi} \approx \mathbf{0}$, $\mathbf{B}_2 \approx \mathbf{B}_2^o$, where $\mathbf{B}_2$ is defined in (6.31) and $\mathbf{B}_2^o$ is $\mathbf{B}_2$ with all the noisy quantities replaced by the true value. Applying the block matrix inversion lemma on $\mathbf{B}_2^o$ gives

$$\mathbf{B}_2^{-1} \approx \frac{1}{2}\begin{bmatrix} [diag(\mathbf{u}^o)]^{-1} & \mathbf{O} \\ -\begin{bmatrix} \frac{\mathbf{s}_1^T}{r_1^o} \\ \vdots \\ \frac{\mathbf{s}_{m_{N-1}+1}^T}{r_{m_{N-1}+1}^o} \end{bmatrix}[diag(\mathbf{u}^o)]^{-1} & \begin{bmatrix} \frac{1}{r_1^o} & & \\ & \ddots & \\ & & \frac{1}{r_{m_{N-1}+1}^o} \end{bmatrix} \end{bmatrix} \tag{6.44}$$

Substituting (6.12),(6.15),(6.31),(6.33) and (6.39), we have

$$
\begin{aligned}
\mathbf{G}_3 = \quad & \mathbf{B}_1^{-1}\mathbf{G}_1\mathbf{B}_2^{-1}\mathbf{G}_2\mathbf{B}_3 \\
= \quad & -\begin{bmatrix}
\frac{(\mathbf{s}_2-\mathbf{s}_1)^T}{r_2^o} + \frac{r_{21}(\mathbf{u}^o-\mathbf{s}_1)^T}{r_2^o\widetilde{r}_1^o} \\
\vdots \\
\frac{(\mathbf{s}_{m_1}-\mathbf{s}_1)^T}{r_{m_1}^o} + \frac{r_{m_1,1}(\mathbf{u}^o-\mathbf{s}_1)^T}{r_{m_1}^o\widetilde{r}_1^o} \\
\vdots \\
\frac{(\mathbf{s}_{m_{N-1}+2}-\mathbf{s}_{m_{N-1}+1})^T}{r_{m_{N-1}+2}^o} + \frac{r_{m_{N-1}+2,m_{N-1}+1}(\mathbf{u}^o-\mathbf{s}_{m_{N-1}+1})^T}{r_{m_{N-1}+2}^o\widetilde{r}_{m_{N-1}+1}^o} \\
\vdots \\
\frac{(\mathbf{s}_{m_N}-\mathbf{s}_{m_{N-1}+1})^T}{r_{m_N}^o} + \frac{r_{m_N,m_{N-1}+1}(\mathbf{u}^o-\mathbf{s}_{m_{N-1}+1})^T}{r_{m_N}^o\widetilde{r}_{m_{N-1}+1}^o}
\end{bmatrix}
\end{aligned}
\tag{6.45}
$$

If the measurement noise is small enough compare to the distance between the source and sensors, the condition $C_1: \frac{n_{j1}}{r_j^o} \approx 0, j = 2, \ldots, M$ and $C_2: \frac{\|\mathbf{V}_j \mathbf{p}\|}{r_j^o} = 0, j = 1, \ldots, M$ are satisfied.

$$
\begin{aligned}
\mathbf{G}_3 = & -\begin{bmatrix}
\frac{(\mathbf{s}_2^o - \mathbf{s}_1^o)^T}{r_2^o} + \frac{r_{21}^o (\mathbf{u}^o - \mathbf{s}_1^o)^T}{r_2^o r_1^o} \\
\vdots \\
\frac{(\mathbf{s}_{m_1}^o - \mathbf{s}_1^o)^T}{r_{m_1}^o} + \frac{r_{m_1,1}^o (\mathbf{u}^o - \mathbf{s}_1^o)^T}{r_{m_1}^o r_1^o} \\
\vdots \\
\frac{(\mathbf{s}_{m_{N-1}+2}^o - \mathbf{s}_{m_{N-1}+1}^o)^T}{r_{m_{N-1}+2}^o} + \frac{r_{m_{N-1}+2, m_{N-1}+1}^o (\mathbf{u}^o - \mathbf{s}_{m_{N-1}+1}^o)^T}{r_{m_{N-1}+2}^o r_{m_{N-1}+1}^o} \\
\vdots \\
\frac{(\mathbf{s}_{m_N}^o - \mathbf{s}_{m_{N-1}+1}^o)^T}{r_M^o} + \frac{r_{m_N, m_{N-1}+1}^o (\mathbf{u}^o - \mathbf{s}_{m_{N-1}+1}^o)^T}{r_{m_N}^o r_{m_{N-1}+1}^o}
\end{bmatrix} \\
= & \begin{bmatrix}
\frac{(\mathbf{u}^o - \mathbf{s}_2^o)^T}{r_2^o} - \frac{(\mathbf{u}^o - \mathbf{s}_1^o)^T}{r_1^o} \\
\vdots \\
\frac{(\mathbf{u}^o - \mathbf{s}_{m_1}^o)^T}{r_{m_1}^o} - \frac{(\mathbf{u}^o - \mathbf{s}_1^o)^T}{r_1^o} \\
\vdots \\
\frac{(\mathbf{u}^o - \mathbf{s}_{m_{N-1}+2}^o)^T}{r_{m_{N-1}+2}^o} - \frac{(\mathbf{u}^o - \mathbf{s}_{m_{N-1}+1}^o)^T}{r_{m_{N-1}+1}^o} \\
\vdots \\
\frac{(\mathbf{u}^o - \mathbf{s}_{m_N}^o)^T}{r_{m_N}^o} - \frac{(\mathbf{u}^o - \mathbf{s}_{m_{N-1}+1}^o)^T}{r_{m_{N-1}+1}^o}
\end{bmatrix} \\
= & \begin{bmatrix}
\frac{\partial r_{21}^o}{\partial \mathbf{u}^o}^T \\
\vdots \\
\frac{\partial r_{m_1,1}^o}{\partial \mathbf{u}^o}^T \\
\vdots \\
\frac{\partial r_{m_{N-1}+2, m_{N-1}+1}^o}{\partial \mathbf{u}^o}^T \\
\vdots \\
\frac{\partial r_{m_N, m_{N-1}+1}^o}{\partial \mathbf{u}^o}^T
\end{bmatrix} \\
= & \mathbf{A} \frac{\partial \mathbf{r}^o}{\partial \mathbf{u}^o}
\end{aligned}
\tag{6.46}
$$

where $\mathbf{r}^o = [r^o_{21}, \ldots, r^o_{m_N,1}]^T$.

Substituting (6.13) and (6.12) into $\mathbf{G}_4$, if C_1 and C_2 are satisfied, we have

$$
\begin{aligned}
\mathbf{G}_4 &= \mathbf{B}_1^{-1}\mathbf{D} \qquad (6.47)\\
&= \begin{bmatrix}
\frac{(\mathbf{u}^o-\mathbf{s}_2)^T\mathbf{V}_2-(\mathbf{u}^o-\mathbf{s}_1+r_{21}\boldsymbol{\rho}_{\mathbf{u}^o,\mathbf{s}_1})^T\mathbf{V}_1}{r^o_2}\\
\vdots\\
\frac{(\mathbf{u}^o-\mathbf{s}_{m_1})^T\mathbf{V}_{m_1}-(\mathbf{u}^o-\mathbf{s}_1+r_{m_1,1}\boldsymbol{\rho}_{\mathbf{u}^o,\mathbf{s}_1})^T\mathbf{V}_1}{r^o_{m_1}}\\
\vdots\\
\frac{(\mathbf{u}^o-\mathbf{s}_{m_{N-1}+2})^T\mathbf{V}_{m_{N-1}+2}-(\mathbf{u}^o-\mathbf{s}_{m_{N-1}+1}+r_{m_{N-1}+2,m_{N-1}+1}\boldsymbol{\rho}_{\mathbf{u}^o,\mathbf{s}_{m_{N-1}+1}})^T\mathbf{V}_{m_{N-1}+1}}{r^o_{m_{N-1}+2}}\\
\vdots\\
\frac{(\mathbf{u}^o-\mathbf{s}_{m_N})^T\mathbf{V}_{m_N}-(\mathbf{u}^o-\mathbf{s}_{m_{N-1}+1}+r_{m_N,m_{N-1}+1}\boldsymbol{\rho}_{\mathbf{u}^o,\mathbf{s}_{m_{N-1}+1}})^T\mathbf{V}_{m_{N-1}+1}}{r^o_{m_N}}
\end{bmatrix}\\
&= \begin{bmatrix}
\frac{(\mathbf{u}^o-\mathbf{s}^o_2)^T\mathbf{V}_2-(\mathbf{u}^o-\mathbf{s}^o_1+r^o_{21}\boldsymbol{\rho}_{\mathbf{u}^o,\mathbf{s}^o_1})^T\mathbf{V}_1}{r^o_2}\\
\vdots\\
\frac{(\mathbf{u}^o-\mathbf{s}^o_{m_1})^T\mathbf{V}_{m_1}-(\mathbf{u}^o-\mathbf{s}^o_1+r^o_{m_1,1}\boldsymbol{\rho}_{\mathbf{u}^o,\mathbf{s}^o_1})^T\mathbf{V}_1}{r^o_{m_1}}\\
\vdots\\
\frac{(\mathbf{u}^o-\mathbf{s}^o_{m_{N-1}+2})^T\mathbf{V}_{m_{N-1}+2}-(\mathbf{u}^o-\mathbf{s}^o_{m_{N-1}+1}+r^o_{m_{N-1}+2,m_{N-1}+1}\boldsymbol{\rho}_{\mathbf{u}^o,\mathbf{s}^o_{m_{N-1}+1}})^T\mathbf{V}_{m_{N-1}+1}}{r^o_{m_{N-1}+2}}\\
\vdots\\
\frac{(\mathbf{u}^o-\mathbf{s}^o_{m_N})^T\mathbf{V}_{m_N}-(\mathbf{u}^o-\mathbf{s}^o_{m_{N-1}+1}+r^o_{m_N,m_{N-1}+1}\boldsymbol{\rho}_{\mathbf{u}^o,\mathbf{s}^o_{m_{N-1}+1}})^T\mathbf{V}_{m_{N-1}+1}}{r^o_{m_N}}
\end{bmatrix}\\
&= \begin{bmatrix}
\frac{(\mathbf{u}^o-\mathbf{s}^o_2)^T\mathbf{V}_2}{r^o_2}-\frac{(\mathbf{u}^o-\mathbf{s}^o_1)^T\mathbf{V}_1}{r^o_1}\\
\vdots\\
\frac{(\mathbf{u}^o-\mathbf{s}^o_{m_1})^T\mathbf{V}_{m_1}}{r^o_{m_1}}-\frac{(\mathbf{u}^o-\mathbf{s}^o_1)^T\mathbf{V}_1}{r^o_1}\\
\vdots\\
\frac{(\mathbf{u}^o-\mathbf{s}^o_{m_{N-1}+2})^T\mathbf{V}_{m_{N-1}+2}}{r^o_{m_{N-1}+2}}-\frac{(\mathbf{u}^o-\mathbf{s}^o_{m_{N-1}+1})^T\mathbf{V}_{m_{N-1}+1}}{r^o_{m_{N-1}+1}}\\
\vdots\\
\frac{(\mathbf{u}^o-\mathbf{s}^o_{m_N})^T\mathbf{V}_{m_N}}{r^o_{m_N}}-\frac{(\mathbf{u}^o-\mathbf{s}^o_{m_{N-1}+1})^T\mathbf{V}_{m_{N-1}+1}}{r^o_{m_{N-1}+1}}
\end{bmatrix}\\
&= \begin{bmatrix}
\frac{\partial r^o_{21}}{\partial \mathbf{p}}^T\\
\vdots\\
\frac{\partial r^o_{m_1,1}}{\partial \mathbf{p}}^T\\
\vdots\\
\frac{\partial r^o_{m_{N-1}+2,m_{N-1}+1}}{\partial \mathbf{p}}^T\\
\vdots\\
\frac{\partial r^o_{m_N,m_{N-1}+1}}{\partial \mathbf{p}}^T
\end{bmatrix} = \mathbf{A}\frac{\partial \mathbf{r}^o}{\partial \mathbf{p}}
\end{aligned}
$$

Substituting (6.46) and (6.47) into (6.41), we have

$$
\begin{aligned}
cov(\mathbf{u})^{-1} = \quad & \mathbf{G}_3^T\mathbf{Q}_a^{-1}\mathbf{G}_3 - \mathbf{G}_3^T\mathbf{Q}_a^{-1}\mathbf{G}_4(\mathbf{Q}_\mathbf{p}^{-1} + \mathbf{G}_4^T\mathbf{Q}_a^{-1}\mathbf{G}_4)\mathbf{G}_4^T\mathbf{Q}_a^{-1}\mathbf{G}_3 \qquad (6.48)\\
= \quad & (\frac{\partial \mathbf{r}^o}{\partial \mathbf{u}^o})^T\mathbf{A}^T(\mathbf{A}\mathbf{Q}\mathbf{A}^T)^{-1}\mathbf{A}(\frac{\partial \mathbf{r}^o}{\partial \mathbf{u}^o}) - (\frac{\partial \mathbf{r}^o}{\partial \mathbf{u}^o})^T\mathbf{A}^T(\mathbf{A}\mathbf{Q}\mathbf{A}^T)^{-1}\mathbf{A}(\frac{\partial \mathbf{r}^o}{\partial \mathbf{p}})\\
& \left[(\tfrac{\partial \mathbf{r}^o}{\partial \mathbf{p}})^T\mathbf{A}^T(\mathbf{A}\mathbf{Q}\mathbf{A}^T)^{-1}\mathbf{A}(\tfrac{\partial \mathbf{r}^o}{\partial \mathbf{p}}) + \mathbf{Q}_p^{-1}\right]^{-1}(\frac{\partial \mathbf{r}^o}{\partial \mathbf{p}})^T\mathbf{A}^T(\mathbf{A}\mathbf{Q}\mathbf{A}^T)^{-1}\mathbf{A}(\frac{\partial \mathbf{r}^o}{\partial \mathbf{u}^o}).
\end{aligned}
$$

From Chapter 3, the CRLB of proposed estimator is

$$
\begin{aligned}
CRLB(\mathbf{u}^o)^{-1} = \quad & (\frac{\partial \mathbf{r}^o}{\partial \mathbf{u}^o})^T\left[\mathbf{Q}^{-1} - \mathbf{Q}^{-1}\mathbf{F}(\mathbf{F}^T\mathbf{Q}^{-1}\mathbf{F})^{-1}\mathbf{F}^T\mathbf{Q}^{-1}\right]\frac{\partial \mathbf{r}^o}{\partial \mathbf{u}^o} \qquad (6.49)\\
& -(\frac{\partial \mathbf{r}^o}{\partial \mathbf{u}^o})^T\left[\mathbf{Q}^{-1} - \mathbf{Q}^{-1}\mathbf{F}(\mathbf{F}^T\mathbf{Q}^{-1}\mathbf{F})^{-1}\mathbf{F}^T\mathbf{Q}^{-1}\right]\frac{\partial \mathbf{r}^o}{\partial \mathbf{p}} \qquad (6.50)\\
& \left[(\tfrac{\partial \mathbf{r}^o}{\partial \mathbf{p}})^T\left[\mathbf{Q}^{-1} - \mathbf{Q}^{-1}\mathbf{F}(\mathbf{F}^T\mathbf{Q}^{-1}\mathbf{F})^{-1}\mathbf{F}^T\mathbf{Q}^{-1}\right]\tfrac{\partial \mathbf{r}^o}{\partial \mathbf{p}} + \mathbf{Q}_p\right]^{-1} \qquad (6.51)\\
& (\frac{\partial \mathbf{r}^o}{\partial \mathbf{p}})^T\left[\mathbf{Q}^{-1} - \mathbf{Q}^{-1}\mathbf{F}(\mathbf{F}^T\mathbf{Q}^{-1}\mathbf{F})^{-1}\mathbf{F}^T\mathbf{Q}^{-1}\right]\frac{\partial \mathbf{r}^o}{\partial \mathbf{u}^o} \qquad (6.52)
\end{aligned}
$$

Denoting $\widetilde{\mathbf{A}} = \mathbf{Q}^{\frac{1}{2}}\mathbf{A}^T$ and $\widetilde{\mathbf{F}} = \mathbf{Q}^{-\frac{1}{2}}\mathbf{F}$,

$$
\mathbf{A}^T(\mathbf{A}\mathbf{Q}\mathbf{A}^T)^{-1}\mathbf{A} = \mathbf{Q}^{-\frac{1}{2}}\widetilde{\mathbf{A}}(\widetilde{\mathbf{A}}^T\widetilde{\mathbf{A}})^{-1}\widetilde{\mathbf{A}}^T\mathbf{Q}^{-\frac{1}{2}} \qquad (6.53)
$$

$$
\mathbf{Q}^{-1} - \mathbf{Q}^{-1}\mathbf{F}(\mathbf{F}^T\mathbf{Q}^{-1}\mathbf{F})^{-1}\mathbf{F}^T\mathbf{Q}^{-1} = \mathbf{Q}^{-\frac{1}{2}}\left[\mathbf{I} - \widetilde{\mathbf{F}}(\widetilde{\mathbf{F}}^T\widetilde{\mathbf{F}})^{-1}\widetilde{\mathbf{F}}^T\right]\mathbf{Q}^{-\frac{1}{2}} \qquad (6.54)
$$

where $\mathbf{I}$ is a $(m_N - 1) \times (m_N - 1)$ identity matrix.

Note that $\widetilde{\mathbf{A}}(\widetilde{\mathbf{A}}^T\widetilde{\mathbf{A}})^{-1}\widetilde{\mathbf{A}}^T$ is the projection matrix onto the subspace defined by the columns of $\widetilde{\mathbf{A}}$.

$\widetilde{\mathbf{F}}(\widetilde{\mathbf{F}}^T\widetilde{\mathbf{F}})^{-1}\widetilde{\mathbf{F}}^T$ is the projection matrix onto the subspace defined by the columns of $\widetilde{\mathbf{F}}$. Using the definition of A and F in (6.18) and (3.29)

$$
\begin{aligned}
\widetilde{\mathbf{A}}^T\widetilde{\mathbf{F}} &= \mathbf{A}\mathbf{Q}^{\frac{1}{2}}\mathbf{Q}^{-\frac{1}{2}}\mathbf{F} = \mathbf{A}\mathbf{F} \qquad (6.55)\\
&= \mathbf{O}.
\end{aligned}
$$

(6.55) indicates that the columns of $\widetilde{\mathbf{A}}$ and that of $\widetilde{\mathbf{F}}$ are orthogonal to each other. Also, the columns of them together span the entire space of dimension $m_N - 1$. Thus

$$
\widetilde{\mathbf{A}}(\widetilde{\mathbf{A}}^T\widetilde{\mathbf{A}})^{-1}\widetilde{\mathbf{A}}^T = \mathbf{I} - \widetilde{\mathbf{F}}(\widetilde{\mathbf{F}}^T\widetilde{\mathbf{F}})^{-1}\widetilde{\mathbf{F}}^T \qquad (6.56)
$$

Or from (6.53) and (6.54),

$$
\mathbf{A}^T(\mathbf{A}\mathbf{Q}\mathbf{A}^T)^{-1}\mathbf{A} = \mathbf{Q}^{-1} - \mathbf{Q}^{-1}\mathbf{F}(\mathbf{F}^T\mathbf{Q}^{-1}\mathbf{F})^{-1}\mathbf{F}^T\mathbf{Q}^{-1} \qquad (6.57)
$$

As a result,

$$cov(\mathbf{u})^{-1} = CRLB(\mathbf{u})^{-1}. \tag{6.58}$$

That is

$$cov(\mathbf{u}) = CRLB(\mathbf{u}) \tag{6.59}$$

when condition C_1 and C_2 are satisfied.

6.4 Summary

In this chapter, we proposed an estimator of the source localization problem in the presence of measurement noise, sensor position manifold uncertainties and clock-bias error. Then, simulation result shows that the proposed method reached the CRLB performance for both near-field and distant source in small error region. In the final part of the chapter, the performance of reaching the CRLB has been proven theoretically under the small noise condition.

Chapter 7

Conclusion and Future Work

7.1 Conclusion

Source localization using TDOA in the presence of sensor position manifold uncertainties and clock-bias offsets, and both the sensor position manifold uncertainties and clock-bias error have been investigated in this thesis. For each of the three cases, first we derived the CRLB of the localization problem. Then, we proposed a computationally efficient closed form estimator of the source location. Simulation were conducted to examine the performance of the proposed estimator. Finally, the proposed estimator has been proven that it reaches the CRLB performance theoretically.

A summary of this research is as follows.

First, we introduced the basic idea of source localization and gave the reasoning of the presence of sensor position manifold uncertainties, clock-bias error and the presence of the two kinds of error.

Then we introduced the concept and the definition of the CRLB. The basic idea of the Taylor-series method and the Chan and Ho's method were also introduced. These two methods were originally developed in the presence of measurement noise only.

In Chapter 3, first, we presented the CRLB with measurement noise only. We next derived the CRLB for source localization in the presence of measurement noise and sensor position manifold uncertainties, the CRLB in the presence of measurement noise and clock-bias error, and

the CRLB in the presence of measurement noise, sensor position manifold uncertainties and clock-bias error. The CRLBs in the latter three cases are bigger than the CRLB when only measurement noise exists because of the presence of other kinds of errors.

In Chaper 4, 5 and 6, we proposed three estimators to locate the source for the three cases.

The first estimator is proposed for the localization problem with measurement noise and sensor position manifold uncertainties. It is a non-iterative method based on Chan and Ho's method. The basic idea is to use the weighting matrix $\mathbf{W}_1$ in Stage 1 to account for the sensor position manifold uncertainties to improve the source location estimation.

The second estimator is also based on Chan and Ho's method and is used to obtain the source location in the presence of measurement noise and clock-bias offsets. The main idea of this estimator is to group the sensors with the same clock together to form m_N sub-arrays. We transformed the original TDOA values to the new TDOA values of which the reference sensors are different for different sub-arrays so that the clock-bias offsets are absent within a sub-array. Through the use of the transformed TDOA measurements, we came up with a closed form estimator of the source location that can reach the CRLB accuracy.

The third source localization estimator is for the case of having measurement noise, sensor position manifold uncertainties and clock-bias offsets. This method combines the previous two proposed technique together. The weighting matrix $\mathbf{W}_1$ takes care of the measurement noise and sensor position manifold uncertainties. Different sub-arrays are created to eliminate the unknown clock offsets by transforming the TDOA measurements, and closed form solution was derived.

The simulations are given for the three proposed estimators and the simulations validated the theoretical analysis that their performance reaches the CRLB under small the noise condition.

7.2 Future Work

In this section, we will discuss some future work on this research topic.

First of all, for sensor position manifold uncertainties, it is worth to investigate moving sensor scenario. If the movement speed of the sensors are related to each other, such as the sensors are

in the same mobile platform, it is possible to get a better performance for the source location estimate by exploring the relationships among sensor velocity uncertainties.

For clock-bias offsets, the present work models them as fixed unknown value. However, they can be modeled as random parameters with certain known probability density functions. The performance of the source location estimate in the presence of clock-bias offsets could be improved. by making use of the prior information about the clock offsets. The CRLB needs to be re-derived and new estimator is needed.

In this thesis, we only consider the use of TDOA to locate the source in the presence of sensor position manifold uncertainties and clock-bias offsets. It is also interesting to investigate the estimators based on other positioning measurements such as TOA and AOA when the two kinds of errors are present.

Bibliography

[1] E. Weinstein, "Optimal source localization and tracking from passive array measurements, *IEEE Trans. Acoust., Speech, Signal Process.,* vol. ASSP-30, pp. 69-76, Feb. 1982.

[2] F. Ahmad and M. Amin, "Noncoherent approach to through-the-wall radar localization, *IEEE Trans. Aerosp. Electron. Syst.,* vol. 42, pp. 1405-1419, Oct. 2006.

[3] G. C. Carter, "Time delay estimation for passive sonar signal processing, *IEEE Trans. Acoust., Speech, Signal Process.,* vol. ASSP-29, pp. 462-470, Jun. 1981.

[4] S. Coraluppi, "Multistatic sonar localization, *IEEE J. Ocean. Eng.,* vol. 31, pp. 964-974, Oct. 2006.

[5] R. J. Vaccaro, "The past, present, and the future of underwater acoustic signal processing," *IEEE Signal Process. Mag.,* vol. 15, pp. 21-51, Jul. 1998.

[6] A. Caiti, A. Garulli, F. Livide and D. Prattichizzo, "Localization of autonomous underwater vehicles by floating acoustic buoys: a set-membership approach, *IEEE J. Oceanic Engineering,* vol. 30, pp. 140-152, Jan. 2005.

[7] T. Gustafsson, B. D. Rao and M. Trivedi, "Source localization in reverberant environments: modeling and statistical analysis," *IEEE Trans. Speech, Audio Process.,* vol. 11, pp. 791-803, Nov. 2003.

[8] B. Mungamuru and P. Aarabi, "Enhanced sound localization, *IEEE Trans. Syst.,Man., Cybern.,* Part B, vol. 34, pp. 1526-1540, Jun. 2004.

[9] P. G. Georgiou and C. Kyriakakis, "Robust maximum likelihood source localization: the case for sub-Gaussian versus Gaussian, *IEEE Trans. Audio, Speech, Language Process.,* vol. 14, pp. 1470-1480, Jul. 2006.

[10] J. C. Chen, K. Yao and R. E. Hudson, "Source localization and beamforming, *IEEE Signal Process. Mag.,* vol. 19, pp. 30-39, Mar. 2002.

[11] J. C. Chen, L. Yip, J. Elson, H. Wang, D. Maniezzo, R. E. Hudson, K. Yao and D. Estrin, "Coherent acoustic array processing and localization on wireless sensor networks, in *Proc. IEEE,* vol. 91, pp. 1154-1162, Aug. 2003.

[12] R. J. Kozick and B. M. Sadler, "Source localization with distributed sensor arrays and partial spatial coherence, *IEEE Trans. Signal Process.,* vol. 52, pp. 601-616, Mar. 2004.

[13] P. Julian, A. G. Andreou, L. Riddle, S. Shamma, D. H. Goldberg and G. Cauwenberghs, "A comparative study of sound localization algorithms for energy aware sensor network nodes, *IEEE Trans. Circuits Syst.,* vol. 51, pp. 640-648, Apr. 2004.

[14] S. Gezici, Z. Tian, G. B. Giannakis, H. Kobayashi, A. F. Molisch, H. V. Poor and Z. Sahinoglu, "Localization via ultra-wideband radios: a look at positioning aspects for future sensor networks, *IEEE Signal Process. Mag.,* vol. 22, pp. 70-84, Jul. 2005.

[15] T. S. Rappaport, J. H. Reed and B. D. Woerner, "Position location using wireless communications on highways of the future," *IEEE Commun. Mag.,* vol. 34, pp. 33-41, Oct. 1996.

[16] G. Sun, J. Chen, W. Guo and K. J. R. Liu, "Signal processing techniques in networkaided positioning: a survey of state-of-the-art positioning designs," *IEEE Signal Process. Mag.,* vol. 22, pp. 12-23, Jul. 2005.

[17] A. H. Sayed, A. Tarighat and N. Khajehnouri, "Network-based wireless location: challenges faced in developing techniques for accurate wireless location information," *IEEE Signal Process. Mag.,* vol. 22, pp. 24-40, Jul. 2005.

[18] F. Gustafsson and F. Gunnarsson, "Mobile positioning using wireless networks: possibilities and fundamental limitations based on available wireless network measurements," *IEEE Signal Process. Mag.,* vol. 22, pp. 41-53, Jul. 2005.

[19] W. Foy, "Position-location solution by taylor-series estimations," *IEEE Trans. erosp. Electron. Syst,* vol. ASSP-33, no. 7, pp. 1387-1396, Dec 1985.

[20] Y. T. Chan and K. C. Ho, "A simple and efficient estimator for hyperbolic location," *IEEE Trans. Signal Process.,* vol. 42, pp. 1905-1915, Aug. 1994.

[21] G. C. Carter, *Coherence and Time Delay Estimation,* IEEE Press, 1993.

[22] B. Yegnanarayana, S. R. M. Prasanna, R. Duraiswami and D. Zotkin, "Processing of reverberant speech for time-delay estimation," *IEEE Trans. Speech, Audio Process.,* vol. 13, pp. 1110-1118, Nov. 2005.

[23] T. Rappaport, J. Reed, and B. Woener, "Position location using wireless communi- cations on highways of the future," *IEEE Communication magazine,* pp. 33-41, Oct 1996.

[24] Y. Zhao, "Standarization of mobile phone positioning for 3g systems," *IEEE Communication magazine,* pp. 108-116, Jul 2002.

[25] D.J. Torrieri, "Statistical Theory of Passive Location Systems," *IEEE Transactions on Aerospace and Electronic Systems,* vol. 20, no. 2, pp. 189-198, 1984.

[26] A. Pages-Zamora, J. Vidal and D. H. Brooks, "Closed-form solution for positioning based on angle of arrival measurements," in *Proc. Int. Symp. Personal, Indoor, Mobile Radio Commun.,* pp. 1522-1526, Sep. 2002.

[27] Y. Rockah and P. Schultheiss, "Array shape calibration using sources in unknown location part i: Far-field source," *IEEE Trans. Acoust., Speech, Signal Processing,* vol. ASSP-35, no. 3, pp. 286-299, Mar 1987.

[28] Y. Chen, J. Lee, and C. Yeh, "Two-dimensional angle-of arrival estimation for uniform planar array with sensor position errors," in *Proc. IEE Radar, Signal Processing,* vol. 140, no. 1, Feb 1993, pp. 37-42.

[29] K. C. Ho, L. Kovavisaruch, and H. Parikh, "Source localization using tdoa with erroneous receiver positions," in *Proc. IEEE ISCAS,* Vancouver, Canada, May 2004, pp. II/453-II/456.

[30] Le Yang; Ho, K.C., "An Approximately Efficient TDOA Localization Algorithm in Closed-Form for Locating Multiple Disjoint Sources With Erroneous Sensor Positions," *Signal Processing, IEEE Transactions,* Volume: 57 , Issue: 12, pp. 4598-4615, 2009.

[31] Fan, H.H.; Chunpeng Yan, "Asynchronous Differential TDOA for Sensor Self-Localization," *Acoustics, Speech and Signal Processing, 2007. ICASSP 2007. IEEE International Conference,* Volume: 2, pp. II-1109-II-1112, 2007.

[32] Chunpeng Yan; Fan, H.H., "Asynchronous differential TDOA for non-GPS navigation using signals of opportunity," *Acoustics, Speech and Signal Processing, 2008. ICASSP 2008. IEEE International Conference,* pp. 5312-5315, 2008.

[33] S. M. Kay, *Fundamentals of Statistical Signal Processing, Estimation Theory.* Engle-Wood CliRs, NJ: Prentice-Hall, 1993.

[34] J. M. Mendel, *Lesson in estimation theory for Signal Processing, Communications, and Control.* EngleWood CliRs, NJ: Prentice-Hall, 1995.